The Effects of Land Cover, Climate, and Urbanization on Groundwater Resources in Dauphin Island

by

Katherine S. Petty

A thesis submitted to the Graduate Faculty of
Auburn University
in partial fulfillment of the
requirements for the degree of
Master of Science

Auburn, Alabama
December 12, 2011

Approved by

Prabhakar Clement, Co-Chair, Arthur H. Feagin Professor of Civil Engineering
Latif Kalin, Co-Chair, Associate Professor of Forestry and Wildlife Science
Xing Fang, Associate Professor of Civil Engineering

Abstract

The effects of land cover change, climate change, and population growth on the groundwater resources of a barrier island were explored in this study. The relationship between land cover and groundwater recharge was studied for seven locations in the Southeast. SEAWAT was used to develop a detailed groundwater model for managing water resources in Dauphin Island, Alabama. Various scenarios were simulated to assess the sensitivity of the groundwater aquifer to parameters such as sea level rise, increased pumping rates, and decreases in recharge due to climate change or land cover change. A heuristic approach was used to estimate sustainable pumping levels for the Dauphin Island aquifer as a function of the annual groundwater recharge.

Based on the model predictions from the Dauphin Island groundwater model, it is expected that decreasing recharge due to climate change would have the greatest effect on the island's groundwater resources. Land cover change, sea level rise, as well as increased water demand due to expected population growth did not have as large of an effect on the aquifer. Some of the scenarios simulated indicated a definite risk of lateral saltwater intrusion occurring in the aquifer. This information is useful for introducing water management practices on the island.

Acknowledgments

This research was funded by the Center for Forest Sustainability at Auburn University, AL. This work would not have been possible without the guidance of my advisors Dr. Clement and Dr. Kalin. I am also grateful to my third committee member, Dr. Fang, for his time and willingness to be a part of this process. Ruoyu Wang kindly provided assistance by providing valuable recharge data used this research. Vaile Feemster from the Dauphin Island Sewer and Water Authority provided well pumping data. Dan O'Donnell was very helpful providing information on his work relating to Dauphin Island. My officemates have been an invaluable resource to me, both in my research and as friends. The unconditional support and encouragement from my parents and grandparents has gotten me to the point I am at today. I am also thankful for the patience and support of my husband, Ben. I am grateful to God for giving me the ability and desire to accomplish all that I have been able to.

Table of Contents

List of Tables

List of Figures

1. Introduction

Dauphin Island is a small barrier island located between the Mississippi Sound and the Gulf of Mexico about 4 miles off the coast of Mobile County, Alabama [*Chandler*, 1983]. The residents of Dauphin Island obtain their water from a shallow lens of freshwater located in the island's unconfined aquifer. According to the United States Census Bureau, the population of Dauphin Island has been steadily increasing for the past 20 years. Due to the ever-growing desire of Americans to live on the coast, it is reasonable to assume that this trend will continue. Because of this, there is a need to understand the capacity, limitations, and characteristics of such shallow coastal aquifers, and understand the impacts of changing climatic factors and hydrologic parameters on these highly vulnerable water resource systems.

This research thesis consists of four sections. The first section investigates recharge issues in the Southeast United States. Several recharge estimation methods were explored. The first research question addressed in this section was which recharge estimation method gave consistent results for our sites in the Southeast and should be used in the rest of the study? The second research question was can a relationship be found between land cover type and amount of water recharged into the aquifer?

The second section of this thesis provides background information about Dauphin Island. It contains information on geology, soil, land use, and water problems of the island. It is intended to introduce the reader to Dauphin Island hydrogeology and present the water issues faced by the island.

The third section specifically focuses on the groundwater resources of Dauphin Island and the effects of changing factors on the island's water-table aquifer. The factors that were examined in this section were the effects of land cover/land use change, climate change, and

increasing population on the groundwater resources. The first research question considered is whether changing the parameters based upon scenarios mimicking land-cover/land-use change, climate change, and population change have a significant impact on the groundwater resources. The second research question was if they did have a significant impact, which factors was the aquifer most sensitive to.

The fourth section focused on assessing what percentage of Dauphin Island's annual recharge could be withdrawn from the wells without significantly impacting the aquifer. This study was done because all of the scenarios modeled in the third study were hypothetical. Since it is impossible to predict what the actual future recharge situation will be, it is important to know what percentage of recharge can be pumped in order to make management decisions. The goal was to estimate what percentage of the annual recharge on the island could be pumped without saltwater contaminating any of the wells on the island.

2. Literature survey

This chapter briefly introduces concepts and surveys relevant literature on several topics, including groundwater aquifers and their importance in barrier islands, estimation techniques for groundwater recharge, numerical modeling of groundwater, and other environmental factors that affect groundwater resources.

2.1 Groundwater concepts for managing island aquifers

Increasing populations, increasing economic and industrial activities, and increasing developments and urban sprawl around the world have significantly amplified demands on water resources around the world. Depletion of surface water is becoming more evident in many areas, putting an increased stress on groundwater sources. Additionally, some areas don't have naturally occurring surface water reservoirs or any considerable river systems. Because of this, the demand for groundwater resources has become increasingly more substantial. Fortunately, the amount of available freshwater in the form of groundwater is much higher than the amount available as surface water, but usage of groundwater must be carefully managed [*Fetter*, 2001].

The existence of groundwater occurs when water is stored in the void spaces of soil, fractured rock, or any other substance that makes up the underlying substrate. Groundwater can occur in unconfined and confined aquifers. Unconfined aquifers have no confining layer between the surface and the saturation zone. Confined groundwater is overlain by a confining unit with a significantly lower hydraulic conductivity than that of the aquifer itself, and prevents the flow of water through the confining strata [*Fetter*, 2001].

On small, barrier islands, the proportion of water used by humans coming from groundwater is very high. Barrier islands are significantly smaller than continental landmasses.

This means that there are no large watersheds feeding water to river systems. Additionally, because of storms, tides, and sediment budget deficits, the morphology of barrier islands changes almost constantly. Further, with sea level rise, there may be observable effects on the morphology of the island [*Morton*, 2008]. Therefore, because of their relatively small size and changing geomorphology, it is unlikely that there would be any well-established, major river channels in these systems. Without any major river systems, reservoirs cannot be used to provide a source of water for human consumption. Because of this, groundwater is extremely important in barrier islands. Most of groundwater pumped from barrier islands comes from island aquifer lens systems, a relatively shallow unconfined layer of water that is exploitable for human use. Typically, these systems are precipitation derived freshwater lenses that overly denser saltwater.

Chesnaux [2008] performed a detailed study of unconfined island aquifers. He specifically developed analytical solutions for groundwater travel times in islands bounded by freshwater as well as by seawater. Figure 2-4 illustrates the cross sectional view of an island aquifer system, showing the lens of exploitable freshwater [*Chesnaux*, 2008].

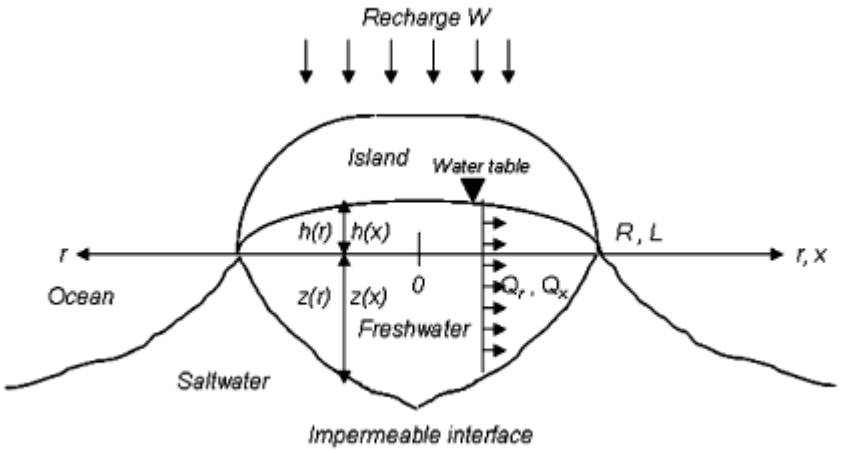

Figure 2-1. Cross-Sectional view of a circular oceanic island [Chesnaux 2008].

As shown in the figure, the sole source of input to the system is precipitation derived recharge. Water is lost from the system via groundwater discharge occurring radially towards the saline ocean. When the groundwater is pumped this is also a loss to the system [*Chesnaux*, 2008]. Withdrawals of water from these systems have serious consequences that must be considered. If withdrawal rates from island aquifers are larger than recharge rates from precipitation, saltwater intrusion will occur since the aquifer is in direct hydraulic contact with the ocean.

Saltwater intrusion occurs because when water is pumped from island aquifers the inland water level is reduced and the higher density salt water flows in due to the head gradient, creating a saltwater wedge. As pumping continues, saltwater intrusion moves further inland and eventually has the potential to contaminate the groundwater resources [*Fetter*, 2001]. In coastal aquifers, intrusion can occur in a variety of modes. As already discussed, saltwater can intrude

upward from deeper, saline zones, but intrusion can also occur laterally from the ocean as well as downward from coastal waters [*Barlow and Reichard*, 2010].

The extent of the saltwater intrusion depends on factors such as rate of groundwater withdrawls, distance between the pumping wells, geological properties of the aquifer, and the hydraulic properties of the aquifer [*Barlow and Reichard*, 2010].

2.2 Groundwater recharge

Groundwater recharge is the process in which surface water reaches the water-table in the aquifer's phreatic zone [*Martinez-Santos*, 2010]. Groundwater recharge can occur in a variety of ways. The two most common vehicles for recharge are deep seepage recharge occurring between aquifer units and by infiltration recharge from precipitation.

As previously discussed, recharge is an integral part of the water budget for a shallow, freshwater aquifer. Understanding and quantifying recharge is extremely important from an aquifer planning and management standpoint so that sustainable abstraction levels can be estimated for the aquifer. The rate and quantity of groundwater recharge directly affects the quantity of freshwater resources contained in the aquifer, and the amount that can be safely withdrawn. Shallow, precipitation driven aquifers are considerably sensitive to recharge rate. Additionally, recharge estimates are important from a hydrogeological standpoint [*Martinez-Santos*, 2010]. In order to accurately understand and model a specific aquifer system, there must be a known estimate for recharge.

Additionally, being able to quantify recharge is also useful if saltwater intrusion occurs in the aquifer. Under natural equilibrium conditions, high inland groundwater levels and flow of fresh water to the sea impede inland movement of saltwater into aquifer systems, and the

position of the boundary is a function of the amount of freshwater discharge [*Fetter*, 2001]. However, when aquifers are over exploited the salt water wedge advances into the aquifer and saltwater intrusion occurs. The effect of recharge intensity and duration on saltwater intrusion was studied by Mahesha and Nagaraja using a one-dimensional finite element model [1995]. They found that a relationship can be developed between interface motion of the saltwater wedge and the intensity and duration of recharge.

There are at least three basic ways to obtain recharge at a certain location. The first, and perhaps most obvious, is to measure it directly. This would include the use of expensive field equipments. A potential drawback to direct measurement is the cost of equipment. Also, it is known that this method is largely site specific [*Sophocleous*, 1991].

A second way to estimate recharge is using the hydrologic continuity equation as the foundation. The equation is

$$\frac{\partial s}{\partial t} = I - Q, \text{ where} \qquad (2\text{-}1)$$

$\frac{\partial s}{\partial t} =$ change in storage per time [L^3/t]; $I =$ inflow [L^3/t]; and $Q =$ outflow in [L^3/t].

This equation suggests that the change in the storage volume is quantified using the difference between the inflow and outflow of a hydrologic system [*Bedient and Huber*, 1992].

This concept can also be applied to small basins by defining the terms that constitute the inflow and the outflow. By doing this, the following water balance equation can be derived:

$$\Delta S = P - R - G - ET - I, \text{ where} \qquad (2\text{-}2)$$

$\Delta S =$ change in storage in a specified time period; $P =$ precipitation; $R =$ surface runoff; $G =$ groundwater flow [recharge]; $ET =$ evapotranspiration, and $I =$ interception [*Bedient and Huber*, 1992].

The main problem with this method of recharge estimation is that while the input term, precipitation, can be easily measured, many of the output terms are not easily measurable. Most of the output terms either have to be measured with expensive equipment or estimated using empirical relationships that are not always accurate for the given circumstance or site location. For these reasons, this method is not always easy to apply or realistic.

The third method, which was the basis for the simpler method used later in this research, is called the Water-Table Fluctuation (WTF) method. This method requires the input of groundwater level data as well as an estimation of the specific yield of the aquifer. Specific yield, S_y, is a property of rock or soil that indicates the ratio of the volume that the soil will yield due to gravity drainage to the total soil volume [*Fetter*, 2001].

By measuring the fluctuations in groundwater level, the groundwater recharge can be estimated. Each positive fluctuation in the groundwater level indicates recharge into the aquifer. By measuring the change in groundwater level and multiplying the change by the specific yield of the system, the value of groundwater recharge is found for that site. Mathematically, recharge is calculated using the following equation:

$R(t_j) = \Delta H(t_j) * S_y$, where (2-3)

$R(t_j) =$ recharge from t_0 to t_j [L]; $\Delta H =$ the peak water level rise during the recharge period [L]; and $S_y =$ Specific yield [dimensionless].

In order to get an accurate ΔH , the height of the increase must be measured from where the antecedent recession curve would be extrapolated had the recharge spike not occurred. This is illustrated in Figure 2-2:

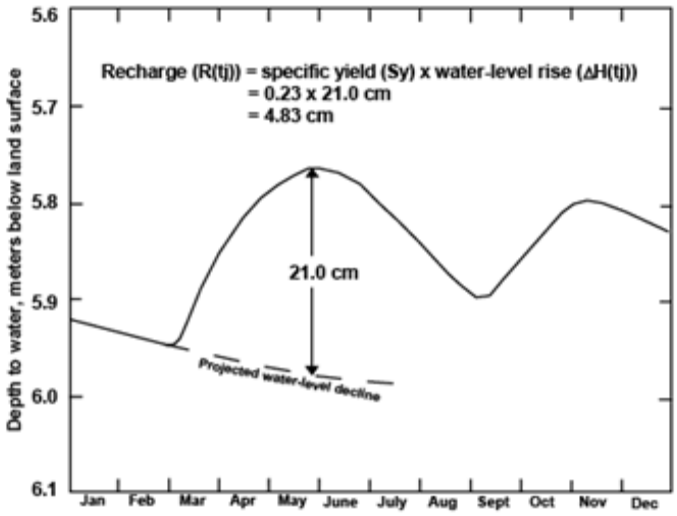

Figure 2-2. Measurement of recharge spike [from USGS Groundwater Information, 2008].

There have been several studies done attempting to estimate groundwater recharge using the methods described above. For example, Delin et al. [2006] used four local and basin scale methods to compare recharge estimations in Minnesota [*Delin et al*., 2006]. The local scale estimates were done using an Unsaturated Zone Water Balance (UZWB), the WTF method, and groundwater age dating. The results of the study showed that the UZWB method gave inconsistent results when compared to other methods. The study also found that the WTF method was the easiest to apply. Additionally, their research illustrated that regionalized recharge estimates compared well to local and basin scale estimates [*Delin et al*., 2006].

Crosbie et al. [2005] also used the WTF method, but combined it with a time series approach to estimate recharge. Using the time series approach, long term water-table and precipitation records were examined and effects due to evapotranspiration, atmospheric tides, the Lisse effect, which occurs when air is trapped by infiltration, and varying specific yields values were removed [*Crosbie et al.*, 2005].

Recharge was estimated by Samper and Pisani [2009] using a combination of the soil water balance and a groundwater flow model for Andújar alluvial aquifer in Spain. The soil water balance alone gave too large of values for recharge estimates. The combined method overcame common problems that are often encountered when recharge estimation is attempted by soil water balance or groundwater flow models alone [*Samper and Pisani*, 2009].

Two recharge estimation methods were also combined by Sophocleous [1990] in an attempt to quantify groundwater recharge in the Kansas Prairies. Sophocleous combined the soil water balance and the WTF method to obtain his "hybrid water-fluctuation method." For each storm event, the recharge amount was calculated using the hydrologic budget. This amount was divided by the measured water-table rise in the groundwater record for the corresponding event, and the estimate of storativity was obtained. After this was done for several events, the average storativity was found, and this value was applied to specific water-table rises to find groundwater recharge values [*Sophocleous*, 1990].

In a study completed by Martínez-Santos and Andreu [2010] results from lumped and distributed approaches to estimate recharge were compared for the Ventós Aquifer in Spain. Lumped models assume the system can be expressed using a combination of transfer functions, and the physics of recharge are rarely considered. Distributed models use detailed data records to establish a relationship and provide spatial information. Both models obtained similar results,

although the results from the lumped model agreed better with the available field data [*Martínez-Santos and Andreu*, 2010].

Another problem that is often encountered in recharge estimation is difficulty in measuring recharge for data poor areas. For example, some areas may not have groundwater monitoring stations, so applying some of the previously discussed methods would be difficult. Crosbie et al [2010] attempted to overcome such problems in their study of almost 200 sites in Australia. They estimated recharge at 172 data rich sites in an attempt to obtain empirical relationships that could relate recharge to national datasets and characteristics such as vegetation, climate, and surface materials. This way the relationships could also be applied for data poor areas. The study found that the relationships were most sensitive to vegetation and soil type [*Crosbie et al*, 2010].

While hydrologic modeling was briefly mentioned earlier, a specific modeling tool to estimate recharge that should be mentioned in depth, as it was used in this research project, is the Soil Water Assessment Tool (SWAT). SWAT is a hydrologic continuous time model that was developed to assess the effects of land management practices and climate on complex watersheds [*Arnold*, 2005]. SWAT uses many input parameters and uses precipitation as the driver. One of the outputs that can be obtained from the model is groundwater recharge for the watershed.

SWAT has been used in many instances to estimate groundwater recharge. For example, Arnold et al. used it to estimate recharge in the upper Mississippi River Basin [*Arnold et al.*, 2000]. It was also used to quantify recharge in the Liverpool Plains of Australia by Sun and Cornish [2005]. The specifics behind the SWAT procedures used in this research will be discussed in later chapters.

2.3 Density-dependent numerical modeling

As previously discussed, over exploitation of aquifers is currently stressing these systems and causing distortion in the natural recharge-discharge equilibrium. Groundwater modeling has become a powerful tool to visualize current groundwater flow conditions as well as predict potential impact of future hypothetical scenarios. This aids in establishing long-term planning practices for the aquifer. Groundwater flow models solve the general groundwater flow equation, and are capable of providing visualization of either two or three dimensional flow in aquifers. Many of these models are based on the popular MODFLOW groundwater model *[Harbaugh*, 2000]. MODFLOW operates by using a finite difference solution scheme to solve the three dimensional groundwater flow differential equation.

In order to simulate the interaction of saltwater and freshwater as well as the occurrence of saltwater intrusion, a density-dependent groundwater flow model can be used [*Lin et al*., 2009]. SEAWAT was developed by combining MODFLOW and MT3DMS [*Zheng*, 1990] into one program and making modifications to account for saltwater-freshwater density variations. By doing this, a finite difference numerical model which is capable of solving the coupled flow and solute transport equations was obtained [*Guo and Langevin*, 2002]. SEAWAT can use either an implicit or explicit solution scheme. When solved implicitly, SEAWAT uses MODFLOW to solve the flow field for each time step, and then MT3D to solve the concentration field. This concentration is used to update the density field, which is used by MODFLOW as the relative density difference term. This is repeated a number of times within the same time step until the difference in density is smaller than the user-defined value [*Rao et al*., 2004]. When solved explicitly, the flow and transport equations are solved alternately and repeated until the allotted amount of stress periods are complete [*Guo and Langevin*, 2002].

The SEAWAT modeling approach was validated by Goswami and Clement [2007] by comparing laboratory data for both steady state and transient experiments to results obtained by modeling done in SEAWAT [*Goswami and Clement*, 2007]. Previous to this, the benchmark for validating saltwater intrusion models was the steady state Henry solution [*Henry*, 1964].

Many coastal aquifer studies have utilized SEAWAT to simulate the freshwater-saltwater interface. For example, SEAWAT was used by Larabi et al. [2008] to model the groundwater quantity and quality contained in the Rmel Coast aquifer in Morocco [*Larabi et al*., 2008]. Pravena and Aris [2010] used SEAWAT to model the aquifer underlying Manukan Island in Malaysia. They modeled six scenarios representing possible human pressures and climate change [*Praveena and Aris*, 2009]. SEAWAT was used by Lin et al. [2008] to model the degree of saltwater intrusion in the Gulf coast aquifers of Alabama [*Lin et al.*, 2008]. The study done by Lin et al. included a 40 year predictive simulation run, which illustrated a large amount of saltwater intrusion potential if groundwater pumping goes beyond the 1996 level. The paper suggested a need for better groundwater development and management strategies for the Gulf Coast, especially for the deep, confined aquifer systems.

An extensive modeling study using SEAWAT was done by Masterson [2004] to model the complex groundwater system of Cape Cod, Massachusetts. The aquifer system at Cape Cod consists of four distinct lenses. Increasing development and demand on the groundwater system had raised serious concerns for the sustainability of the system. Using a complex groundwater model, the current groundwater situation was simulated, as well as future groundwater levels with predicted pumping rates [*Masterson*, 2004].

SEAWAT has also been used as a tool in a more unconventional manner to quantify aquifer parameters. For example, Cecan et al. [2008] used it to analyze pumping test data in order to

find horizontal hydraulic conductivity and vertical anisotropy in Cape Cod, Massachusetts. The results of the study showed that classical methods such as the Hantush-Jacob method and numerical models that do not account for density difference do not predict horizontal hydraulic conductivity and vertical anisotropy values as accurately as SEAWAT [*Cecan et al.*, 2008].

Rao et al. [2004] utilized SEAWAT in an unusual and interesting way. They used SEAWAT to model the saltwater intrusion dynamics in a hypothetical coastal aquifer, but then also explored if the SEAWAT model could be replaced by a trained artificial neural network. An artificial neural network (ANN) is a computational tool that attempts to mimic the structure and/or function of the biological neural network. Because of the computational burden that corresponds with complex groundwater models, ANN was used to replace the model. In this study, the ANN was improved by data training sets from repeated runs of SEAWAT. Once this was done, the ANN was able to produce results very similar to the results obtained from SEAWAT [*Rao et al.*, 2004].

Other density dependent groundwater flow models have been used to model groundwater flow in coastal aquifer systems. Joscon et al. [2001] used the SWIG2D to find the depth to the saltwater interface in the Northern Guam Lens Aquifer [*Joscon et al.*, 2001]. The region of the Biscayne Aquifer underlying Hallandale, Florida was modeled by Anderson et al. [1988] using the program SWICHA [*Anderson et al.*, 1988]. Sherif and Singh [1999] used 2D-FED to model the effects of climate change on two coastal aquifers, one in Egypt and one in India [*Sherif and Singh*, 1999].

2.4 Additional factors affecting groundwater resources in islands

While increased demand due to increasing population and pumping rates can cause large stresses on an aquifer, there are other confounding factors that can affect the quality and quantity of groundwater resources. Some of these factors are land cover/land use change and climate change. Climate change includes scenarios such as changing precipitation patterns, increase in hurricanes and other large storm events, and sea level rise.

Studies have been done that have illustrated the significant effects of land use on groundwater recharge. By monitoring water level measurements from two monitoring wells for 122 days, Zhang and Schilling [2005] were able to observe the effects of land cover on the water-table, evapotranspiration, soil moisture, and groundwater recharge. The two wells were on either side of Walnut Creek, in Iowa. One of the wells was located in grassy field and the other well was located in bare ground. The water level data showed significant variations in water level between the two sites. Because of increased ET at the grass covered well, much less groundwater recharge reached the water-table. They also found that soil moisture was also less in the grass covered site due to ET [*Zhang and Schilling*, 2005].

Since there is often an obvious relationship between land use and recharge, scientists have attempted to estimate recharge using land cover data. Cherkauer and Sajjad [2005] outlined a method to estimate recharge which uses ground-surface information instead of long-term groundwater monitoring data. They used the topography, hydrogeology, and land cover of the site to estimate recharge. The method obtained a conservative approximation for recharge, but recommended that the estimate should be refined with other methods [*Cherkauer and Sajjad*, 2005]. Similarly, Ranjan et al. [2005] estimated recharge based on land use and climatic factors. They then used the estimated recharge amounts as inputs into a numerical groundwater model.

Researchers have not only studied the effect of land use/land cover on groundwater resources, but they have also studied the effect of land use/land cover *change* on aquifer systems. Scanlon et al. [2005] completed a study on the Southwestern United States to test their hypothesis that the land use/land cover (LU/LC) change of a natural rangeland into an agricultural ecosystem will affect the groundwater recharge and chloride mass balance. By examining three types of LU/LC they were able to detect significant differences in mean chloride concentrations as well as mean matric potential. Information gained from this study and similar studies suggest that groundwater resources can be somewhat managed through modification of LU/LC [*Scanlon et al*., 2005].

Another factor that has the potential to significantly affect groundwater resources is climate change. Since the mid-twentieth century carbon dioxide levels in the atmosphere have been steadily rising. If this phenomenon continues, many researchers believe that the global and local climate characteristics will be significantly altered [*Ranjan et al*., 2006]. This trend has been termed climate change, and would likely have large effects on the hydrologic cycle around the world. Increased atmospheric carbon dioxide levels would lead to an increased "greenhouse effect," in which solar radiation is trapped by the increased gases. This results in increased temperatures, which in turn affects evapotranspiration, precipitation, and soil moisture.

While increased temperatures would likely lead to an overall global increase in precipitation, it will lead to both increases and decreases on the local scale, depending on the location and topography of the region [*Ranjan et al*., 2006]. There have been numerous studies done which assess the impact of climate change and decreased precipitation on fresh groundwater resources. Ranjan et al. [2006] used the high and low emissions scenarios from the Hadley Centre climate model to predict the change in climate that should be input into their

groundwater model. Among the five locations modeled, which were located around the globe, all but one showed increasing losses of fresh groundwater resources.

Drought due to climate change could not only cause a decrease in groundwater recharge, but also a decrease in water levels in surface reservoirs that would force more of a demand onto groundwater. This situation was studied by Mollema et al. [2010] for Terceira Island in Portugal. The water demands of the island are currently met by rain fed springs, but with increased droughts they may need to begin to exploit the freshwater lens that underlies the island. The study was devoted to understanding the size, characteristics, and limitations of the lens, so that it could be exploited if necessary.

Another effect of climate change is sea-level rise. Sea level rise is caused by changes in atmospheric pressure, expansion of ocean water, and the melting of ice sheets and glaciers [*Sherif and Singh*, 1999]. The effects of sea level rise on saltwater intrusion have been studied by Webb and Howard [2011], Loáiciga et al. [2011], and Chang et al. [2011]. Webb and Howard [2011] found that the hydraulic properties of the aquifer played a large role in rate of intrusion. Loáiciga et al [2011] found that groundwater pumping had a much larger effect on saltwater intrusion than sea level rise. Chang et al. [2011] found that sea level rise does not have a long-term impact on confined aquifers. While the sea level rise will initially cause saltwater intrusion, a reversal effect will drive the wedge back out over time [*Chang et al*., 2011].

3. Recharge and land cover estimation for the southeastern United States

This section discusses the process used to relate land cover type to groundwater recharge in the Southeastern U.S. It discusses how land cover type and groundwater recharge values were quantified as well as the methods used to find a relationship between the two factors.

3.1 Background

In order to obtain a relationship between groundwater recharge and land cover type, seven sites were examined in the Southeast region. These sites were mostly located in coastal Alabama and Florida, although two were located more inland than the others (Figure 3-1). They are all located in un-consolidated and semi-consolidated shallow unconfined aquifers. The regional aquifers that the well sites are located in are the Southeastern Coastal Plains aquifer, Coastal Lowland aquifer, and the Floridian Sand and Gravel Surficial aquifer. The aquifers were all unconfined with similar soil types, and the aquifer characteristics of the various regional aquifers are similar. Therefore, after a small adjustment to specific yield values based on the site's soil characteristics, we can assume differences in recharge are due to land cover differences.

The sites labeled later in the research as FL1, FL2, and FL4 are in the Gonzalez/Ensley/Pace area of Florida. Site FL3 is located in Pensacola, FL. The site labeled as Covington was located in Covington County, AL, near Opp, AL. The site labeled Baldwin was located in Baldwin County, AL, near Fairhope, AL. The site labeled Montgomery was located in Montgomery, AL.

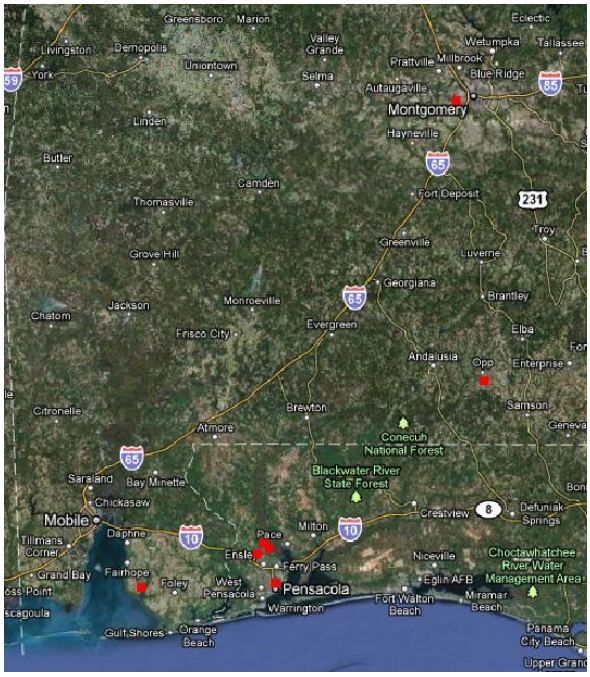

Figure 3-1. Map of well locations used in this study.

3.2 Research objectives

The primary research objective of this section was to determine whether a relationship could be derived between the groundwater recharge values and the land cover characteristics for the seven sites in the Southeast. A significant relationship between the two factors would indicate that land cover and land use is an important aspect in relation to groundwater resources and the management of these resources. In an effort to obtain this relationship between groundwater recharge and land cover characteristics, both continuing abstractions, which is the amount of water taken into the soil once ponding begins, and infiltration were examined for the seven sites.

This effort is valuable because whether or not a relationship can be derived between groundwater recharge and LU/LC for the particular sites chosen is an interesting issue that is worth investigating. If a relationship is found, the same concepts and methods could be later

applied to find recharge in areas where there is no groundwater elevation data, but there is land cover data. Specifically, the same methodology could be applied for Dauphin Island. As already discussed, groundwater recharge is an important input for groundwater modeling. Dauphin Island does not have publically available groundwater data from non-pumping wells, therefore; a relationship between land cover and recharge would enable us to use the island's land cover data to calculate recharge.

Research methodology for this chapter is divided into three distinct parts. The first step was estimating groundwater recharge for the seven sites. This was done using daily groundwater level data from seven USGS groundwater monitoring wells. The recharge was calculated for a year-long time period and summed to obtain an annual cumulative recharge value. A year-long time period was used to eliminate the effects of differences in recharge rates due to seasonal factors, such as changing evapotranspiration patterns in different seasons. The second section describes how the Curve Number (CN) was used to relate recharge to land-cover and the third part describes how the CN was calculated for each site.

3.3 Recharge estimation

This section discusses the methods examined for recharge estimation at the seven sites. The results from the various methods are shown for a few of the sites in order to illustrate the methods and then one method was selected as the best method for this study.

3.3.1 Methods and input data

The Water-Table Fluctuation (WTF) method, which was previously discussed, was the method used to estimate cumulative recharge for the year-long time periods for each site. Since the WTF method requires the peak water table rise during the recharge period, or ΔH , as input to calculate recharge, multiple methods were used and compared to generate ΔH values.

Perhaps the simplest method to measure groundwater recharge is the graphical method. Using a hydrograph for a given site, which has groundwater elevation vs. time, the graphical method can be completed manually. An example hydrograph for Baldwin County, AL is shown in Figure 3-2. For each hydrograph spike, the height of the increase was measured from the location the antecedent recession curve would be extrapolated had the spike not occurred. Prior to extrapolating the curves, it is useful to examine the entire data set in order to get an estimate for recession rates [*USGS*, 2008]. The measured heights were multiplied by the specific yield values for each site. The recharge amounts were found, and Table 3-1 lists the values used for specific yield in these calculations. The specific yield values were obtained by examining the soil type at each of the seven sites. By summing the spikes for the year-long time period, the cumulative recharge was found. The graphical method is prone to subjectivity when performed manually as each person would likely draw the recession curve differently.

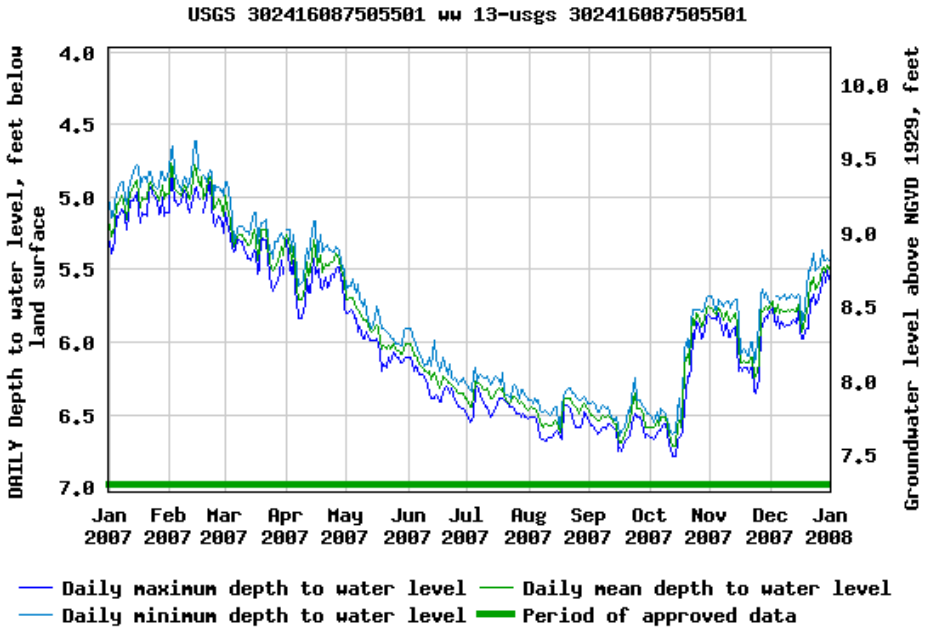

Figure 3-2. Example of a hydrograph from the Baldwin County, AL well.

The second method of recharge estimation that was used was the Master Recession Curve (MRC) approach to the WTF method. Developing a MRC is a similar idea to the graphical method, but instead of manually extrapolating the hydrograph recession beneath each positive fluctuation a MRC is developed to calculate the antecedent recession curve. A MRC is a water-table recession hydrograph that is unique to the evaluated site. For a specific site it represents the average behavior of a declining water-table [*Heppner and Nimmo,* 2005]. A MRC can be developed using MATLAB [*Heppner and Nimmo,* 2005] or in Excel.

For this project, Excel was used to find the MRC for the various sites and the general method is described in Heppner and Nimmo [2005]. In this method time and water level data for the desired site is required. This data is used to calculate the water-table fluctuation rate for each time step. The water table fluctuation rate is the change in water table elevation divided by the change in time for each time step. The water-table fluctuation rate is plotted on the y-axis against the water-table elevation on the x-axis.

This method assumes that at a certain water-table elevation, there will be a characteristic water-table decline rate. Due to this, we would expect a linear relationship when the data is plotted. However, due to various factors, this may not always be the case. The type of MRC that can be created is selected based on the trend in the plotted data. In addition to a linear method, power and bin averaged may also be used [*Heppner and Nimmo,* 2005]. The bin averaged method was used for this research, so it will be discussed more in depth.

The bin-averaged method is best suited for large data sets that may have an irregular pattern when initially plotted [*Heppner and Nimmo,* 2005]. After inspecting the range of elevation values from the lowest to highest observed water-table elevations, the user decides on an appropriate number of bins, which are ranges of elevation, based on the elevation range. The

total range is then divided into equally spaced bins of elevation range. As the elevation levels are placed into the appropriate elevation bins, the corresponding decline rates are placed in the bins [*Heppner and Nimmo*, 2005]. Each elevation and decline rate bin is averaged and plotted. Once these values are plotted the relationship usually appears more linear and a trend line equation can be obtained that is specific for the particular site and time period.

The equation obtained represents the MRC. For example, a hypothetical MRC may be represented by the equation $y = mx + b$. Given a dataset that contains time as well as groundwater elevation values, the equation can then be used to find total recharge. For each time step, the groundwater level in from the previous time step is used as the x-value, and the y-value is the predicted groundwater level from the Master Recession Curve. By subtracting the predicted value from the actual value, ΔH is obtained. This ΔH is subsequently multiplied by the specific yield of the aquifer to obtain the recharge.

The third method used to obtain ΔH and thus cumulative recharge, mimicked the RISE program developed by Rutledge [2007]. This program calculates the daily rise in a given observation well by calculating the amount of water level increase from the previous day. The value for that day is set to zero if the difference is negative, but it is considered groundwater recharge if the difference is positive [*Delin et al*., 2006]. Daily recharge values are evaluated using this program and the positive recharge values are summed to obtain a cumulative annual rise in the aquifer (cumulative ΔH). This estimate was multiplied by the specific yield of the subsurface material to obtain the cumulative annual recharge.

Specific yield values were varied based on the soil material of the site. Soil data was obtained from the SSURGO database and imported into ArcMap program as a shapefile. The well locations were marked on their latitude and longitude. Using the soil types of the region, a

specific yield value was assigned to each site. The values that were used for specific yield were based on values from Fetter [2001], Nachabe [2002], and estimations based on these ranges and soil types. The specific yield was used to multiply ΔH to obtain the daily and cumulative annual recharge for each site. Table 3-1 shows the values specific yield values of each site:

Table 3-1. S_y values used for recharge estimations.

Location	Soil type	S_y
FL1	Sand, Loamy sand, Sandy loam	0.13
FL2	Sandy loam, Loamy sand	0.13
FL3	Sandy loam	0.13
FL4	Sandy loam, Loamy sand	0.13
Covington	Loamy sand, Loamy fine sand	0.12
MGM	Fine sandy loam	0.12
Baldwin	Loamy fine sand, Loamy alluvial	0.15

Since the RISE approach does not take into account the hydrograph recession that would have occurred if recharge had not taken place, this method generally underestimates actual recharge. While this is not ideal, it is acceptable for our study because all of the sites will be underestimated so it will not skew the relationship found between the recharge values and land cover. It does, however, slightly underestimate groundwater recharge when the estimate is used for future predictions. This is actually ideal, because it will result in a more conservative estimation, which is usually desired when dealing with groundwater resources management. For this research, this method was done using MS Excel instead of the actual RISE program but an identical protocol was followed to obtain the annual recharge estimates for each of the seven sites.

3.3.2 Results

The results for bin-averaged MRC obtained from Baldwin, AL and Montgomery, AL are shown in Figures 3-3 and 3-4. The Baldwin County MRC had a relatively linear relationship,

while the Montgomery MRC did not. The y-axis, labeled "rate of decline," is the change in water table elevation divided by the change in time for each time step.

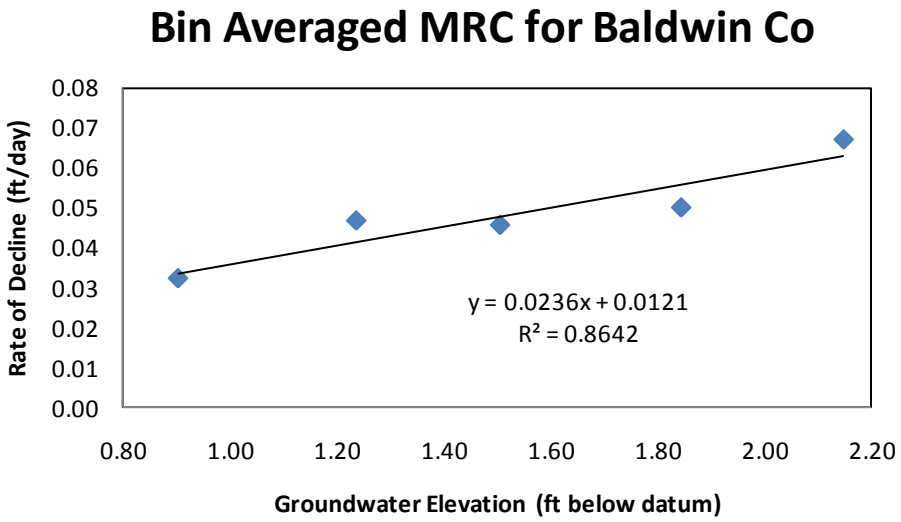

Figure 3-3. Bin averaged MRC for Baldwin County, AL.

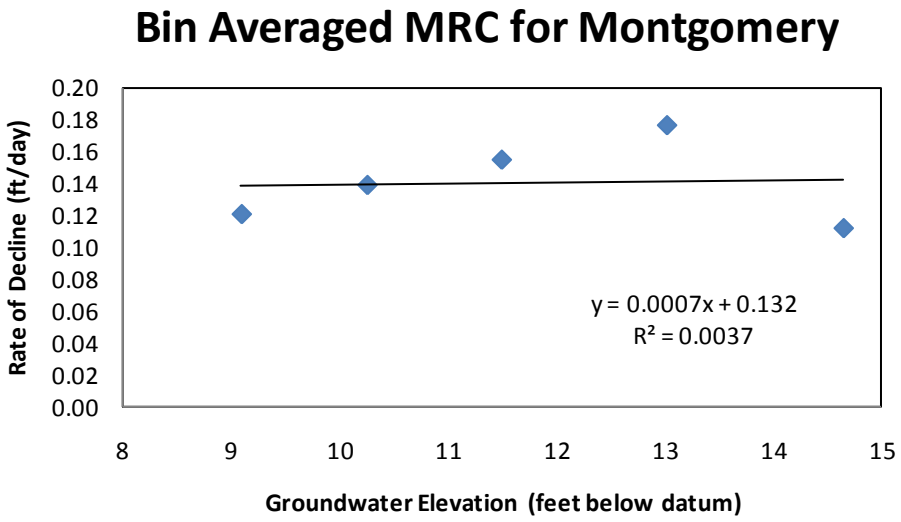

Figure 3-4. Bin averaged MRC for Montgomery, AL.

Figure 3-5 is from Delin et al. [2006] in which the graphical, MRC, and RISE approaches were used to calculate percent of water recharged in a Minnesota site. Delin's figure is shown as a comparison to Figure 3-6, which we obtained by using the same methods for recharge estimation described in Delin's study and applying them to Baldwin County, AL. As shown, the Baldwin County estimates that were obtained have larger values for percentage recharged, but this would be expected due to site characteristics. The important aspect to note in this comparison is that the main trends are similar, with the MRC estimate being generally the largest, followed by the graphical and RISE approach respectively.

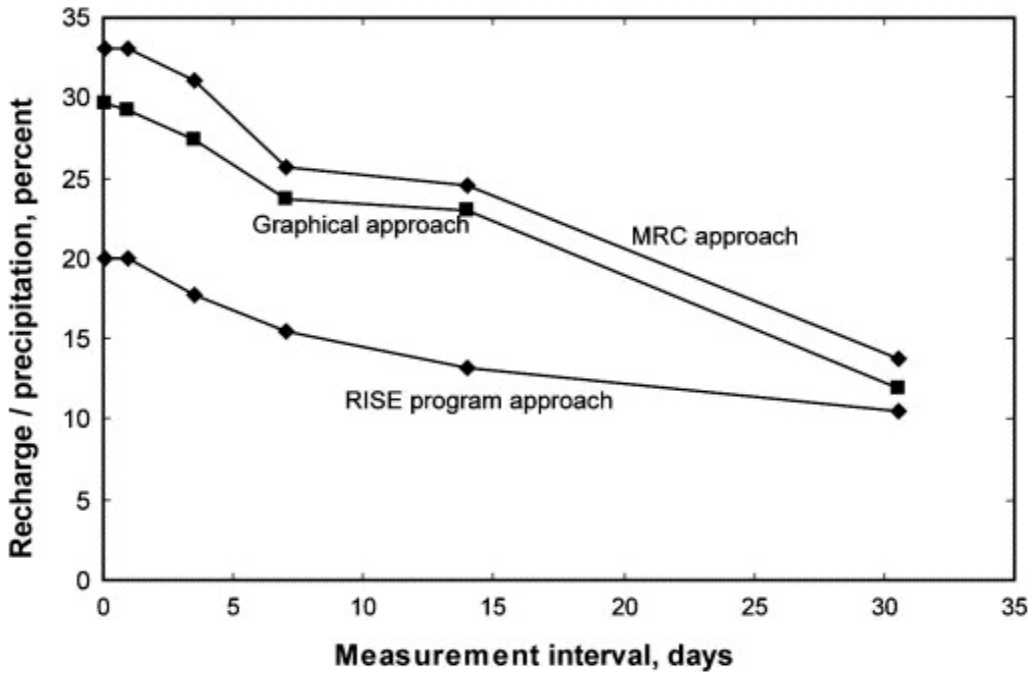

Figure 3-5. Comparison of recharge methods in Minnesota [Delin et al, 2006].

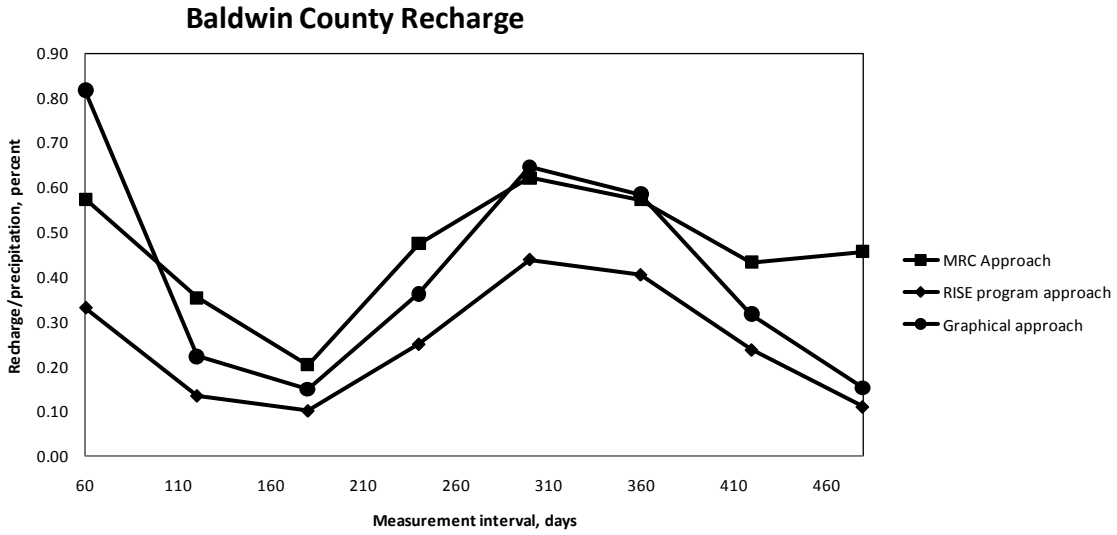

Figure 3-6. Comparison of recharge methods in Baldwin Co, AL.

Table 3-2 summarizes the values obtained for cumulative recharge at each site using the RISE method.

Table 3-2. Recharge values using the RISE method.

Site Location	Dates Evaluated	Rise Recharge Estimate [ft]	Precip [ft]
FL1	7/1/1981-6/30/1982	1.75	3.79
FL2	10/1/1983-9/30/1984	3.60	4.94
FL3	9/7/1983-9/6/1984	1.21	5.36
FL4	1/15/1980-1/14/1981	2.10	4.05
Covington Co	5/1/2007-4/30/2008	3.53	4.56
Montgomery Co	1/27/1990-1/26/1991	1.81	4.13
Baldwin Co	11/1/2007-10/31/2008	1.63	6.28

3.3.3 Observations

The graphical method was deemed inefficient and subjective because different results are obtained by different users of the method, hence the results of this method will not be used further in this study. For some of the sites evaluated in this study, the line of best fit generated using the MRC method had a high R^2 value (Figure 3-2) and the relationship would have been

acceptable for use in estimating recharge. For other sites, however, the relationship had a relatively low R^2 value (Figure 3-3) and the relationship was deemed insignificant and not acceptable for use in this study. This is most likely due to other factors causing a difference in recharge rate, such as antecedent moisture conditions, the Lisse Effect, and heterogeneities in the subsurface material. Due to this, the RISE method of recharge estimation was employed in order to quantify the amount of annual recharge at the seven sites, and the RISE estimates were used in the following sections of this chapter.

3.4 Quantify LU/LC effects on Recharge

This section discusses the method used in an attempt to relate LU/LC to the amount of water recharged into the aquifer at each of the seven sites.

3.4.1 Study methodology and input data

The Soil Conservation Service Curve-Number (SCS-CN) method was developed by the United States Department of Agriculture-Soil Conservation Service (USDA-SCS) in the 1950's. The SCS-CN method can be used to predict flood-flow volumes for ungauged watersheds for runoff generating rainfall events [*Lyon et al.*, 2004]. Accumulated rainfall (P) and accumulated runoff (Q) are important variables in the SCS-CN method. Therefore, the general form of the SCS-CN equation is as follows:

$$Q = \frac{(P - I_a)^2}{P - I_a + S} \tag{3-1}$$

where Q is runoff [in], P is the event precipitation [in]; I_a is the initial abstractions [in]; and S is the potential maximum retention after runoff begins [in]. This equation is only valid if $P>I_a$. If this precipitation is not greater than the initial abstractions, Q=0. The CN is used to calculate both S and I_a [*Michel et al.*, 2005]. The equations for both of these variables will be outlined

below. The CN is a function of LU/LC, Hydrologic Soil Group (HSG), and the Antecedent Moisture Condition (AMC) of the soil.

Once the appropriate adjusted CN was found for each day in the precipitation record, it was used along with daily precipitation records for the area to calculate the continuing abstractions, Fa, for events that qualify. As will be illustrated in the following calculations, Fa is calculated using both CN and precipitation, so it takes into account land cover type as well as precipitation events. This makes it a sensible value to use in developing a relationship between recharge and LU/LC type.

The value of initial abstractions, or I_a, is calculated to determine which events qualify as large enough to generate continuing abstractions. I_a includes interception by vegetation and water that ponds on the surface [Lecture Notes, *Kalin*, 2010]. In order to obtain I_a, the adjusted CN value was used to first calculate S using equation 3-2. The method and calculations for obtaining the CN will be described in Section 3.5:

$$S = \frac{1000}{CN} - 10 \qquad (3\text{-}2)$$

where S is the potential maximum retention after runoff begins [in]; and CN is the curve number [dimensionless].

With S, the value of the initial abstraction of water during a rainfall event could be calculated using the following equation:

$$I_a = 0.2 * S \qquad (3\text{-}3)$$

The calculated I_a values were used to determine which rainfall events were large enough to generate continuing abstractions. As already stated, for each rainfall event, the total amount of

precipitation must be larger than or equal to $0.2 * S$ in order for the event to generate continuing abstractions. The values of I_a and S were subsequently used to calculate the value of runoff, or Q, using equation 3-1 that was presented above.

Using the obtained values the continuing abstractions can be calculated through equation 3-4:

$$F_a = P - I_a - Q. \qquad (3\text{-}4)$$

The sum of the F_a values for the annual period for each site were plotted against the recharge values for the respective sites on the same scatter plot (Figure 3-7) to seek a relationship between recharge and F_a . If a relationship is found between recharge and F_a, this relationship could be related back to land cover type as described above. With a relationship between the two factors, recharge could be calculated using the average CN of a particular site.

As an alternative, a relationship between infiltrating depth and recharge was also sought to see if a relationship between LU/LC and recharge could be developed. First interception depth was calculated using the following equation [*Bras*, 1990] :

$$I = a + b * P^n \qquad (3\text{-}5)$$

where I is interception [in]; $a, b,$ and n are empirical values that vary with vegetation type; and P is the amount of precipitation [in].

Interception is the amount of rainfall that is intercepted by vegetation before it is able to reach the ground [*Fetter*, 2001]. Once interception was calculated, infiltration was estimated by subtracting Q and interception from total precipitation for each rain event.

The values that were calculated for each site were plotted against the recharge values for the respective sites on the same scatter plot to find a relationship between recharge and land cover

(Figure 3-8). Additionally, the data points from a few of the sites seemed less reliable and these locations were removed from the analysis. The relationship was observed for the time period of December to April (Figure 3-9). This time period was examined because it can be assumed that the least evapotranspiration would be occurring during this time period, causing the infiltration values to be greater. The sites that were not included in this last plot were the Montgomery, AL site and the Baldwin County, AL site since Montgomery is more inland than the others and the Baldwin County site could have been tidally influenced as it is very close to the coast.

3.5 Land cover analysis and curve number calculations

This section details the method used to utilize land cover/land use data in order to calculate the curve number for a given land area. Average curve numbers were obtained for each of the seven study sites. As previously explained, the SCS-CN method has been widely used for years as a tool to calculate the volume of surface runoff for rain events, reflecting factors such as LU/LC effects [*Mishra and Singh*, 2011].

3.5.1 Study methodology and input data

After an annual recharge estimate was found using the RISE estimation method for the seven sites, the next step was to quantify land cover type for each site. Land cover data was obtained from the National Land Cover Database (NLCD). Using the latitude and longitude of the well locations, data was downloaded for the region surrounding the well. Landcover data downloaded from NLCD was imported into ArcMap and cropped. An ellipsoid shaped boundary with 100 meters from the well to the side of the ellipse and 200 meters to the top of the ellipse was applied around the well. The orientation of the ellipse was decided by the direction of flow on the surface, as it was assumed that the shallow subsurface flow approximately mimics the direction of the surface flow.

The land cover map was cropped and a measured grid was applied with grid cells of 20 m x 20 m (Figure 3-6). Each grid cell was assigned a land cover type that occupied the majority of each cell.

Figure 3-7. Land Cover/Land Use sites for FL Site #3, Baldwin, Covington, and Montgomery, AL.

A curve number was assigned to each grid based on land cover type. The curve number, CN, is an empirical value that is used in predicting runoff or infiltration and is a function of hydrologic soil group, land cover type, land cover treatment, and hydrologic condition such as antecedent moisture condition [*USDA SCS TR-55 Manual*, 1986].

The curve number for each land cover type depends on the hydrologic soil group of the soil in area. The hydrologic soil group indicates the soil's tendency for infiltration or runoff. The hydrologic soil group for each soil type was obtained from the NRCS Web Soil Survey

(***websoilsurvey****.nrcs.usda.gov/)*. Using the hydrologic soil group, a CN value was assigned for each grid.

Next, the distance between the monitoring well and the center of each cell was calculated. The inverse of the distances were used to weight the CN of each cell, and an average CN was obtained for each well site using the weighted CN values.

In order to accurately use the average CN, the antecedent moisture condition (AMC) had to be taken into account. The average CN that was calculated in the previous step is for normal conditions (CN_2) and a CN_1 can be found for a dry AMC, while conversely a CN_3 is used for a wet AMC. Table 2-2 outlines the antecedent moisture values that dictate which CN value should be used [*Chow et al*., 2005]:

Table 3-3. Values used to determine AMC.

AMC	Total 5-day antecedent precipitation [in]	
	Dormant Season	Growing Season
I	< 0.5	< 1.4
II	0.5 to 1.1	1.4 to 2.1
III	> 1.1	> 2.1

Daily precipitation data was obtained from the National Climatic Data Center (NCDC) for the same year-long time period for each site in which the recharge measurements were made. Table 3-4 lists the appropriate weather station ID used for each of the wells, and the approximate distance from the weather station to the groundwater well.

Table 3-4. Approximate distance from well to weather station

Site Name	Well ID	Weather Station	Distance: well to station [mi]
FL 1	USGS303610087165001	Pensacola Reg Airport	13
FL 2	USGS303558087155501	Pensacola Reg Airport	13
FL 3	USGS30283008711390	Pensacola Reg Airport	1.25
FL 4	UGSG303614087190901	Pensacola Reg Airport	13
Covington Co	USGS311319086153601	Andalusia, AL	18
MGM Co	USGS322047086214301	MGM Airport	6
Baldwin Co	USGS302416087505501	Fairhope, AL	12

Using this data, the AMC for each day in the record was calculated by summing the five previous day's precipitation amounts. Based on this sum for each day, the CN number was calculated accordingly using equations 3-6 and 3-7 for wet and dry conditions respectively [*Chow et al*., 2005]:

$$CN_1 = \frac{4.2CN_2}{10 - 0.058CN_2}(dry) \tag{3-6}$$

$$CN_3 = \frac{23CN_2}{10 + 0.13CN_2}(wet). \tag{3-7}$$

3.5.2 Results

The Table 3-5 shows the average calculated values of CN. As illustrated, the values that were calculated vary widely from site to site, depending on the land cover type. For example, the site labeled FL3, which has a very large CN is located in the Pensacola Regional Airport. In contrast, the site labeled FL1 is located in an area that is heavily forested.

Table 3-5. Calculated average CN values.

Site Location	Calculated Avg CN
FL1	50
FL2	59
FL3	93
FL4	76
Covington Co	84
Montgomery Co	77
Baldwin Co	78

Figure 3-8 is the scatter plot of the seven site's cumulative recharge values plotted against each site's cumulative continuing abstraction values.

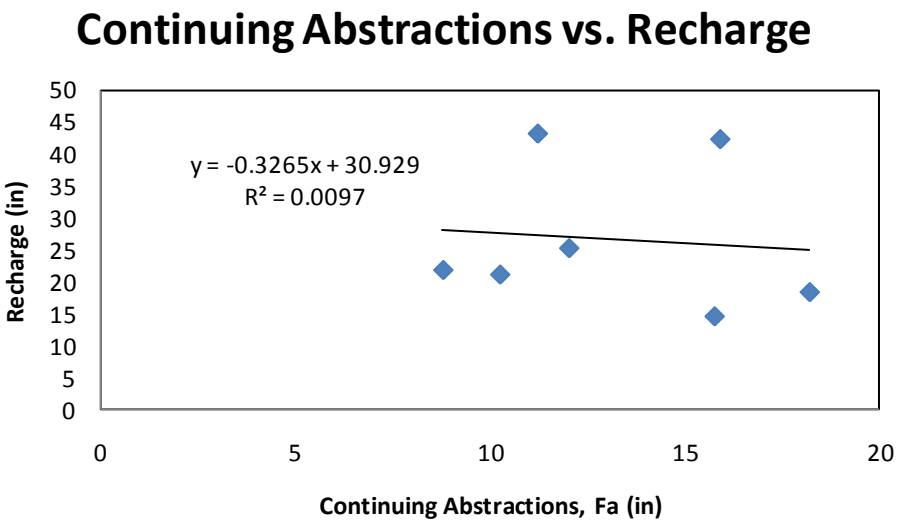

Figure 3-8. Recharge versus continuing abstractions.

Figure 3-9 shows the scatter plot of cumulative recharge and cumulative infiltration for each site.

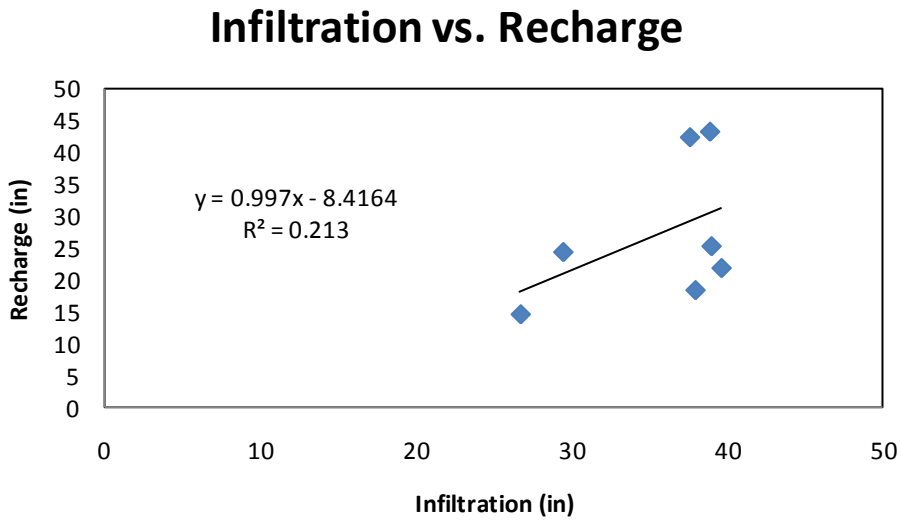

Figure 3-9. Cumulative Infiltration vs. Cumulative recharge

Figure 3-10 shows the scatter plot of cumulative recharge plotted against cumulative infiltration at five of the sites for December to April. As stated earlier, these calculations were done using only data from December to April, as the least evapotranspiration occurs during these months, and the sites of Baldwin County, AL and Montgomery, AL were not used in an effort to obtain a better relationship. As stated previously, these sites were left out since Montgomery is more inland than the other sites and the Baldwin County site could have been tidally influenced.

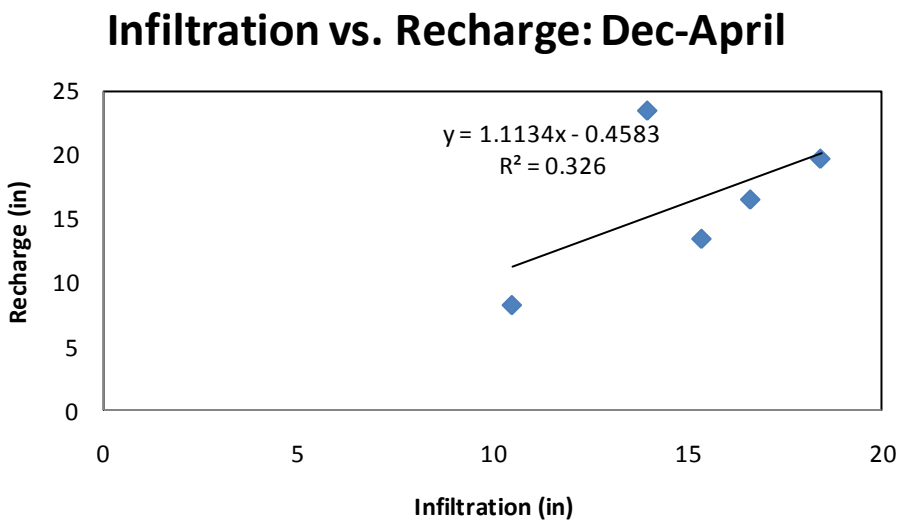

Figure 3-10 Cumulative Infiltration vs. Cumulative Recharge for December-April

3.5.3 Discussions

As illustrated in the figures, no significant linear relationship was found between F_a and recharge or the infiltration values and recharge. The seasonal investigation of infiltration and recharge did not yield any significant results either. This is likely due to a number of confounding factors. Some factors that may have contributed to an unclear relationship between land use and recharge could have been due to some of the water-tables being deeper than others, unpredictable heterogeneities in the soil profiles causing flow impediment or changing specific yield values, or the Lisse effect, which occurs when air is trapped by recharging water causing the water level to be at a higher level than it would appear if only the recharged water height was taken into account. Many of the recharge values calculated using the RISE method seemed larger than would be expected. For example, there was an instance that the recharge value exceeded the infiltration value for the same site, which is physically impossible. This would suggest that there were factors influencing the recharge estimate. Also, it is possible that the area

of land taken into account for the CN calculations was too large, although the weighting scheme should have taken this into account.

Due to the fact that there was no clear relationship found between land cover and recharge in this study, this method was not used to calculate average annual recharge on Dauphin Island with land cover data. Instead, recharge estimates were obtained by directly applying the Soil Water Assessment Tool (SWAT) which will be explained in further detail in Chapter 5.

4. Geography and ground water issues of Dauphin Island

This chapter provides necessary background information on Dauphin Island and also summarizes the island's current water issues.

4.1 Location, size, and morphology

Dauphin Island is a small barrier island located between the Mississippi Sound and the Gulf of Mexico about 4 miles off the coast of Mobile County, Alabama (Figure 4-1). The island is shaped like an oval on the east end, with a thin strip of land coming off the oval to make up the west end (Figure 4-1). The east end oval is about 1.5 miles wide at its widest and 3 miles long. The thin strip of land that makes up the west end is about 12 miles long and 0.5 miles wide. In total, Dauphin Island is about 6.3 square miles in size. Elevation on the island mostly varies between 5 to 15 feet but can reach up to 40 feet at the locations of the island's sand dunes [*Chandler*, 1983].

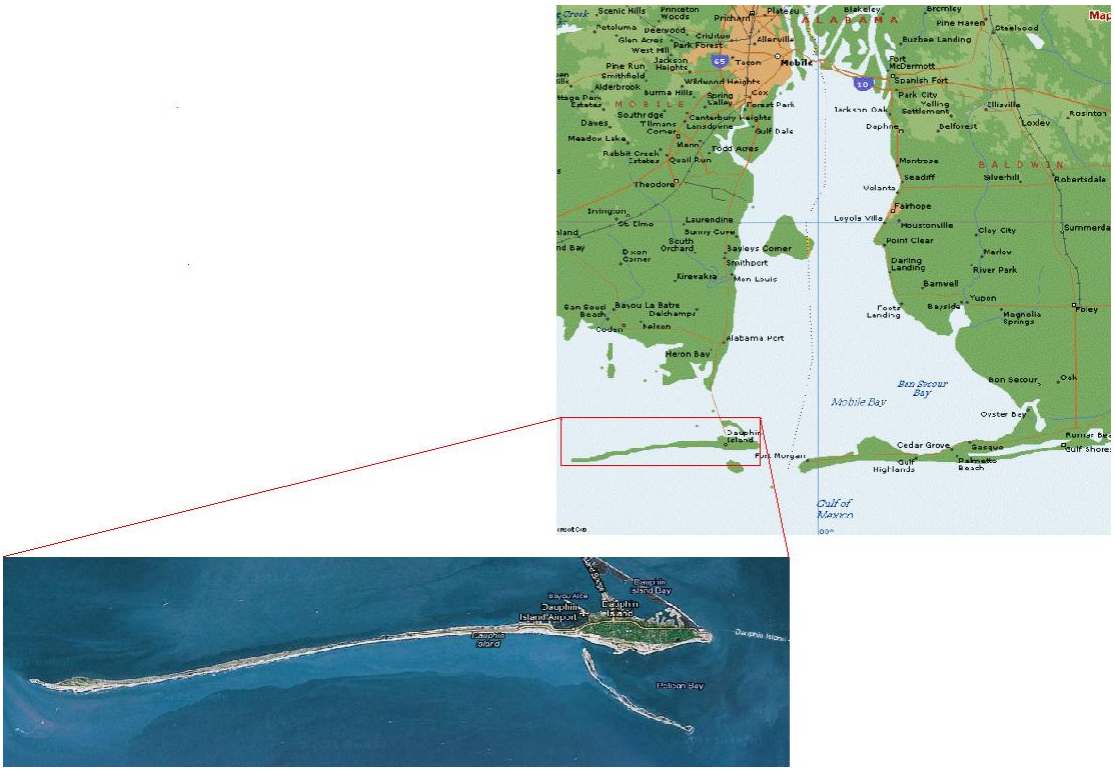

Figure 4-1. Map of Mobile Bay and Dauphin Island.

Since Dauphin Island is a barrier island its morphology is constantly changing as a result of coastal winds, tides, and currents. The shoreline of the island has greatly varied throughout history, mostly due to longshore drift and hurricanes. Longshore drift, which is the process of sediment transport along the coast, is likely responsible for the formation of the long,thin sandy-spit extension on the west end of the island. Vegetation on this island is important as it prevents erosion and promotes accretion in some areas. Additionally, the marsh areas are nutrient processing sites [*Chandler*, 1983].

4.2 Climate and tides

The climate of Dauphin Island is significantly influenced by the Gulf of Mexico and is warm to subtropical. Temperature variations on Dauphin Island in 2008 are shown in Figure 4-2. Monthly average temperature variations are less than 20°F from the annual mean [*Chandler*, 1983]. The annual average maximum temperature is 74.8 °F and the average minimum temperature is 63.1 °F.

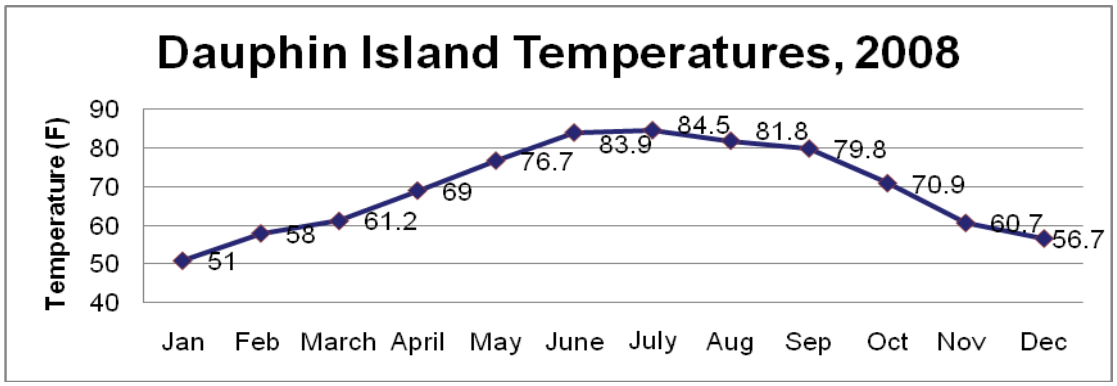

Figure 4-2. Monthly temperatures for Dauphin Island in 2008.

The island receives on average 163 cm (62.4 inches) of rain per year. The precipitation record for Jan 1995-Dec 2005 is shown in Figure 4-3.

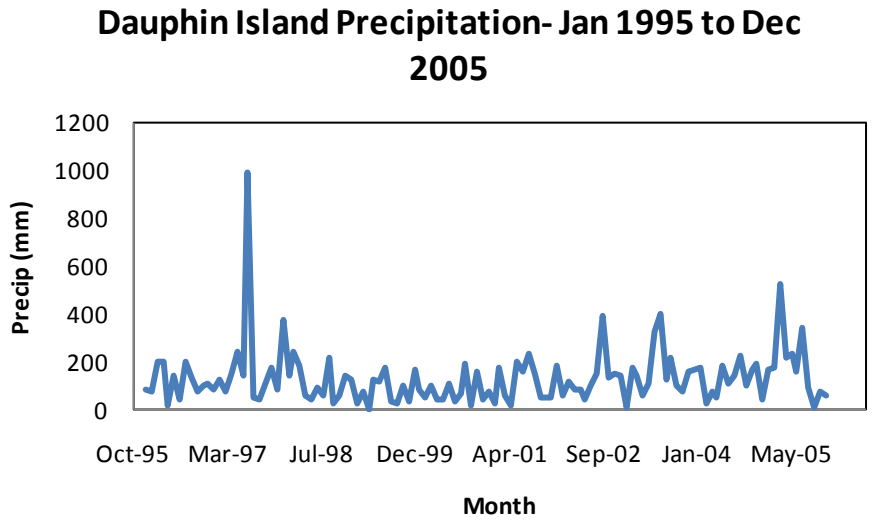

Figure 4-3. Monthly Precipitation for Dauphin Island from January 1995-December2005, data from NCDC

Because of its location in the Gulf of Mexico the island has been hit numerous times by hurricanes, including Hurricane Katrina, which brought extensive damage to large portions of the island. The tides on Dauphin Island are diurnal, with a high tide and low tide occurring once a day, and average about 1.5 feet [*Chandler*, 1983].

4.3 Soil types

As illustrated in Figure 4-4, the majority of the soil types on the island are sands or loams, both of which have a relatively high permeability. The Hydrologic Soil Group (HSG) of a land area indicates the "minimum rate of infiltration obtained for bare soil after prolonged wetting" [*USDA SCS TR-55 Manual*, 1986]. Dauphin Island has an interesting HSG condition. Dauphin Island is generally classified as A/D because of the relatively high water-table on the island. Although the soil types on the island would generally be classified as A, the high water-table on

the island creates some drainage problems. Therefore, the HSG is A/D indicating that drained soil is type A and undrained soil is type D [*USDA SCS TR-55 Manual*, 1986].

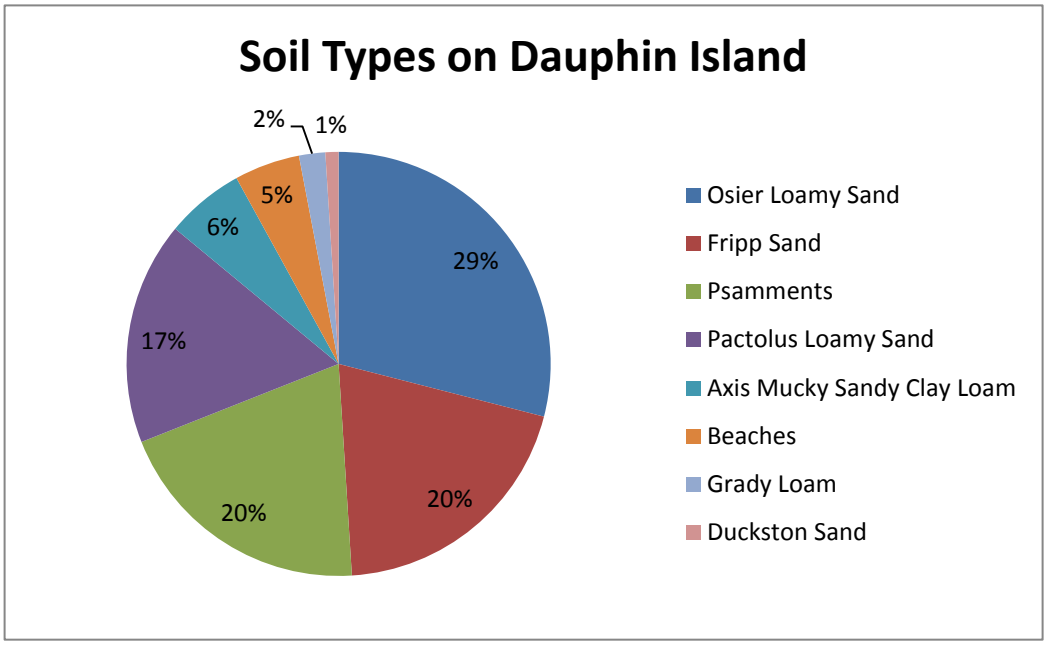

Figure 4-4. Soil types on Dauphin Island from USDA NRCS Soil Survey Database.

4.4 Geology

Dauphin Island is located in the Coastal Lowland Aquifer system. There are three distinct hydrogeologic units underlying Dauphin Island. These units are the Pleistocene-Holocene interval, shallow Miocene Siliclastic interval, and the deep Miocene Siliclastic interval. These units are considered hydraulically separate for a number of reasons: they outcrop in entirely different locations, they are separated by confining clay layers, and water quality parameters such as concentration of certain dissolved solids are different [*O'Donnell*, 2005].

As already noted, Dauphin Island's main source of water resources is the shallow aquifer underlying the barrier island. While the island does possess two relatively small reservoirs, they do not have the capacity to meet the freshwater demands of the island. The island's shallow

aquifer consists of a thin layer of Holocene sand, which is underlain by a Pleistocene unit known as the Gulfport Formation. The aquifer is approximately 28-42 feet thick with a thick layer of marine clay at the base. The water in Dauphin Island's aquifer is generally low in chloride content except near the island's coast. Recharge to the aquifer occurs through rainfall. Freshwater is lost from the aquifer due to seepage to surface water, evapotranspiration and pumping [*Kidd and Moody*, 1987].

As discussed, the top unit visible from the ground level is the Water-Table Aquifer. This aquifer extends about 42 feet below ground level and is composed of fine to coarse grain sand [*O'Donnell*, 2005]. A layer of clay underlies this aquifer and separates it from the Shallow Sand Aquifer, which occurs at about 70 feet below ground level and is composed of very fine to very coarse grain quartzose sand [*O'Donnell*, 2005]. The top surficial aquifer is hydraulically separate from the other aquifers located below it.

There are three layers of the Shallow Sand Aquifer, each of which has a clay layer underneath. Another clay layer underlies the Shallow Sand Aquifer. Beneath this clay layer is the Deep Sand Aquifer, which begins at about 441 feet below the surface.

The Water-Table Aquifer and the Shallow Sand Aquifer are the only units deemed potential sources of freshwater without rigorous treatment. The water pumped from the Deep Sand Aquifer has a chloride concentration too high to be used for human consumption [*O'Donnell*, 2005]. There are eight shallow wells drilled into the Water-Table Aquifer and two wells tapping the Shallow Sand Aquifer. There has also recently been a well drilled into the Deep-Sand Aquifer. Water pumped from this well will be treated by reverse osmosis before it is distributed to the island's customers [*O'Donnell*, 2005]. In this research, only the Water-Table Aquifer and its wells will be examined. In Figure 4-5 shown below, the Water-Table Aquifer is shaded.

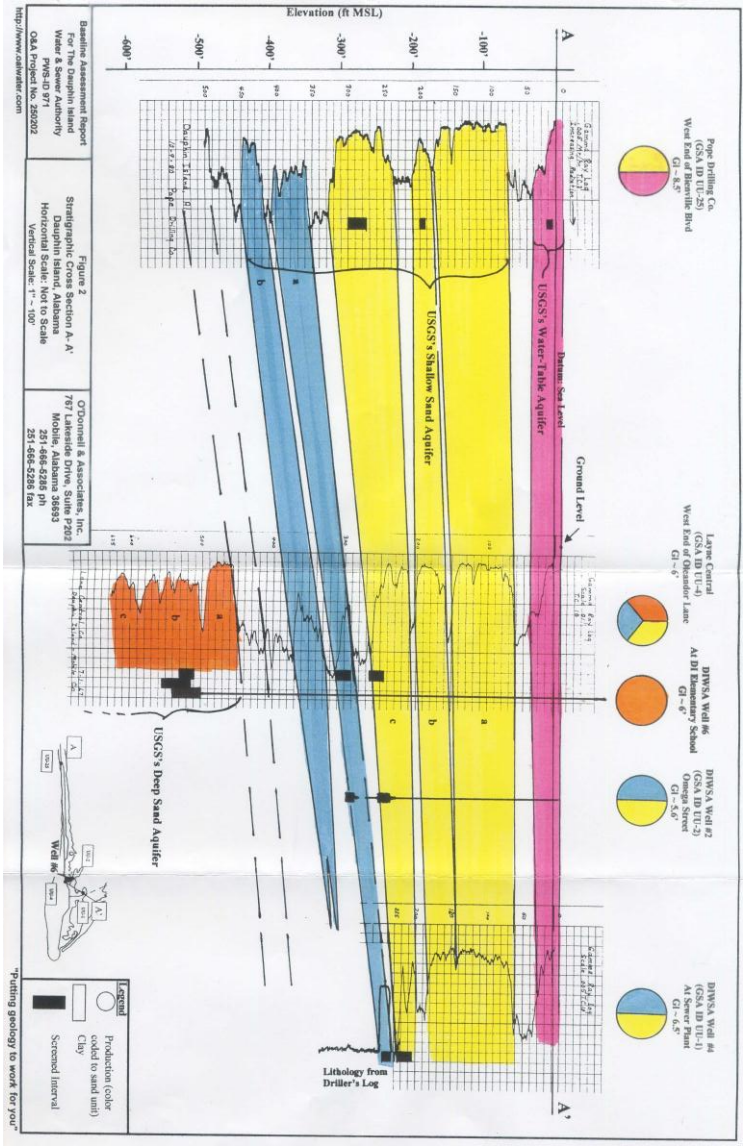

Figure 4-5. Details of the layering of the aquifers beneath Dauphin Island O'Donnell, 2005].

4.5 Land Use/Land Cover

Land Cover/Land Use (LC/LU) data was obtained from the National Land Cover Database for the year 2001. As illustrated in Figure 4-5 and Table 4-1 the island is mostly in various stages of development, with some forests and wetland areas. As previously discussed, the sandy soil types on the island generally allow for quick infiltration. However, due to the large amount of residential development on the island and high water table, there is the potential for considerable runoff in large rain events, resulting in a relatively high average curve number.

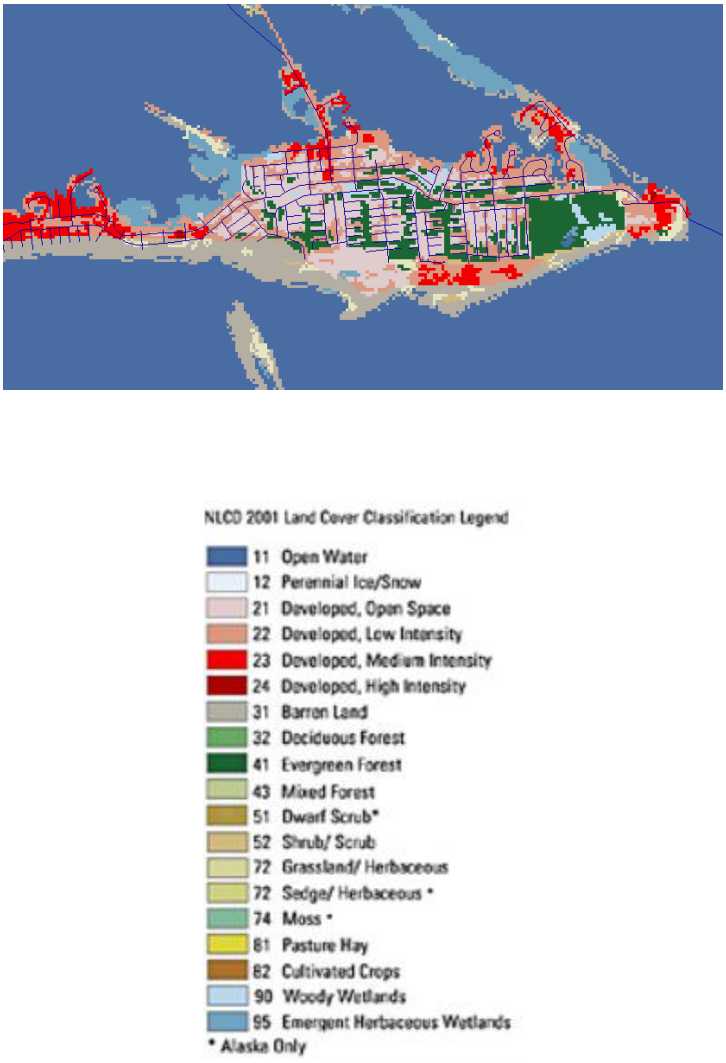

Figure 4-6. Land cover data from the Multi-Resolution Land Characteristics Consortium

Table 4-1. LC/LU by percentage for Dauphin Island in 2001, data obtained from NLCD.

NLCD 2001	Area [ha]	Percent [%]
Water [WATR]	7.19	1.60
Residential-Low Density [URLD]	158.09	35.25
Residential-Medium Density [URMD]	113.89	25.39
Residential-High Density [URHD]	13.76	3.07
Wetlands-Forested [WETF]	14.69	3.28
Wetlands-Non-Forested [WETN]	8.19	1.83
Southwestern US [Arid] Range [SWRN]	10.32	2.30
Range-Grasses [RNGE]	6.62	1.48
Forest-Evergreen [FRSE]	112.86	25.16
Range-Brush [RNGB]	2.79	0.62
Industrial [UIDU]	0.13	0.03

4.6 Water issues

This section discusses the island's water demands, current system in place to meet these demands, and current issues as well as potential future problems.

4.6.1 Freshwater-saltwater interaction and the hydrologic cycle

It is important to understand the dynamics of a freshwater lens in order to fully understand Dauphin Island's freshwater situation. Barrier Islands often form a freshwater lens because of the unique saltwater-freshwater relationship. Since freshwater is less dense than saltwater, the freshwater "floats" on the salt water due to the density differences, water-table elevation, layers of low permeability, and the slow rate of diffusion to surrounding salt water. The lens that forms is generally irregularly shaped and influenced by landforms. The subsurface flow of freshwater

towards the saline water results in the formation of a stable, wedge shaped surface that defines the lens. Evapotranspiration and pumping losses may cause the lens shape to change.

Dauphin Island is surrounded by brackish water on the Mississippi Sound side and saline water on the Gulf of Mexico side. The lens is recharged solely by precipitation. The precipitation that does not reach the freshwater lens is lost to the atmosphere as evaporation and transpiration or lost to the ocean as runoff. Losses from the system occur as diffusion to the surrounding saltwater and losses from pumping [*Chandler*, 1983].

4.6.2 Water demands

Dauphin Island is mainly a residential community with a fairly small amount of commercial development. According to the 2000 Census, there were about 1300 permanent residents on the island, with the total population soaring temporarily during vacation and holiday periods. Because of the ever-growing desire of Americans to live on the coast, it is reasonable to assume that the number of permanent residents has grown since then, and will continue to grow well into the future.

While many of the residents of the nearby Fort Morgan Peninsula have switched to municipal water supply from Gulf Shores Water Authority, groundwater is still heavily used on Dauphin Island itself [*Liu et al*, 2008]. Tourism is very important to the economy of Dauphin Island, and the hotels and tourist attractions rely on groundwater. Because of the large influx of people at certain times of the year there are peaks in water demand throughout the year. These demand peaks may not coincide with peaks in precipitation, and may occur in months with historically little rainfall, such as May and June.

4.6.3 Current water supply system

Dauphin Island's surficial aquifer is about 50 to 100 feet thick, and is composed of alluvial, low terrace and coastal deposits. The aquifer is elliptical in shape oriented east west along Dauphin Island, and consists of fine to coarse grain sands [*Chandler*, 1983].

Previous to the drilling of the shallow water-table aquifers, the island was obtaining all of their freshwater from deeper wells that were extracting water from the aquifers underlying the surficial sand aquifer. The water obtained from the deeper wells was extremely high in chlorides and iron, so test drills were installed in the water-table aquifer in order to assess the capacity of the shallow aquifer to meet the island's freshwater needs [*Caldwell*, 1996].

Through a variety of tests, it was determined that the shallow aquifer was capable of providing sufficient freshwater for the island. Up to this point, however, the residents on the island had been using septic tanks to deal with their sewage. When it was decided that the shallow sand aquifer was going to be exploited, an island wide sewer system was installed to eliminate the need for septic tanks. Once the sewer system was in place, the shallow wells were drilled [*Caldwell*, 1996].

The first four shallow wells were installed and came on line in 1990. These were wells #10, #20, #30, and #40. In 1992, four more shallow wells were added to this supply when they installed well #50, #60, #70, #80 (see Figure 4-7 and Table 4-2). The water system supply on the island contains approximately 55 miles of water mains. The wells extended about 35 feet into the ground. When the four additional wells were added in 1992, the total pumping for the eight shallow wells and one deep well was 520 gallons per minute or about 700,000 gallons per day [*Caldwell*,1996].

Because of a few instances in which the demand of water exceeded the production from the eight shallow wells and single deep well, alternative options had to be considered. One of the options to obtain additional freshwater included installing two additional shallow wells in the Water-Table aquifer. The addition of two more shallow wells would bring the total number of shallow wells to the number that the Unites States Geological Survey had deemed the maximum for the island. Another option was to pipe water about 18 miles from the main land. The option that was ultimately chosen was to build a reverse osmosis plant that could treat high levels of chloride. This would allow another deep well that was not in use to be brought back online. The final inspection and approval of this plant was completed at the end of 1996. The reverse osmosis plant was successful in removing the large majority of chlorides in the water, thus making it potable and safe for public consumption [*Caldwell*, 1996].

In addition to the construction of the reverse osmosis plant, another deep well is currently under construction and should be coming on line soon. This well extends to a depth of 547 feet. With this deep well, the pumping capacity for the island will be nearly doubled [*McElroy*, 2010]. Figure 4-7 shows the location of the island's water-table pumping wells.

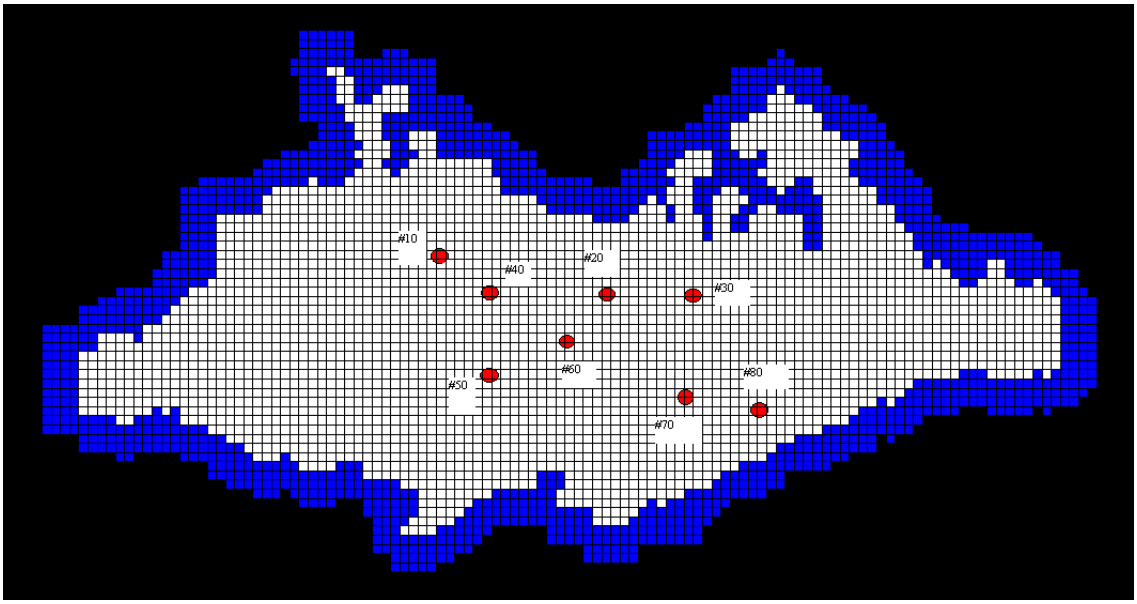

Figure 4-7. Well locations on Dauphin Island (well size is exaggerated). Blue color indicates discharge towards the ocean.

Table 4-2. Well depth, screened interval, and location; data obtained from DIWSA.

Well ID #	Well Depth [ft below sea level]	Screened Interval [ft below sea level]	Lat/Long
10	30.0	18.00-28.00	30.25380/88.11003
20	32.5	20.50-30.50	30.25156/88.10153
30	34.5	22.50-32.50	30.25124/88.9686
40	33.0	21.00-31.00	30.25168/88.10746
50	40.0	23.65-33.65	30.24913/88.10757
60	40.0	24.75-34.75	30.24940/88.10377
70	40.0	26.10-36.10	30.24767/88.09223
80	40.0	26.65-36.65	30.24676/88.09223

4.6.4 Current and future water issues

Due to increasing stresses on the island's groundwater system, concerns about the quantity and quality of groundwater resources on the island have been raised. There are multiple factors that already have or have the possibility to affect the groundwater resources on the island. One of these factors is increasing population which increases the daily demand for freshwater. The DIWSA has reported several high capacity weekends in which the water demands put a much larger than normal stress on the system [*Caldwell*, 1996]. Additionally, increasing population on the island would likely lead to increasing development on the island resulting in more impervious surfaces. Additional impervious surfaces would increase runoff and decrease groundwater recharge.

Another factor is climate change which has the possibility of altering precipitation patterns, evapotranspiration patterns, and increasing sea level rise. Climate change could also increase the number of large storm events such as hurricanes. Large storms and hurricanes can be devastating for small barrier islands. For example, Hurricane Katrina caused a 1.9 km breach in the island landform after the storm. There was approximately 2 m of overwash flow during the storm [*Fritz et al*, 2007].

In addition to issues with water demand, Dauphin Island has multiple water quality problems such as high iron, manganese, chloride, dissolved solids content, color, and turbidity. Iron content increases and manganese content decreases with hydrogeologic depth [*Chandler*, 1983].

While some of these problems are already being addressed by the addition of the new deep well, it is important to fully understand the dynamics of the Water-Table Aquifer. The Water-Table Aquifer is the easiest and most economically feasible aquifer to exploit. There are already

eight wells installed in the aquifer as well as an extensive water piping system. Although Dauphin Island may switch to deep wells for part of their water in the near future, it is still important to understand the capacity, limitations, and characteristics of the shallow aquifer, as well as how it responds to certain changing climate factors and the sensitivity to hydrologic parameters.

5. Sensitivity of Dauphin Island's Water-Table aquifer to changing factors

This section will discuss the details of the groundwater model and sensitivity analysis. The sensitivity analysis was performed to detect which factors most affected the island's groundwater resources.

5.1 Background

The coastal regions of Baldwin County are experiencing steadily increasing development as well as an increasing economy [*Murgulet and Tick*, 2008]. As previously discussed, this phenomenon is specifically of concern in Dauphin Island because their entire water supply is derived from the freshwater lens underlying the island. Because of the possibility of decreasing supply of freshwater and the threat of saltwater intrusion, groundwater modeling was performed to predict the impact of various anthropogenic factors. Using the information gained in this section, it is possible to develop better management practices that could be integrated on the island to preserve the island's valuable freshwater resources.

5.2 Research objectives

There were multiple objectives to this section of research. The first objective was to create an accurate groundwater model using SEAWAT to simulate the steady-state and transient groundwater situations at Dauphin Island. The second objective was to determine the effects of different factors on the island's freshwater resources. In order to do this, some of the parameters and inputs in the model were altered to model future scenarios (from the time period of 2010-2030). For example, recharge patterns were changed due to land cover change or climate change to determine which parameters have the most effect on the position of the saltwater-freshwater boundary and the total volume of usable freshwater in the Water-Table Aquifer.

5.3 Input data, methods, and study methodology

This section will discuss the data used in the Dauphin Island groundwater models, as well as the methods used in the development of the model. Additionally, the different scenarios that were simulated to detect the effects of the changing factors will be introduced.

5.3.1 Input data

The MODFLOW family code, SEAWAT, was used to simulate the Dauphin Island aquifer and the freshwater/saltwater interactions occurring for a variety of scenarios. As previously discussed, SEAWAT was developed by combining MODFLOW and MT3DMS into one program and making modifications to account for saltwater-freshwater density variations [*Guo and Langevin,* 2002]. SEAWAT operates by solving the flow and solute transport equations. The groundwater flow equation is as follows [*Langevin and Guo,* 2006]:

$$-\nabla \cdot (\rho \vec{q}) + \bar{\rho} q_s = \rho S_p \frac{\partial h}{\partial t} + \theta \frac{\partial \rho}{\partial C} \frac{\partial C}{\partial t} \qquad (5\text{-}1)$$

where ρ = density of saline groundwater; C = concentration of dissolved salts in groundwater; h = fresh water equivalent hydraulic head; t = time variable; ∇ = the gradient operator in Cartesian three-dimensional coordinates.

The solute transport equation is as follows [*Diersch*, 2006, *Langevin and Guo*, 2006]:

$$\frac{\partial C}{\partial t} = \nabla \cdot \left(D \cdot \nabla C \right) - \nabla \cdot \left(\vec{v} C \right) - \frac{q_s}{\theta} C_s + \sum_{k=1}^{N} R_k \qquad [5\text{-}2]$$

where D = hydrodynamic dispersion tensor; $\vec{v}$ = fluid velocity; C_s = solute concentration of water entering from sources or sinks, and R_k= the rate of solute production or decay in reaction of k of N different reactions.

All scenario simulations were modeled with the same parameters and values for the time period 1990-2010. The only values that differed before 2010 between scenarios were the

recharge values. This will be explained below. The following list details which values were used for each parameter as well as the reasoning behind the values used.

- Number of Columns: The number of columns used in the model was 126.
- Number of Rows: The number of rows used in the model was 78.
- Grid Size: The cells used in the model are 164 feet on each side. Usually a convergence test is done to determine the appropriate grid size, but this grid size had already been used in a successful Dauphin Island finite difference model [*Kidd*, 1988].
- Number of Layers: Fifteen layers were used for the model. The top ten layers represent the sandy water-table aquifer. Layers eleven through fifteen represent the underlying confining clay unit.
- Layer Elevations: The sandy water-table aquifer was estimated to extend to approximately 42 feet below mean sea level. This value was obtained from records of subsurface lithology taken when a well on the island was being drilled [*O'Donnell*, 2005]. While the bottom elevation of this layer likely varies slightly throughout the island, it was assumed to be flat for this simulation. The elevations for the ten layers representing the water-table aquifer were obtained by dividing 42 by the number of layers. The clay, confining layer was estimated to go to 70 feet below mean sea level, so this was used as the bottom elevation of this layer. This value was also obtained from the drilling records mentioned previously. The clay unit was split into 5 layers. They are not all of equal size, as the first two layers in the clay unit are thinner than the last three layers. This was done because in preliminary simulations the bottom freshwater-saltwater interface fluctuated around the region of the last layer of sandy unit, and the top two layers of the clay unit. By making the top two layers of

the clay unit thinner, a greater resolution of the bottom interface position could be obtained. Table 5-1 lists the layer elevations.

- Hydraulic Conductivity: The hydraulic conductivity values used in the model for the water-table aquifer were obtained from ranges presented in O'Donnell's report titled "Dauphin Island Water and Sewer Authority's Public Water Supply Wells" which were obtained from Kidd's USGS report on Dauphin Island titled "Hydrogeology and water-supply potential of the water-table aquifer on Dauphin Island". Two well tests were done in order to estimate the hydraulic conductivity in the water-table aquifer. The first test that was done was a 48 hour aquifer test performed with multiple observation wells around the island [*O'Donnell*, 2005]. The range obtained from this study was 45-55 ft/day. The second well test was a 26 day test, and the range that this test produced was 56-59 ft/day [*Kidd*, 1988]. The values for the water-table aquifer were changed slightly during the calibration process, but they remained within the ranges found in the literature. It should also be noted that the hydraulic conductivity values were not varied spatially within the same layer, as it was assumed that the value was homogeneous in each layer. This is acceptable, because aquifer tests reported in Kidd's report indicate that the aquifer properties are uniform across the island [*Kidd*, 1988]. The hydraulic conductivity values used for the clay confining layer were based off of the generally accepted range for clay, which is 10^{-9} to 10^{-6} cm/s [*Fetter*, 2001]. Table 5-2 shows the hydraulic conductivity values used for each layer in the model.
- Storage/Porosity: Inputs required for the SEAWAT model are S_s, S_y, and Porosity (*n)*. O'Donnell's report gives a range of specific yield values from the previously mentioned well tests. This range was 0.03-0.15 [*O'Donnell*, 2005]. The value used for S_y was 0.1. The

value used for S_s was 0.002. The value used in this model for porosity was 0.3, which is a generally accepted porosity value for sand.

- Well Locations: The well locations for the shallow wells were obtained from the latitude and longitude given by the Dauphin Island Water and Sewer Authority (DIWSA). The latitude and longitude values were used to mark the well locations in ArcMap. This figure was then used to place the wells within the Groundwater Vistas interface by importing a bitmap that could be seen under the finite difference grid. Table 4-3 lists data for each well, including location. Since the wells were not all at a constant depth below sea level, they were located in different layers of the model based upon their depth. Wells #10 and #20 were placed in layer 7. Wells #30 and #40 were placed in layer 8. The rest of the wells were placed in layer 9 of the groundwater model.
- Well Pumping: Pumping rates were also obtained from DIWSA. The DIWSA provided 4 years of pumping data, from September 2000 - August 2002 and January 2009 - December 2010, but were unable to provide the rest. To overcome this, the missing years were estimated using the years that were provided. Appendix 9-6 lists the Dauphin Island well pumping rates as provided by the DIWSA.

  In regards to assigning pumping rates to the simulation time it is easiest to view the simulation period as broken up into 6 time periods. The first time period is from 1990 to 1994. This is the time period in which only the first four shallow wells (#10, 20, 30, and 40) were on line and pumping. The pumping rates used for this time period were each wells average pumping rate as calculated from the DIWSA data. In 1994, the other four wells (#50, 60, 70, and 80) came on line and began pumping. For the time period between 1994 and August 2000 (which is the last month before the DIWSA data begins), the same averages

that were previously used for 1990-1994 were also used. The first set of pumping data provided by the DIWSA starts in September 2000. From September 2000 to August 2002, the known pumping values that were provided were used. In order to reduce the number of stress periods in the model, which in turn reduces computational time, similar consecutive pumping rates were grouped together and averaged. Using this method for September 2000-August 2002, the number of stress periods for this time span was reduced from 24 to 8 stress periods. For the time period between September 2002 and September 2008, the average values used from 1990 to 2000 were used here as well. Pumping data was provided from the DIWSA for the months between October 2008 and December 2010. Similar consecutive pumping rates were grouped for this time periods as well in order to reduce the number of stress periods. This reduced the number of stress periods for this period from 27 to 19. For the years after 2010, which are deemed the "future years" for this study, average values from the previous years of pumping were also used. In some scenarios, such as an increased pumping scenario, different pumping schemes were used and this will be discussed in a later section.

- Recharge: The SEAWAT model allows the user to define recharge that can vary both with time and space. For this study, the recharge was assumed to be spatially constant since the island is small, but it did vary temporally.

  As previously mentioned, the recharge assessments described earlier did not yield usable relationships between land cover and recharge that could be applied to Dauphin Island to estimate recharge. Due to this fact, recharge estimates to be used as inputs to the model had to be obtained by another method. SWAT was used to estimate recharge for Dauphin Island [*Wang*, 2011]. SWAT was chosen as the tool to estimate recharge because SWAT had

already been successfully calibrated and applied to several watersheds close to Dauphin Island [*Wang*, 2011, *Singh*, 2010].

Two different SWAT methods were used to calculate the retention parameter within SWAT. The more traditional method calculates the retention parameter based on the soil profile water content. The retention parameter is then used to find the curve number. An alternate method uses accumulated plant evapotranspiration to calculate the daily curve number. The daily curve numbers from each method are used to calculate infiltration. As would be expected, differing curve numbers produce differing infiltration values. Recharge is directly derived from these infiltration values. Equation 5-3 is used within SWAT to calculate recharge [*Arnold et al*., 1996]:

$$w_{rchrg,i} = (1 - \exp[-1/\delta_{gw}]) \cdot w_{seep} + \exp[-1/\delta_{gw}] \cdot w_{rchrg,i-1} \qquad (5\text{-}3)$$

where $w_{rchrg,i}$ = the amount of water entering the aquifer on day *i* [mm], δ_{gw} = the delay time or drainage time of overlying geologic units [days], w_{seep} = the total amount of water exiting the bottom of the soil profile on day *i* [mm], $w_{rchrg,i-1}$ = the amount of recharge entering the aquifer on day *i*-1 [mm].

Figure 5-1 shows both precipitation and recharge estimated using the plant evapotranspiration method.

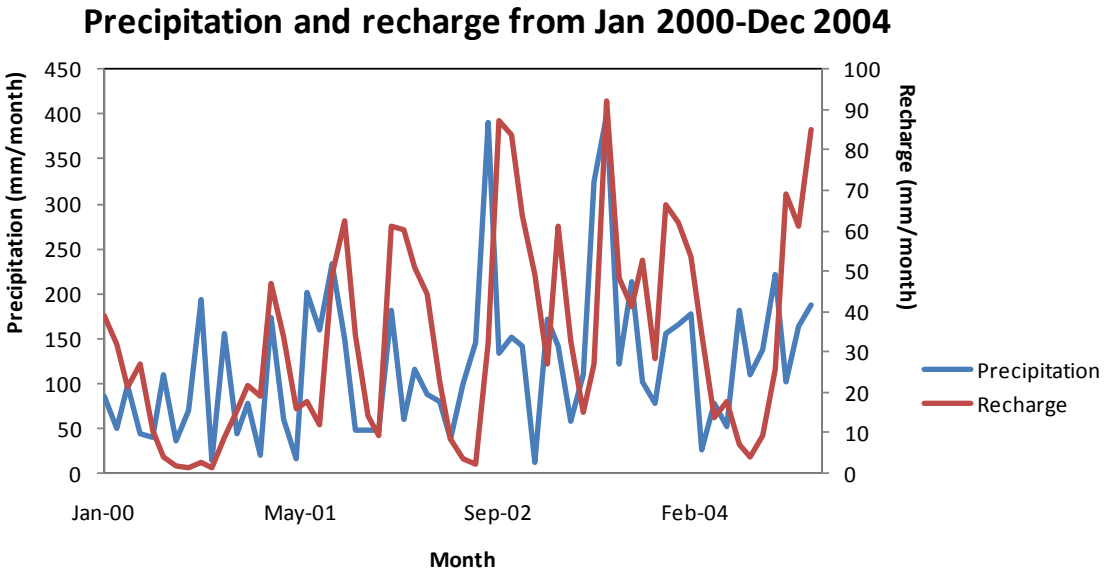

Figure 5-1 Comparison of precipitation and recharge on Dauphin Island, Jan 2000-Dec 2004

- Dispersivity: The model uses longitudinal dispersivity, transverse dispersivity, and vertical dispersivity as input parameters to model the effect of dispersion in the model. Dispersion is the process in which a solute in groundwater mixes with uncontaminated water and thus decreases in concentration. This is caused by the differences in velocity in pore travel and difference in flow rate through different strata [*Fetter*, 2001]. In order to calculate dispersion, dispersivity is multiplied by flow velocity.

  For this model, dispersivity values were set to zero, which is a common practice in field models [*Masterson*, 2004]. There are multiple reasons for using this approach. It was assumed that the flow system in Dauphin Island was an advection dominated flow system because of the large recharge rates used and the relatively high hydraulic conductivities of the sandy layer. It was also assumed that any possible effects from dispersion were taken into account by numerical dispersion.

As the discretization yielded grid cells that were 164 feet by 164 feet, numerical dispersion was certainly an issue. This reasoning was adapted from prior work done on Cape Cod, Massachusetts [*Masterson,* 2004].

- Surface Water Bodies: In cells that contained surface water bodies such as ponds, the hydraulic properties were changed so that they would be simulated appropriately. The two notable surface water bodies are Alligator Lake and Oleander Pond, which are shown in Figure 5-2, and are located on the southeastern shore of the island. Table 5-4 shows the values K, porosity, S_y, and S_s used at these nodes.
- Time Step Size: The time step size used for the model was one month. This time step size was chosen because the pumping and recharge data that was obtained was all in the monthly time scale.
- Density of Saltwater: The density of saltwater used was 2.18 lbs/ft^3.

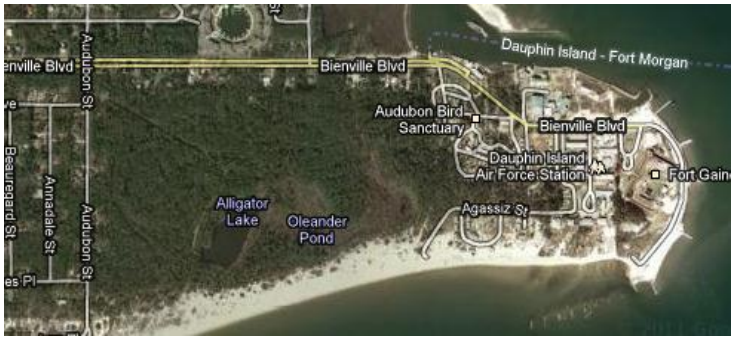

Figure 5-2. Locations of Alligator Lake and Oleander Pond on Dauphin Island.

Table 5-1. Top and bottom layer elevations.

Layer	Top Elevation [ft]	Bottom Elevation [ft]
1	0.0	-4.2
2	-4.2	-8.4
3	-8.4	-12.6
4	-12.6	-16.8
5	-16.8	-21.0
6	-21.0	-25.2
7	-25.2	-29.4
8	-29.4	-33.6
9	-33.6	-37.8
10	-37.8	-42.0
11	-42.0	-45.5
12	-45.5	-49.0
13	-49.0	-56.0
14	-56.0	-63.0
15	-63.0	-70.0

Table 5-2. Hydraulic conductivity values used for Dauphin Island.

Layer	Kx [ft/month]	Ky [ft/month]	Kz [ft/month]
1	1370	1200	30
2	1370	1200	30
3	1370	1200	30
4	1370	1200	30
5	1370	1200	30
6	1370	1200	30
7	1370	1200	30
8	1370	1200	30
9	1370	1200	30
10	1370	1200	30
11	0.00262	0.00262	0.000262
12	0.00262	0.00262	0.000262
13	0.00262	0.00262	0.000262
14	0.00262	0.00262	0.000262
15	0.00262	0.00262	0.000262

Table 5-3. Well depth, screened interval, and location; data obtained from DIWSA.

Well ID #	Well Depth [ft below sea level]	Screened Interval [ft below sea level]	Lat/Long
10	30.0	18.00-28.00	30.25380/88.11003
20	32.5	20.50-30.50	30.25156/88.10153
30	34.5	22.50-32.50	30.25124/88.9686
40	33.0	21.00-31.00	30.25168/88.10746
50	40.0	23.65-33.65	30.24913/88.10757
60	40.0	24.75-34.75	30.24940/88.10377
70	40.0	26.10-36.10	30.24767/88.09223
80	40.0	26.65-36.65	30.24676/88.09223

Table 5-4. Parameter values used for surface water bodies.

Parameter	Value	Unit
K	50000	ft/day
Porosity	0.1	dimensionless
S_y	1	dimensionless
S_s	1	$Feet^{-1}$

In order to refine the finite difference grid to delineate the island, discharge regions, no flow boundaries, etc, numerous modeling steps were used. First, a map of the island was obtained from the National Land Use Consortium in a format that could be imported into ArcMap and retain its spatial information. This was beneficial because the information regarding latitude, longitude, and distances across the island remained with the image while it was being altered in ArcMap. Once the map was in ArcMap, it was cropped and gridded to mark the distances so that scale would be known.

The map developed in ArcMap was then imported into Groundwater Vistas as a bitmap. This way, the map was overlain with the finite difference grid. Using the map, the island could be delineated using a constant head boundary at the shoreline around the island. The constant

head boundary condition grid extended offshore on the first three layers in order to mimic aquifer discharge into the surrounding surface water. The width of the discharge area was largest on the first layer, and decreased in width in both the second and third layer. The protocol used in the Cape Cod Study [*Masterson*, 2004] was closely followed with respect to demarcating the offshore discharge. Past this discharge area, island was surrounded by no flow boundary cells. The no flow boundaries around the island were intended to terminate lateral groundwater flow past the island-lens boundary.

5.3.2 Steady-state and transient models

With all of the inputs listed above a general steady state and transient models were developed to simulate the density dependent flow and saltwater-freshwater interactions using SEAWAT. Before differing scenarios could be simulated, it was necessary to develop an accurate steady state model. Steady state is reached in a groundwater flow model when equilibrium has been achieved and the head distribution stops changing. This occurs when the inflows to the system equal the outflows [*Fetter*, 2001].

A steady state model is necessary because the output head files and concentration files that are created at the final time in which the model reaches steady state are important input files for the transient simulation. In the transient model, the matrix of head values is used as the initial heads for the first time step. Additionally, the initial concentration values in the transient model are the concentration values at the last time step of the steady state model.

Once the steady state model was developed, the general transient model was developed for the years 1990-2010 using the recharge and pumping data described above. The benefit of transient simulations is the ability to vary input values over time and be able to view the simulation results at various time steps, instead of just at the final equilibrium state.

5.3.3 Calibration

Once the initial Dauphin Island steady state and transient models had been developed based on data obtained and past studies, they were tested using the model data available in Kidd's USGS report. The study done by Kidd [1988] used data from 40 test wells to develop a two-dimensional finite difference groundwater flow model for the island's water-table aquifer. This was done in order to assess the freshwater resources in the shallow aquifer and determine if it would be a feasible source of freshwater for the island at the time. The model was calibrated for both high and low water-table conditions. Using the data collected from the monitoring wells and the groundwater model that was developed, Kidd estimated that the water-table aquifer could produce up to 0.6 million gallons per day without lateral encroachment of seawater.

Three figures in Kidd's report were used to validate the model. The model was calibrated to reach approximately the same head contours found in Kidd's figures as shown in the top layer of the aquifer. The recharge values used in the calibration were given in the Kidd report.

There were multiple steps taken in order to calibrate the model. As previously described, a steady state and a transient groundwater model for Dauphin Island was built based on data collected from previous studies and literature that outlined the hydrologic properties of the island. Since many of the properties were given in ranges, such as hydraulic conductivity or porosity, our models were built with values in the middle of the given ranges as a starting point. With these models, several steady state and transient simulations were done to mimic situations presented in the Kidd report. Using the results, specifically the water-table elevation contour lines, the results from our models and Kidd's results were compared visually. The results of the Kidd model, which are accepted as valid, were compared to the results of the study model to validate the latter, a validation method known as comparison testing [*Balci*, 1998].

After comparison, certain model parameters were adjusted in order to better match Kidd's figures based on the response of the aquifer and prior knowledge of unconfined aquifer behavior. It is important to note, however, that the changes always remained within the published range of values for the hydrologic properties on the island. This process was continued until the contour lines from our models and Kidd's results matched fairly well upon visual inspection. Visual inspection was done to ensure the contour shapes were similar between ours and Kidd's, the same maximum and minimum head values were obtained, and that the same contour lines surrounded the pumping wells during pumping. The final steady state and transient model that remained after the tweaking process were the models used in the remainder of this Dauphin Island study.

Matching these figures was a valuable effort. The validity of a groundwater model depends on how accurately the model is able to predict field conditions [*Wang and Anderson*, 1982]. Since the Kidd study used data from 40 monitoring wells on the island, and the simulations were being run for the same time period, Kidd was able to compare the observed groundwater monitoring data to the results obtained from the numerical model. For example, in the steady state simulations, sixty percent of the observed groundwater levels were within 0.5 feet of the simulated levels. Additionally, all of the observed groundwater levels were within 1 foot of the simulated values [*Kidd*, 1988]. Therefore, these figures provided an indispensable point of reference to calibrate and develop the initial steady state and transient models.

Figures 5-3 and 5-4 show the figure from the Kidd report and from our study, respectively. The figures depict the groundwater flow situation using the water-table altitude at steady state in the year 1985.

Figures 5-5 and 5-6 show the figure from the Kidd report and from our study, respectively. The figures were obtained after a transient simulation of a time period. During the beginning of the simulation, the recharge was 15 inches/year, but the simulation time period ended with about two months of no recharge. Due to this, the water-table levels were lower than in the previous figure.

Figures 5-7 and 5-8 show the figure from the Kidd report and from our study, respectively. The figures were matched for a steady state simulation that included pumping. In this simulation, there are four wells on the island pumping a total of 0.3 MGD. The recharge value used for this simulation was also 15 inches/year.

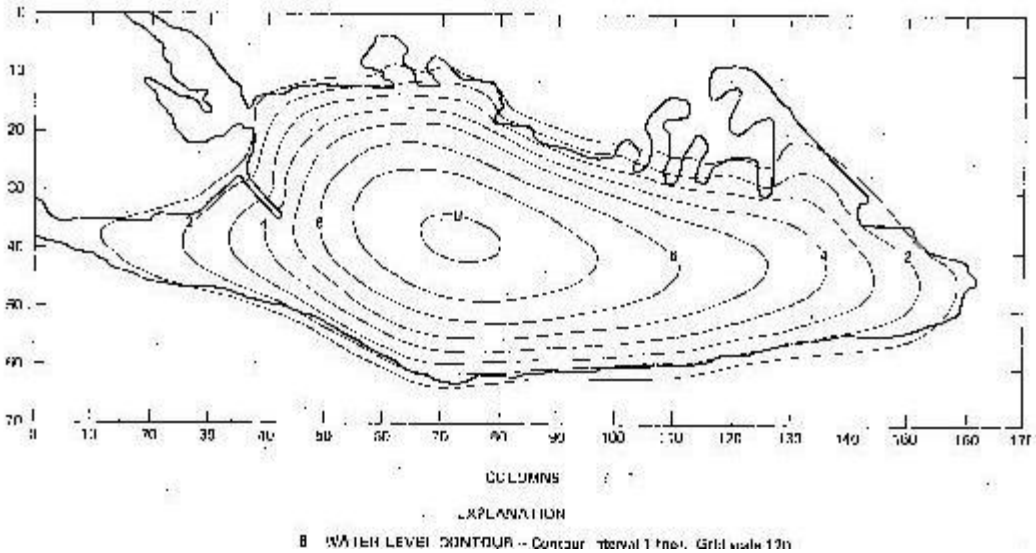

Figure 5-3. Steady State Head Distribution, April 2, 1985, from Kidd [1998]

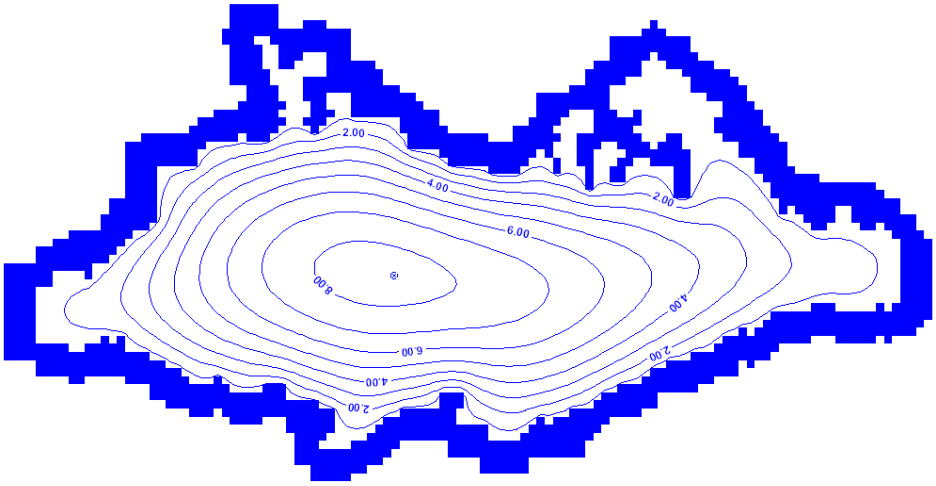

Figure 5-4. Steady State Head Distribution, April 2, 1985, from model developed in this study

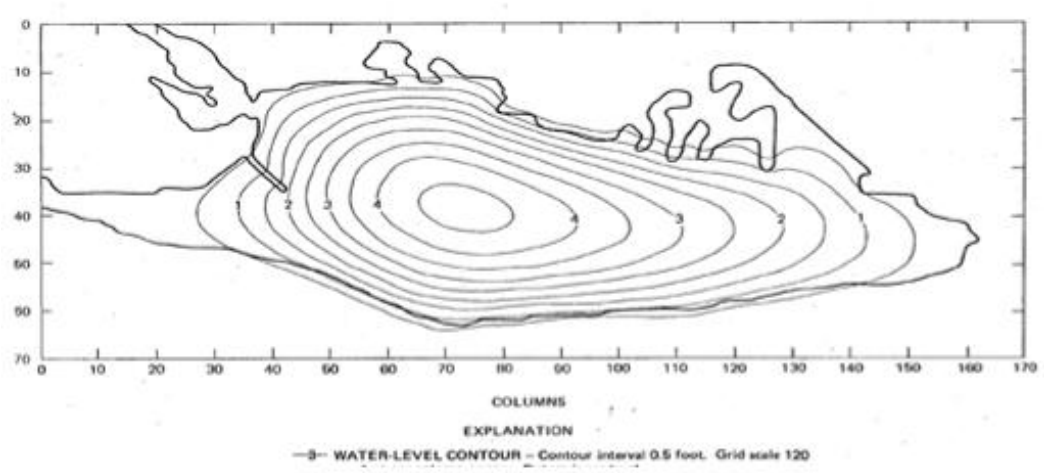

Figure 5-5. Head Distribution after Transient Simulation from May 22-June 15, 1985, from Kidd [1998]

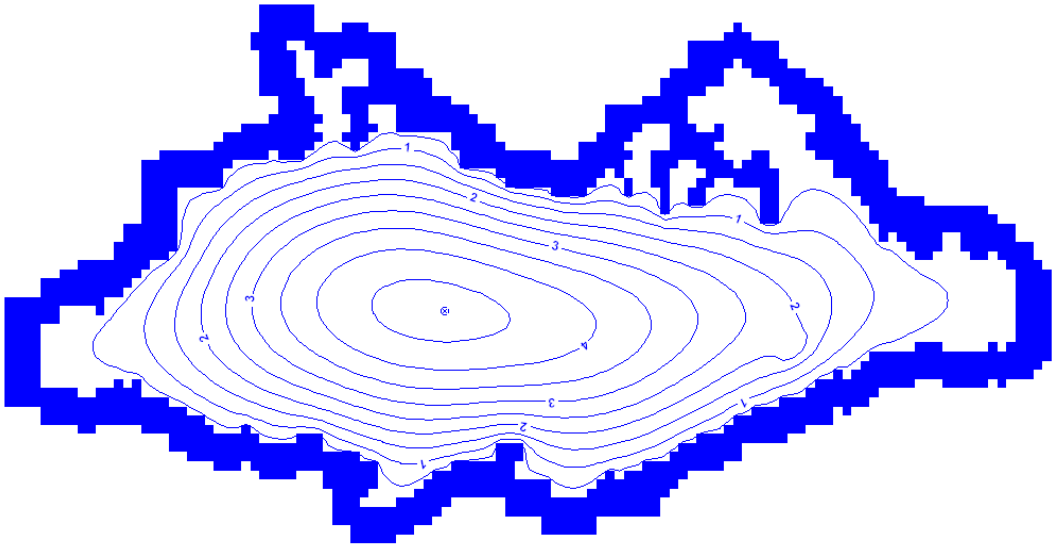

Figure 5-6. Head Distribution after Transient Simulation from May 22-June 15, 1985, from model developed in this study

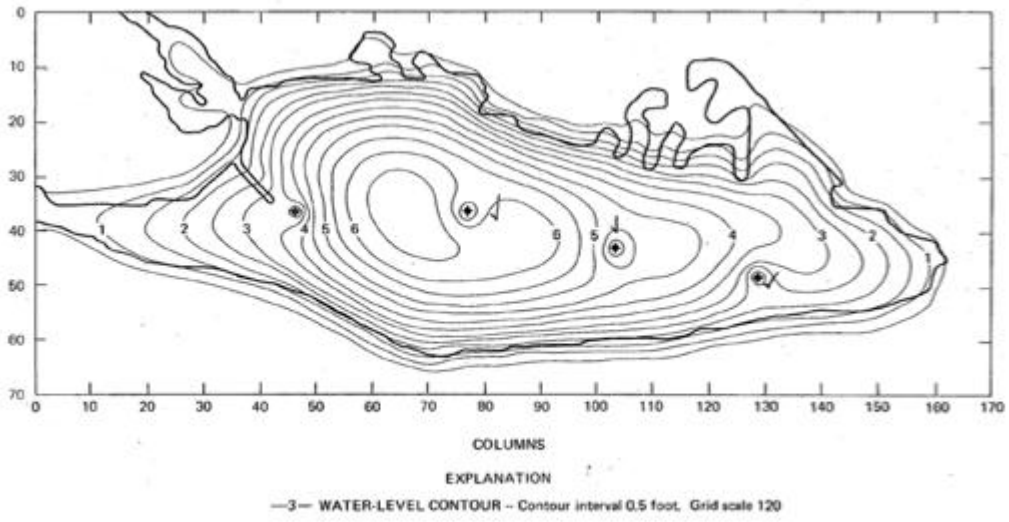

Figure 5-7. Head Distribution after Pumping Simulation in 1988, from Kidd

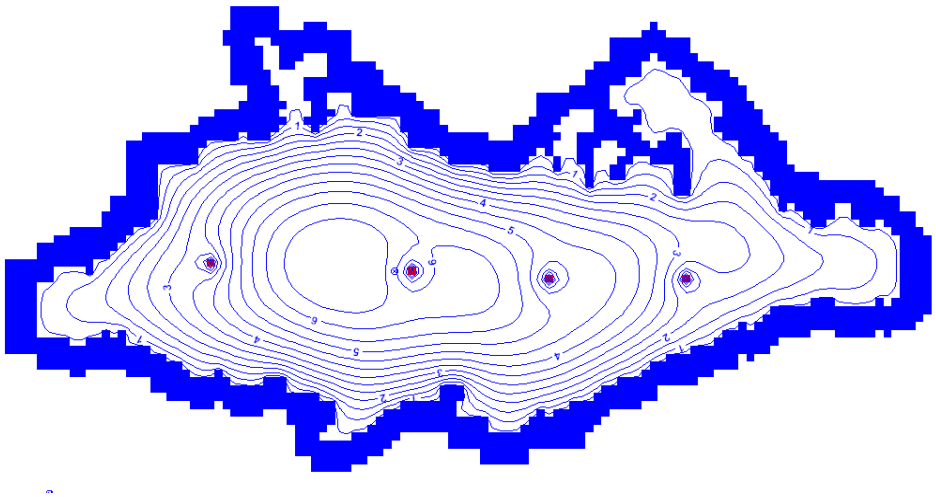

Figure 5-8. Head Distribution after Pumping Simulation in 1988, from model developed in this study

5.3.4 Scenario simulations

Six scenarios were simulated for Dauphin Island in an attempt to both visualize and quantify the effects of different factors on the unconfined aquifer. All of the scenarios were modeled for the same time period, 1990-2030. The simulation start time of 1990 was chosen because that was when the first four shallow wells came on-line. The end year of 2030 was chosen because that gave about a 20-year prediction into the future.

In all of the scenarios, the values used as inputs were similar to those described before, and they remained constant. Additionally, they all had the same initial head values that were obtained from the steady state simulation described above. Therefore, each model run should be identical until the year 2010. After the year 2010, the input data was modified to simulate various scenarios. The following section describes in detail each of the scenario simulated in this study. Table 5-5 summarizes the factors examined in each scenario, although they will each be described extensively in the following section.

Table 5-5 Summary of Scenarios Simulated

Simulation	Description
Scenario 1	Base-case
Scenario 2	Land-cover change
Scenario 3	Land-cover change+dry climate change
Scenario 4	Land-cover change+wet climate change
Scenario 5	Land-cover change+dry climate change+sea level rise
Scenario 6	Land-cover change+dry climate change+increased pumping

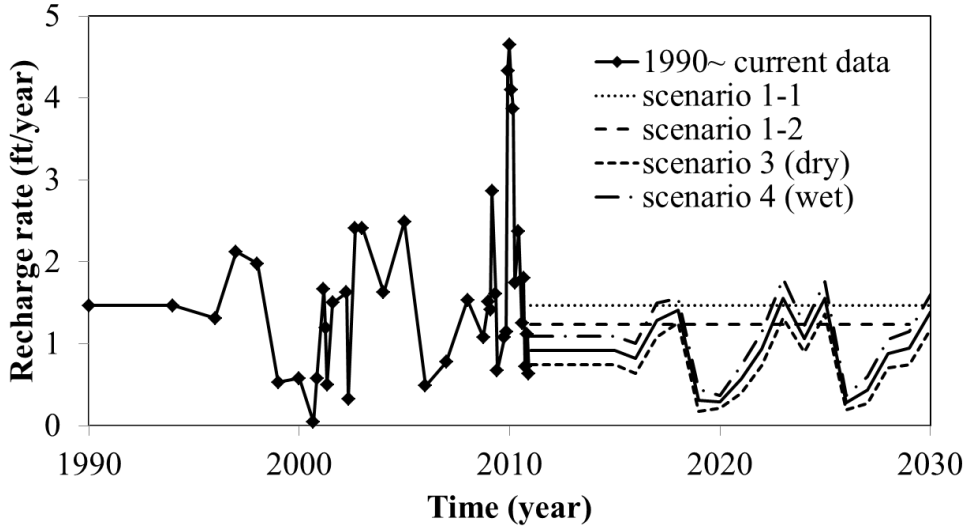

Figure 5-9. Summary of Recharge Values used for six scenarios as obtained from SWAT

Scenario 1:Base Case- The first scenario simulated was the general, no-change scenario modeling the groundwater situation with base-line inputs for the time period 1990-2010 and then no changes from the current condition were applied for the time period of 2011-2030. This means future pumping values were the same average pumping values used in previous years. Also, the recharge patterns were assumed to remain approximately constant, so an average recharge value based on the data from 1990-2010 was assigned. The Scenario 1 model was run twice (and the two runs were labeled 1.1 and 1.2). The first simulation was run with the SWAT recharge estimates that were obtained using the soil moisture method and the second simulation was run with the recharge estimations based on the plant evapotranspiration method. Since the recharge values for the two regimes varied, this gave a good range for the simulation results.

While it is highly unlikely that the situation on Dauphin Island would not change from 2010 into the future, this scenario was still an important base-case scenario. The results of the simulations provide a reference datum to compare other scenarios against.

Scenario 2: LU/LC change- The second scenario was developed to explore the effects of land cover change induced by urban development. By altering the land cover scenario we are able to simulate the change in groundwater resources on the island with a hypothetical land cover change that could possibly occur in the future. The scenario modeled is an extreme case which illustrates what would likely be the largest possible change in land cover. The following table illustrates the changes that were simulated:

Table 5-6. Land Use/Land Cover change scenarios simulated in this study.

NLCD 2001 LU/LC	Future LU/LC	Area [ha]	Percent [%]
Water [WATR]	Water [WATR]	7.19	1.60
Residential-Low Density [URLD]	Residential-Medium Density [URMD]	158.09	35.25
Residential-Medium Density [URMD]	Residential-High Density [URHD]	113.89	25.39
Residential-High Density [URHD]	Residential-High Density [URHD]	13.76	3.07
Wetlands-Forested [WETF]	Wetlands-Forested [WETF]	14.69	3.28
Wetlands-Non-Forested [WETN]	Wetlands-Non-Forested [WETN]	8.19	1.83
SW US [Arid] Range [SWRN]	SW US [Arid] Range [SWRN]	10.32	2.30
Range-Grasses [RNGE]	Range-Grasses [RNGE]	6.62	1.48
Forest-Evergreen [FRSE] 50%	Forest-Evergreen [FRSE]	56.43	12.58
Forest-Evergreen [FRSE] 50%	Residential-Low Density [URLD]	56.43	12.58
Range-Brush [RNGB]	Range-Brush [RNGB]	2.79	0.62
Industrial [UIDU]	Industrial [UIDU]	0.13	0.03

For this scenario, the recharge values used for the years of 2010-2030 were obtained using Global Climate Models (GCMs) to predict the future recharge patterns based on changing precipitation patterns. Both dry and wet future climate scenarios were used to calculate the recharge for the future time period between 2010-2030. Using a combination of four GCMs and three greenhouse gas emission scenarios, 12 temperature estimates and 12 precipitation estimates were obtained for each month in the time period [*Wang*, 2011]. Figure 5-10 shows the change in mean temperature and precipitation as predicted from the GCMs and greenhouse gas emission scenarios. A dry future climate was modeled by choosing the highest temperature values and

lowest precipitation values for each month. Those values were then used as input to SWAT to calculate recharge. In order to mimic a wet future climate, the estimates that had the lowest temperature values and the highest precipitation values for each month were chosen to run SWAT [*Wang*, 2011]. The dry climate change scenario was used for Scenario 3. The wet climate change scenario was used for Scenario 4. The average of the dry climate change and wet climate change recharge estimates were used for Scenario 2, since we just wanted to examine the effect of land cover change.

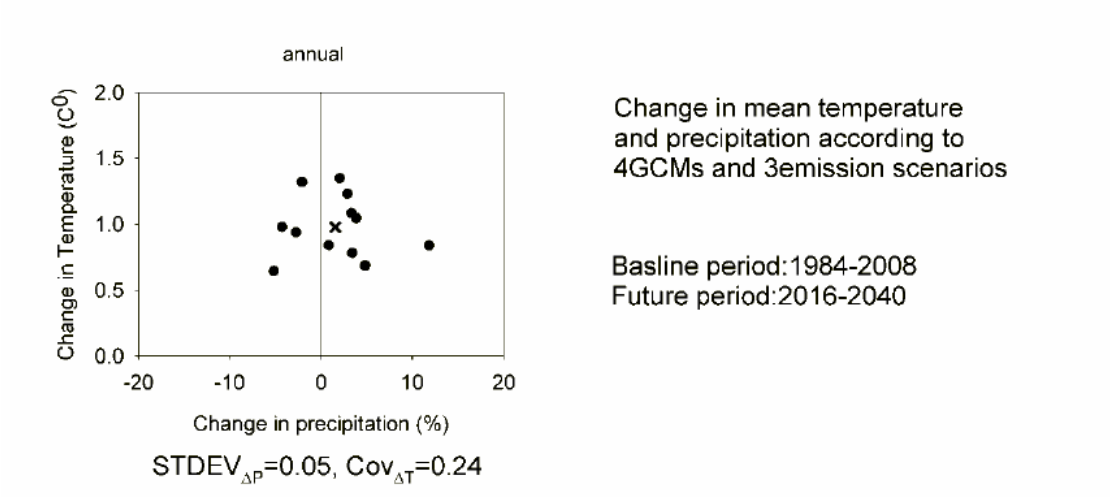

Figure 5-10 Changes in temperature and precipitation predicted by 4GCMs and 3 emission scenarios [Wang, 2011]

The recharge values used for the future years can be found in the Appendix in Table 9-3. It should be noted that the recharge values used for the years 2011-2030 were actually some extreme values simulated by SWAT for later years. We used them to study worst-case conditions.

Scenario 3: LU/LC and climate (dry) change- The third scenario that was developed to simulate both effects of LC/LU change as well as a dry climate change scenario. The dry climate

change scenario mentioned previously was used for the recharge estimates for this simulation. The recharge values assumed for future years can be found in the Appendix Table 9-4.

Scenario 4: LU/LC and climate (wet) change- The fourth scenario that modeled was identical to the third scenario that was modeled, but instead of using the dry climate change scenario, the wet climate change scenario was used. The same time shift that was previously mentioned for the recharge predictions was also applied for this scenario, and all other scenarios in which the climate change recharge values were used.

Scenario 5: LC/LU change, climate (dry) change, sea-level rise- The fifth scenario simulated was the dry climate change scenario discussed earlier, land cover/land use change, with the addition of sea level rise.

The rate of sea level rise used was 9.09 mm/year, or 0.36 inches/year. This value was estimated by Rahmstorf [2007] using a semi-empirical approach which connected global sea level rise to global mean surface temperature [*Rahmstorf*, 2007]. This is a relatively extreme value when compared to other values that have been suggested. Since our simulation time for sea level rise is 20 years, we can estimate a cumulative sea level rise of 7 inches. This value was used as the elevation at the head boundaries surrounding the island. Since the model was set to not use the same head values for the beginning and end of the simulation, the model is able to mimic a rising sea level. It should be noted that this is a somewhat idealized boundary condition since hypothetical vertical rise was assumed and inundation was ignored.

Scenario 6: LC/LU change, climate (dry) change, increased pumping- The sixth scenario that was simulated combined the dry climate change scenario and land use/land cover change, with the addition of increased pumping in the years of 2010-2030. The dry climate change as well as the land cover change scenarios has already been described. The increased pumping scenario depicts the groundwater situation with an increase in pumping due to a growing population on the island and increasing demand for freshwater. As seen in Figure 5-11, the population of Dauphin Island has been steadily increasing over the past 20 years.

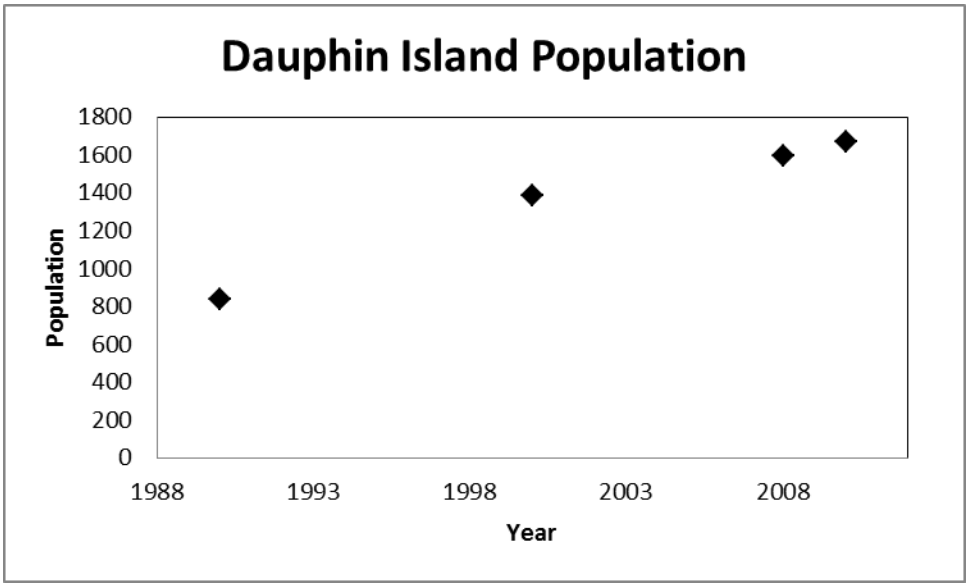

Figure 5-11. Dauphin Island population; data obtained from the United States Census Bureau.

If it is assumed that water demand will be directly reflected by the rate of population growth, then an approximation for the increase in water demand in the time period from 2010 to 2030 can be made. From the population data shown above, a percentage increase per year was calculated. It was estimated that the population increased about 2.5% every year. Using this as a guide, the pumping values were also increased 2.5% every year for each well starting in the year 2011. The exception to this was Well #40, as it is out of service and was assumed to remain

offline for the remainder of the simulation. The pumping values used for the years of 2011-2030 can be found in the Appendix Table 9-7.

While it may be extreme to assume that water demand so closely mirrors population growth, it will give us a conservative estimate for the demand on freshwater resources. This is beneficial because it best motivates more conservative water management and preservation practices on the island.

5.4 Results

The results of the scenario simulations will be presented in four formats. The first format will be the water-table elevation above sea level at the end of each simulation time. The second format will be plots of the location of the bottom of the saltwater-freshwater interface over time from 1990-2030. This will reveal whether or not upward intrusion occurs in any of the scenarios. The third format is the location of the saltwater-freshwater interface along the perimeter of the aquifer after each simulation in order to detect lateral intrusion. The fourth way will be the cumulative amount of freshwater stored in the water-table aquifer in the year 2030 at the end of each simulation.

5.4.1 Water-table elevations

The simulated groundwater elevation profile was plotted for Row 40 (Figure 5-14) of the model after each scenario was run. As shown in Figure 5-12 below, the head profiles all share a similar shape due to the well positioning but the height differs. The highest head profile was obtained from the Scenario 5, which was the sea level rise simulation. This is due to the "lifting effect." The increase in sea level "lifts" by acting as a wedge beneath the freshwater lifting the lens from below. It does not necessarily indicate anything about the quantity of freshwater in the

aquifer. The smallest profile was obtained from Scenario 6, which was the increased pumping simulation.

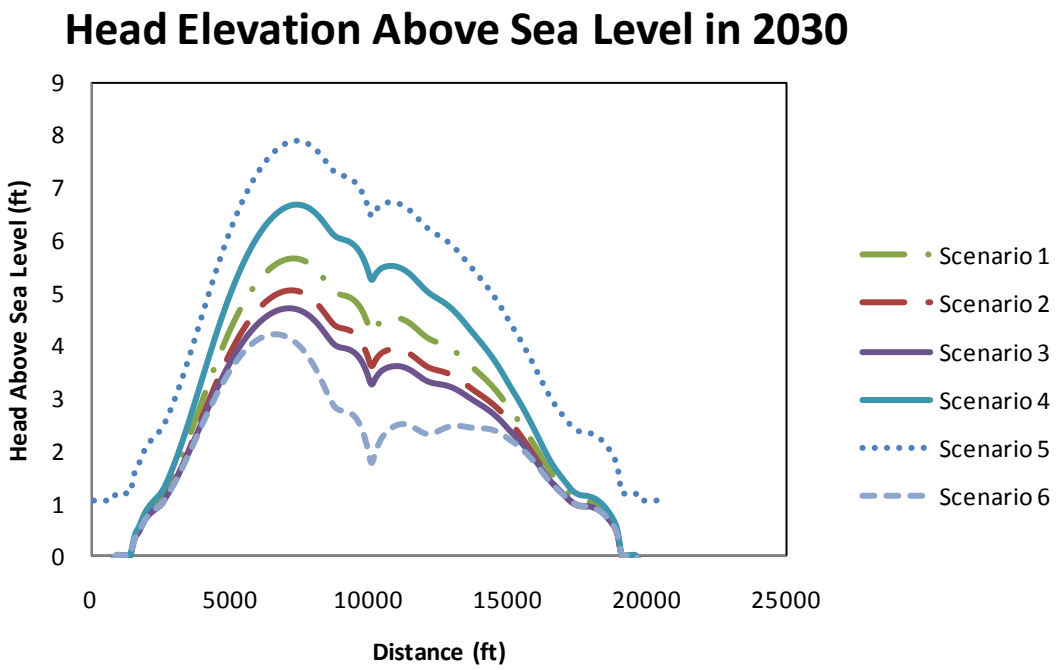

Figure 5-12. Predicted head Profiles at Row 40 under various scenarios.

5.4.2 Saltwater-freshwater interface

In order assess the position of the bottom freshwater-saltwater interface, a point in the grid was chosen and the bottom interface was found for this point at each time step. The interface was assumed to occur at 50% of the saltwater concentration. As shown in Figure 5-13, the lens was relatively flat along the bottom, so the crosscut was taken towards the middle in Row 40.

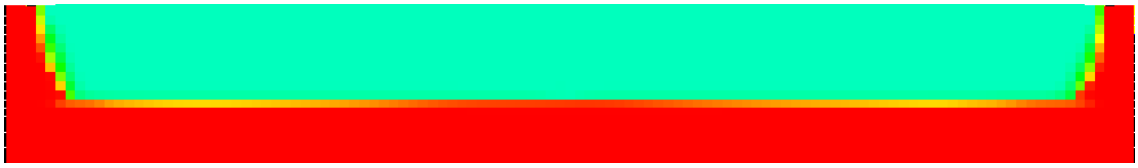

Figure 5-13. Cross-sectional view of freshwater lens beneath Dauphin Island.

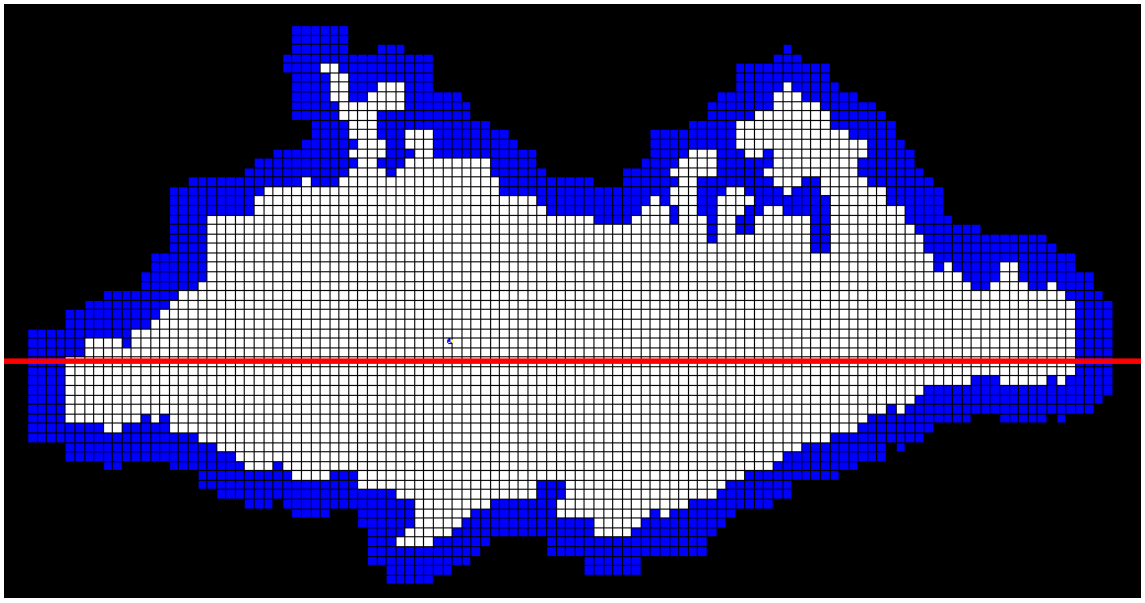

Figure 5-14. Location of Crosscut taken at Row 40

Figure 5-15 shows the comparison of the freshwater-saltwater interface using the soil moisture method for recharge estimation and using the plant evapotranspiration method for recharge estimation. As illustrated in the figure, the soil moisture method for estimating recharge push the interface down slightly as compared to the plant ET method. This is because the soil moisture method gives larger recharge values. Eventually, the interfaces match up at the depth where they hit the clay confining layer.

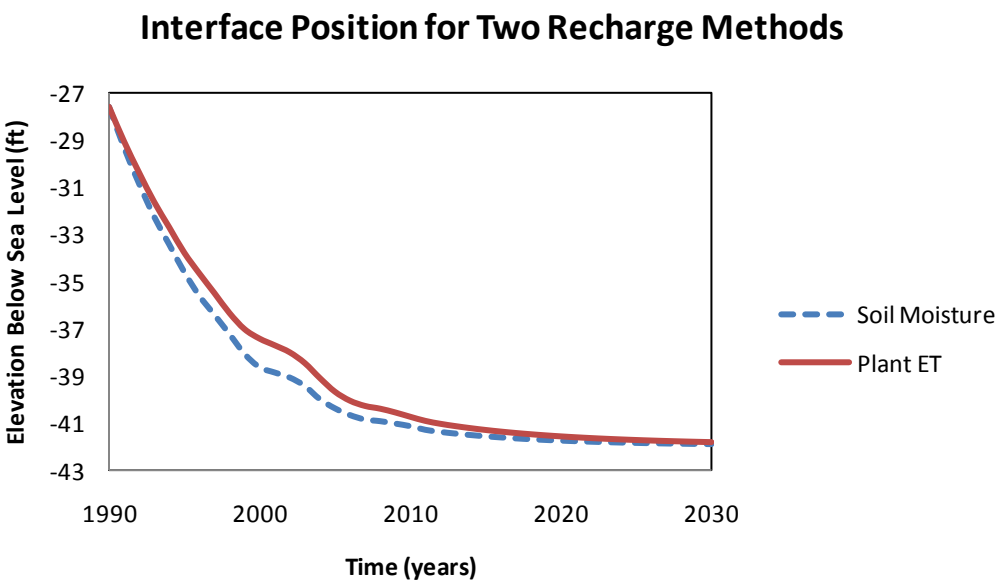

Figure 5-15. Comparison of interface using two recharge methods.

Figure 5-16 illustrates a comparison of both the soil moisture and plant ET based scenarios (the differences between the soil moisture and plant ET methods were described in Section 5.3.1) as well as Scenario 5, which includes LU/LC change and sea level rise. Interestingly, the interface position for the plant ET method for recharge estimation almost exactly matches the interface position for the sea level rise scenario.

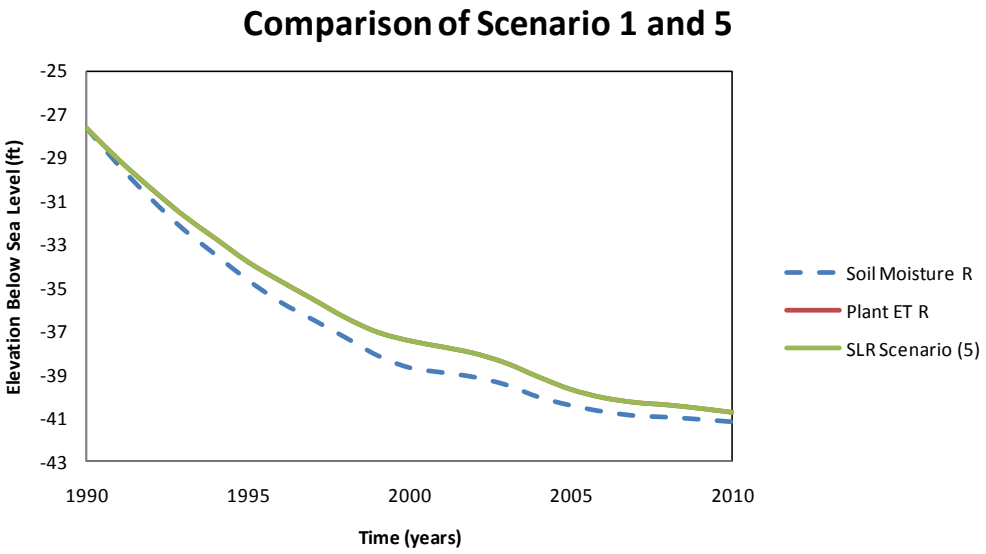

Figure 5-16. Comparison of interface position using scenarios 1 and 5.

Figure 5-17 displays the interface positions for each scenario. It should be noted that the recharge pattern used for the beginning of Scenarios 2, 3, 4, 5, and 6 was the plant ET recharge estimation method.

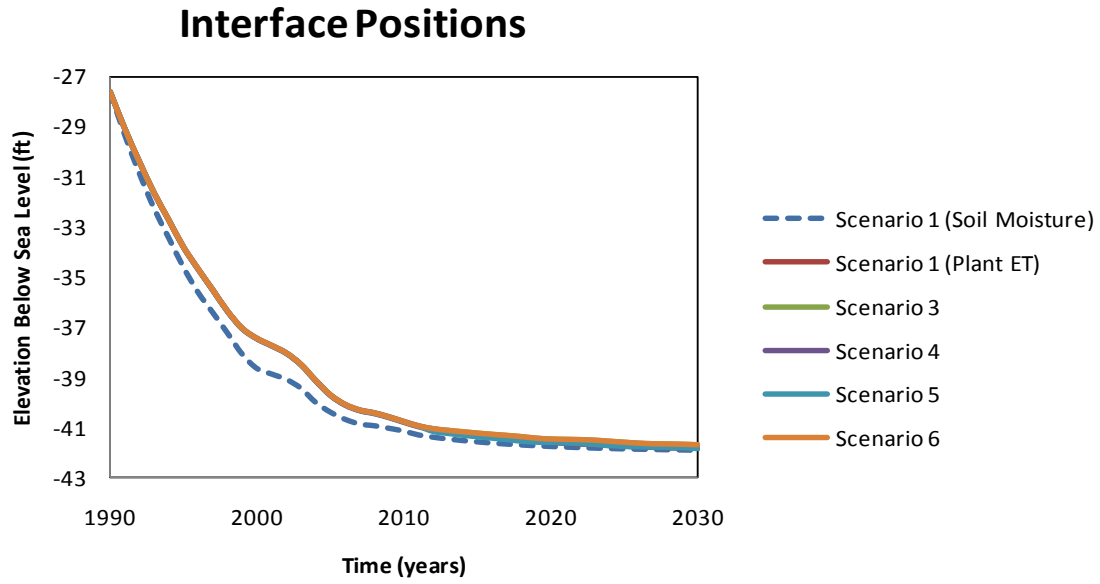

Figure 5-17. Comparison of interface position for all scenarios.

As shown in Figure 5-17, the bottom interface position is extremely insensitive to the changing factors on the island. Almost all of the interface positions are identical, especially after the model has been run for a long time. This response indicates no upward intrusion is occurring and is expected because of the characteristics of the aquifer, such as the confining layer below the shallow water-table, as well as the relatively large recharge inputs. Due to this response, it could be anticipated that lateral intrusion was occurring instead of upward intrusion.

5.4.3 Lateral movement of the saltwater-freshwater interface

The following figures are plan views of the island. In each comparison pair, the first figure is a plan cut at layer 9 at the beginning of the transient simulation [i.e., at steady state conditions] and the second figure is the same layer 9 cut at the end of the simulation period, 2030. The contour lines displayed are the head contours. The red indicates saltwater, the aqua indicates freshwater, and the colors in between indicate the mixing-interface. The 50% isochlor is located in this mixing interface. The figures illustrate significant intrusion occurring in some of the scenarios. Layer 9 is examined because that is the layer where most of the intrusion is occurring.

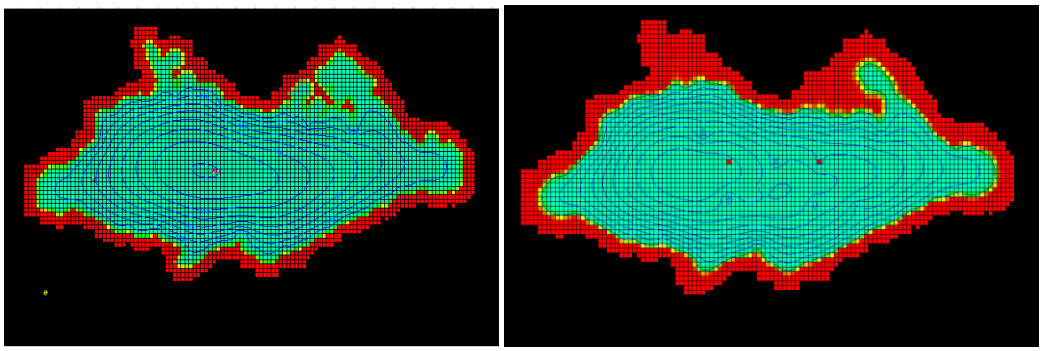

Figure 5-18. Saltwater-freshwater interface movement in Scenario 1.1.Red indicates saltwater, aqua indicates freshwater.

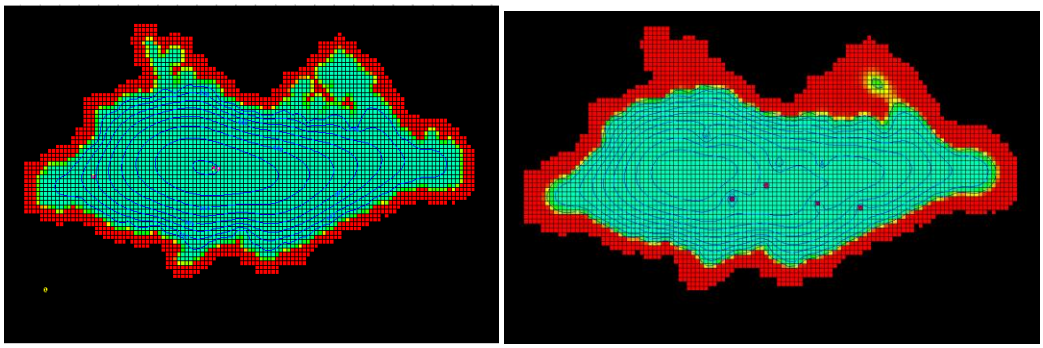

Figure 5-19. Saltwater-freshwater interface movement in Scenario 1.2. Red indicates saltwater, aqua indicates freshwater.

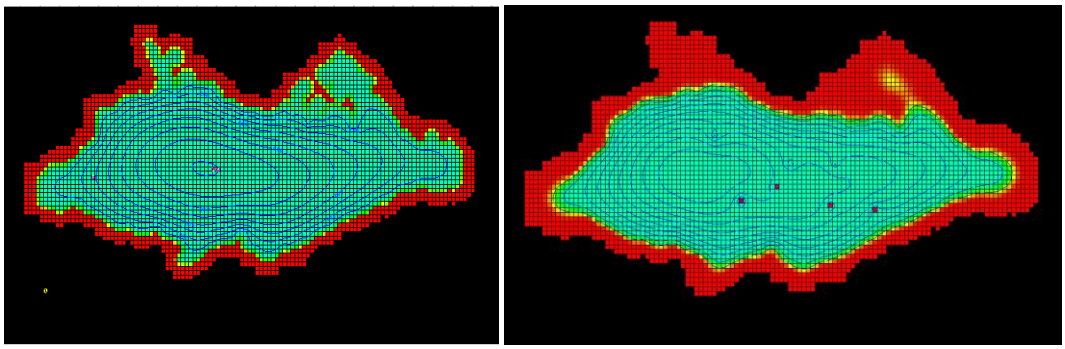

Figure 5-20. Saltwater-freshwater interface movement in Scenario 2. Red indicates saltwater, aqua indicates freshwater.

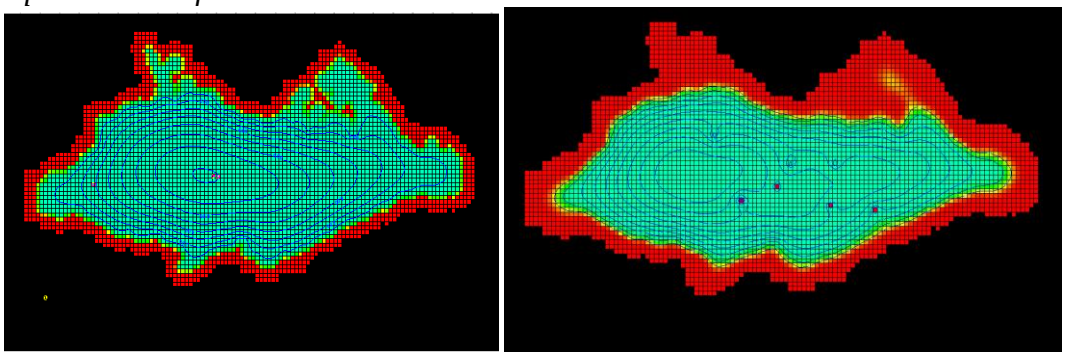

Figure 5-21. Saltwater-freshwater interface movement in Scenario 3. Red indicates saltwater, aqua indicates freshwater.

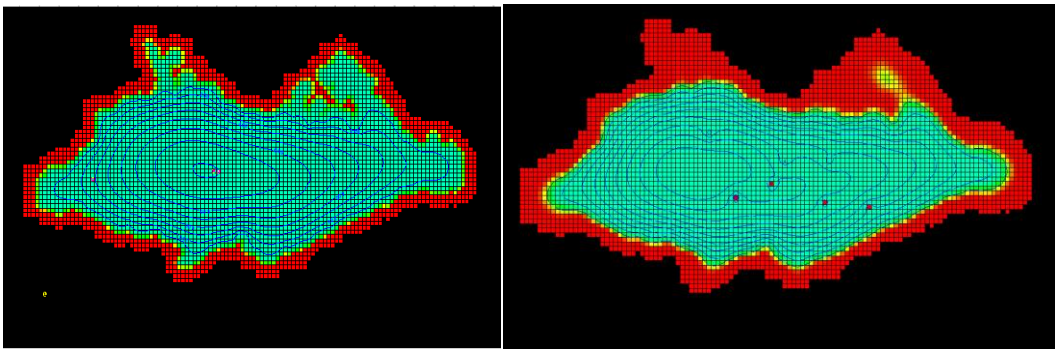

Figure 5-22. Saltwater-freshwater interface movement in Scenario 4. Red indicates saltwater, aqua indicates freshwater.

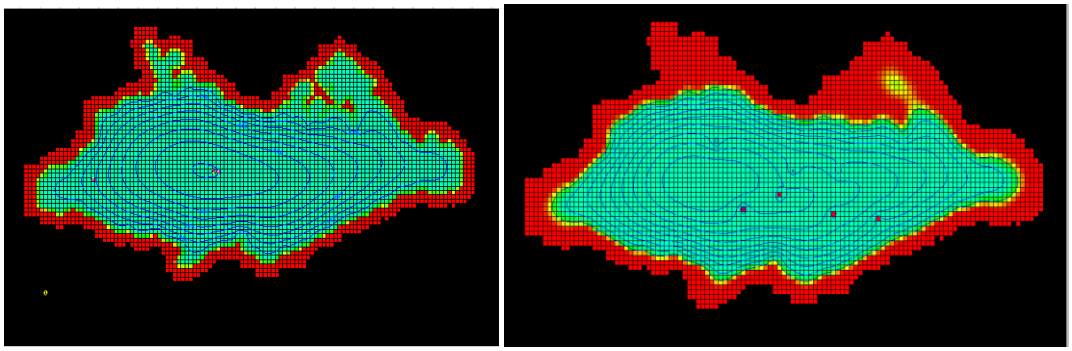

Figure 5-23. Saltwater-freshwater interface movement in Scenario 5. Red indicates saltwater, aqua indicates freshwater.

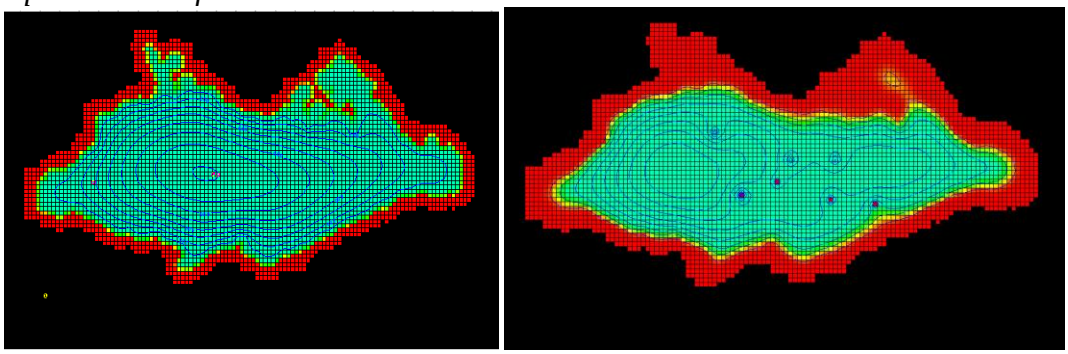

Figure 5-24. Saltwater-freshwater interface movement in Scenario 6. Red indicates saltwater, aqua indicates freshwater.

The following figures (Figures 5-25 through 5-31) are sectional cuts through the island at Column 91. The contour lines that are displayed are concentration contours, and they provide useful points of reference to compare the different concentration contours and intrusion occurring in the different scenarios.

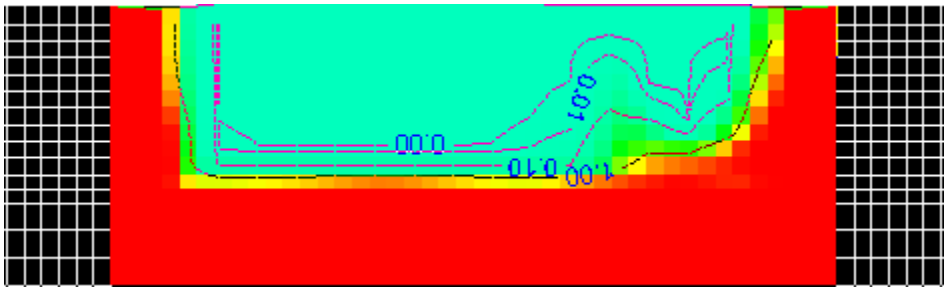

Figure 5-25. Saltwater-freshwater interface sectional cut for Scenario 1.1.

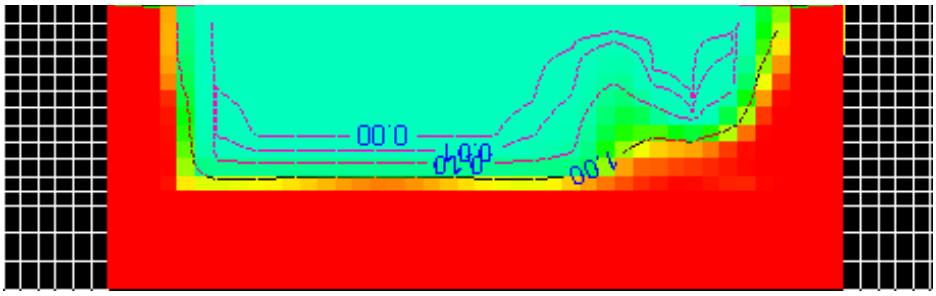

Figure 5-26. Saltwater-freshwater interface sectional cut for Scenario 1.2.

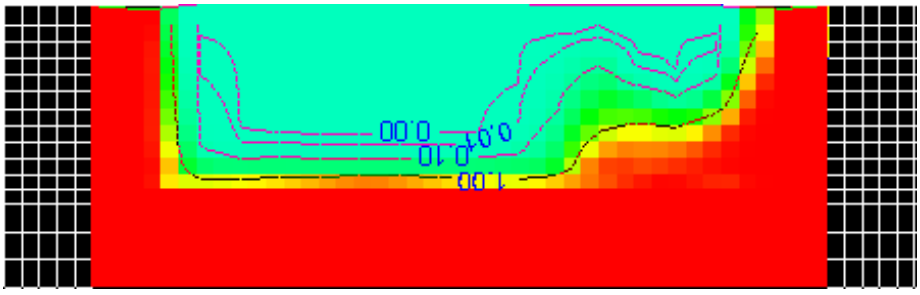

Figure 5-27. Saltwater-freshwater interface sectional cut for Scenario 2.

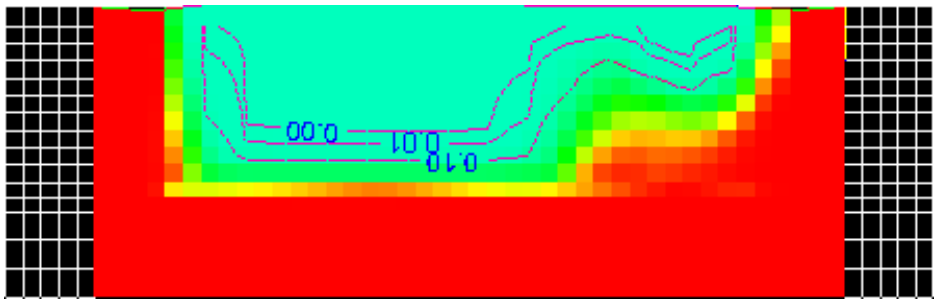

Figure 5-28. Saltwater-freshwater interface sectional cut for Scenario 3.

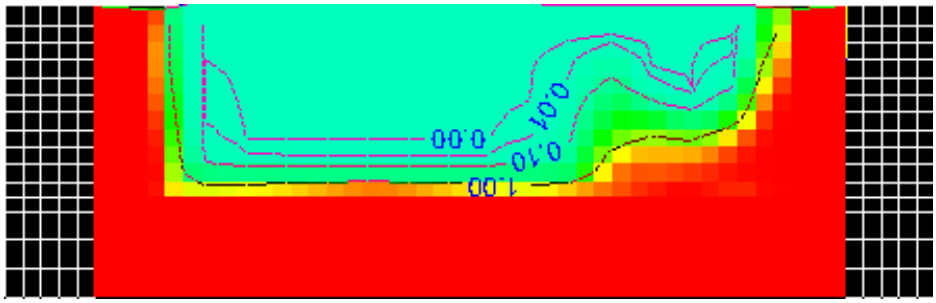

Figure 5-29. Saltwater-freshwater interface sectional cut for Scenario 4.

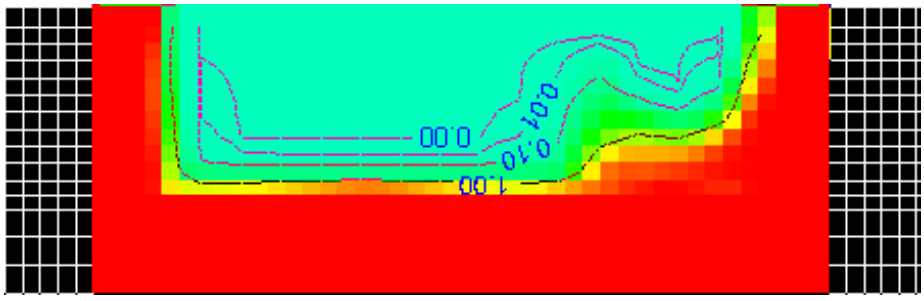

Figure 5-30. Saltwater-freshwater interface sectional cut for Scenario 5.

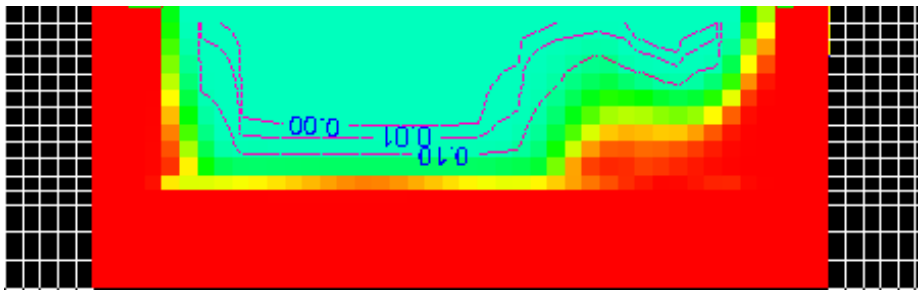

Figure 5-31. Saltwater-freshwater interface sectional cut for Scenario 6.

Figure 5-32 shows the same interface sectional cut view as seen in Figures 5-25 through 5-31 but all of the scenarios are displayed at once for the purpose of comparison. The values displayed in Figure 5-32 are the 50% isochlor positions for all of the scenarios. The saltwater intrusion is seen beginning to occur in some of the scenarios starting at around -27.5 below mean sea level. Figure 5-33 shows where the crosscut was taken in order to construct Figure 5-32.

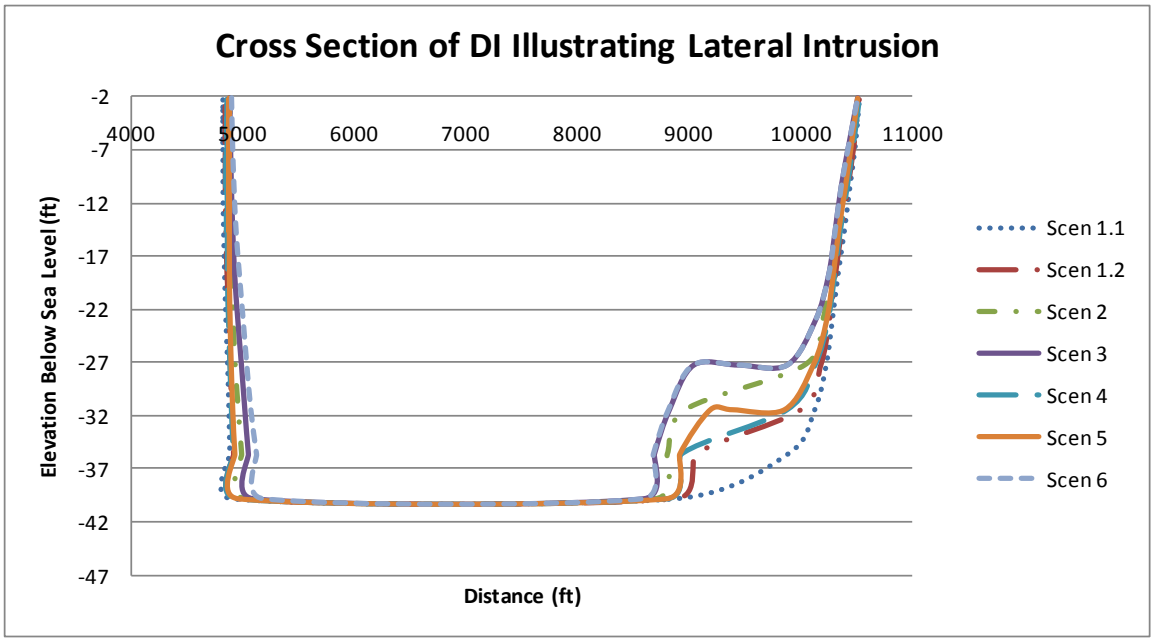

Figure 5-32. Cross Section of DI illustrating lateral intrusion (crosscut taken at Col 91)

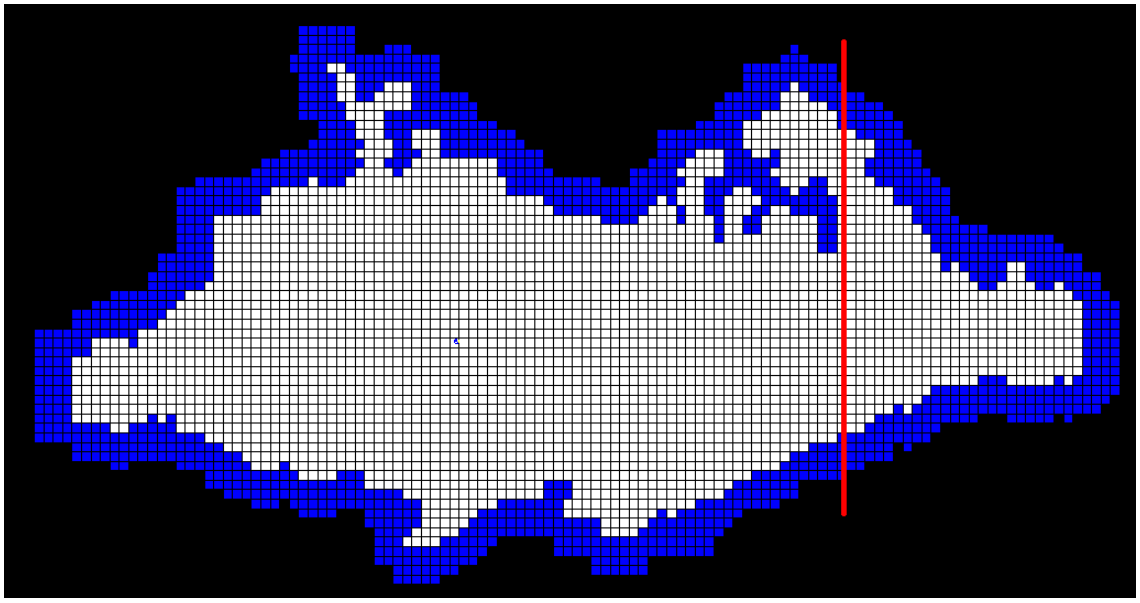

Figure 5-33. Location of crosscut taken at Column 91

5.4.4 Volume of freshwater contained in the water-table aquifer

Another method to express the effects of the different factors in each scenario is to quantify the results of each run by calculating the amount of freshwater contained in the aquifer at the end of each simulation. Freshwater was defined using the same protocol used in defining the saltwater-freshwater interface used in the earlier study. Water with a saltwater concentration less than 1.09 lbs/ft^3 was considered freshwater. This value was chosen because it is 50% of the concentration of pure saltwater. In reality, the secondary standard for drinking water is much lower than this 50% value. The standard set by the EPA is 250 mg/L of chloride [*EPA Drinking Water Contaminants*, 2011]. This is equivalent to about 0.016 lbs/ft^3.

A short code was written in Visual Basic to calculate the number of total grid cells containing freshwater at the end of each scenario run. Since the size of the grid cells was known, the volume of the total number of grid cells containing freshwater could be calculated. Then, the volume of freshwater was calculated by multiplying the volume of cells that contained water

with a saltwater concentration less than 1.09 lbs/ft^3 by the porosity of the medium, which was 0.3. Table 5-7 shows the volume calculations.

Table 5-7. Volume of Freshwater in Aquifer after Scenarios are Simulated.

Scenario	# Freshwater Grid Cells	Volume of Cells [ft^3]	Volume of Freshwater [ft^3]	% of Vol of 1.1
1.1	29004	3276384653	9.83E+08	
1.2	28325	3199682640	9.60E+08	100.00
2	27840	3144895488	9.43E+08	98.29
3	27085	3059608272	9.18E+08	95.62
4	28293	3196067818	9.59E+08	99.89
5	26998	3049780474	9.15E+08	95.32
6	26739	3020523005	9.06E+08	94.40

The percentages were calculated in relation to Scenario 1.2 since that was the base-case recharge used for the years 1990-2010 in all of the simulations except 1.1. As illustrated by the percentage change in volume, decreasing recharge due to climate change had the largest effect on the groundwater resource. Land cover had the next largest effect, while sea level rise and increased pumping had a significant effect on the aquifer.

5.5 Discussions

The sensitivity simulation results indicate that the aquifer was most sensitive to change in climate causing a decrease in recharge patterns. The largest change in aquifer volume attributed to a single factor was from a decrease in recharge due to climate change. The only volume reported smaller than the volume after the dry climate change was the scenario with LC/LU change. The addition of dry climate change to the LC/LU simulation led to the greatest change in percentage, so it was concluded that climate change had the largest effect.

The other factors did not cause as much of a change in the amount of freshwater contained in the aquifer. These conclusions are based on the volume of freshwater contained in the aquifer at the end of the simulation period. The figures showing lateral intrusion from a plan view are

helpful for visualization purposes, but they do not provide the full picture since only one layer (layer 9) is shown.

When the simulation results are represented as percentage decrease in freshwater from the initial conditions, it does not appear as though the aquifer is very sensitive to changes in climate and pumping scenarios. The largest decrease in percentage of freshwater was about 6%. This does not indicate, however, that the aquifer should be exploited without concern.

While it does seem that the pumping from the aquifer is very sustainable, careful attention should be drawn to the figures that show the lateral movement of the saltwater-freshwater interface. In some of the scenarios, especially the increased pumping scenario (6), the interface moves in towards Well 80, located on the southeast coast of the island. If pumping were to increase over what was simulated, especially in Well 80, the water being pumped could be significantly contaminated.

6. Sustainable yield study for Dauphin Island

6.1 Background

An additional study was done in order to quantify the percentage of the annual average values that could be pumped without serious problems occurring. For this study, a "serious problem" was defined as saltwater being pumped into any of the wells and thus contaminating the water source.

This was a valuable study because all of the scenarios presented in the previous section were hypothetical. It is impossible to accurately predict how much land cover and climate change will occur in the coming years. By studying what percentage of recharge the aquifer can safely yield, the future management practices can be tailored to fit the actual scenarios on a yearly basis. Once again, the concentration identified as problematic was anything over 1.09 lbs/ft^3, or 50% saltwater concentration, detected by the wells.

6.1.1 Research Objectives

The main objective for this section was to identify what percentage of annual recharge could be safely extracted from the aquifer without the possibility of saltwater contaminating any wells. This was found for both uniform average annual recharge as well as for recharge values that varied year to year.

6.2 Input Data and Study Methodology

The same general groundwater model developed in SEAWAT for the previous transient simulations was used. The simulation period was kept the same for this study (1990-2030), as we already had recharge values for that time period. Additionally, all other parameter values that were used in the previous section, such as hydraulic conductivity, porosity, etc. were all kept the same.

In the model, we inserted a new monitoring well in the grid right next to the cell containing Well 80. Refer to Figure 4-7 to see the location of Well 80, located on the southeast shore of the island. It was inserted in this location because Well 80 is most prone to saltwater intrusion since it was closest to the shore and one of the deepest wells. By monitoring the cell next to Well 80 we can get a conservative estimate for the amount of water that can be pumped, as we would be detecting the contamination right before it would reach the well. Also, the cone of depression caused by pumping could become large enough to reach the surrounding cells around Well 80. The monitoring well is capable of monitoring head and concentration over time, without pumping, so it does not affect the groundwater levels or concentration.

For the first part of the study, the model was simplified and a uniform average recharge value was used for every year. Therefore, the recharge was the same year to year, and this also resulted in the pumping being the same year to year as that was a percentage of recharge. Some conversions had to be done to calculate pumping rates.

Since recharge is input in the model in the units of [L/T], the recharge values had to be multiplied by the simulated area of the island. By doing this, recharge was obtained in the units $[L^3/T]$, and we were able to calculate percentages from this to be pumped.
The first scenario simulated was 20% of the recharge, next was 30% and so on. This was continued until the monitoring well detected concentrations at or above 1.09 lbs/ft^3, which would indicate saltwater intruding and reaching the well.

Once the concentration in the monitoring well reached or exceeded 1.09 lbs/ft^3 the value was noted. However, since the pumping had been increased in rather large increments (10% at a time) and it was possible that saltwater had also reached the well at percentages between the last simulation and the simulation it was detected in. The next task was to attempt to find a smaller

range that would provide a sustainable yield. The pumping rates were then decreased in smaller increments until a level was reached where intrusion did not occur. This provides us with a range of values to recommend for future pumping scenarios.

A similar protocol was followed for the second part of the study where instead of uniform yearly recharge, the recharge varied from year to year. The annual recharge estimates used in this section of the study were the same ones used previously for Scenario 1.2 in the previous chapter. These were the SWAT recharge estimations that were run for Dauphin Island using the plant evapotranspiration method within SWAT, and assuming no climate change.

6.3 Results

This section discusses the results obtained when the uniform recharge and varying recharge simulations were simulated in an effort to determine what percentage of recharge could be pumped without introducing saltwater into any of the wells.

6.3.1 Uniform Recharge

Concentrations at or above 1.09 lbs/ft^3 were first detected at the pumping rate of 60% of the average annual recharge values. Since the last simulation that had been done was pumping at the rate of 50% of the recharge values, the scenario of 55% was simulated in order to try to narrow the range in which saltwater is introduced. When 55% of the recharge was pumped, the monitoring well detected concentrations above 1.09 lbs/ft^3 at about 124 months into the simulation, as shown in Figure 6-1. Since the 50% pumping scenario did not yield concentrations above 1.09 lbs/ft^3, it is gathered that saltwater flows into the well at pumping rates of somewhere between 50%-55% and higher. Figure 6-2 shows the 50% isochlor reaching well 80. While the percentage range could have been narrowed down farther, this is acceptable

for our screening calculations, as there will be some degree of uncertainty caused by natural properties and heterogeneities not taken into account by this preliminary model.

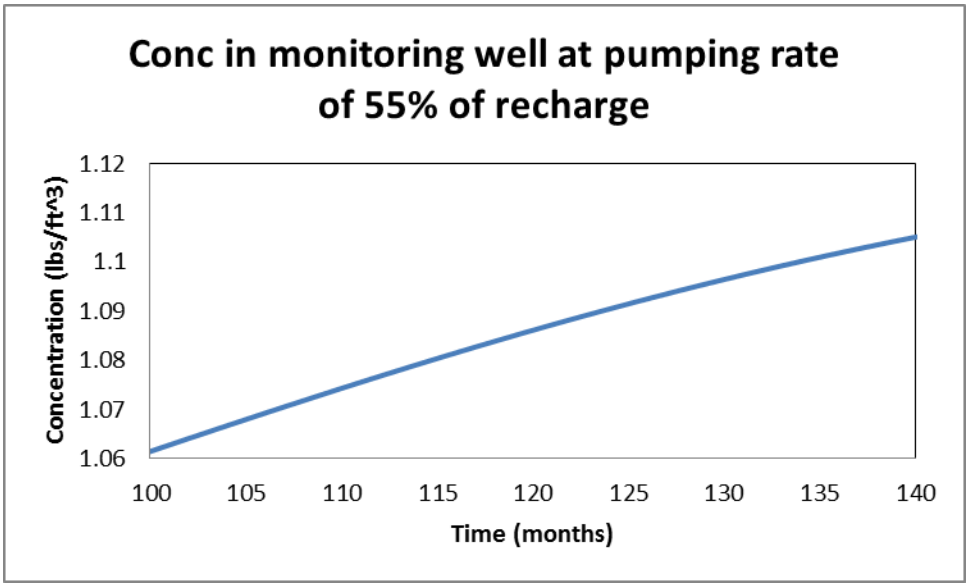

Figure 6-1. Concentration at Monitoring well, detected conc. of 1.09 lbs/ft^3 at 124 months

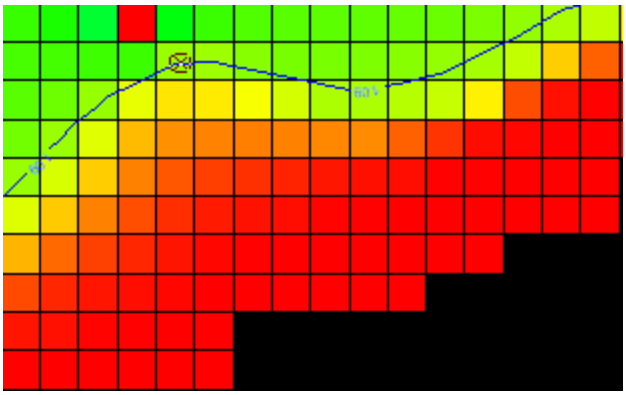

Figure 6-2. Isochlor at 124 months, showing conc. of 1.09 lbs/ft^3 reaching the monitoring well.

6.3.2 Varying Recharge

Using the varying annual recharge values, concentrations at or above 1.09 lbs/ft^3 were first detected at the pumping rate of 60% of the annual recharge values. The concentration was

detected at 1.09 lbs/ft^3 at about 73 months into the simulation, as shown in the figure below. Concentration had not met or exceeded 1.09 lbs/ft^3 in the 55% simulation, so saltwater contamination at the monitoring well is suggested to occur in the range of 55%-60% of the annual recharge values.

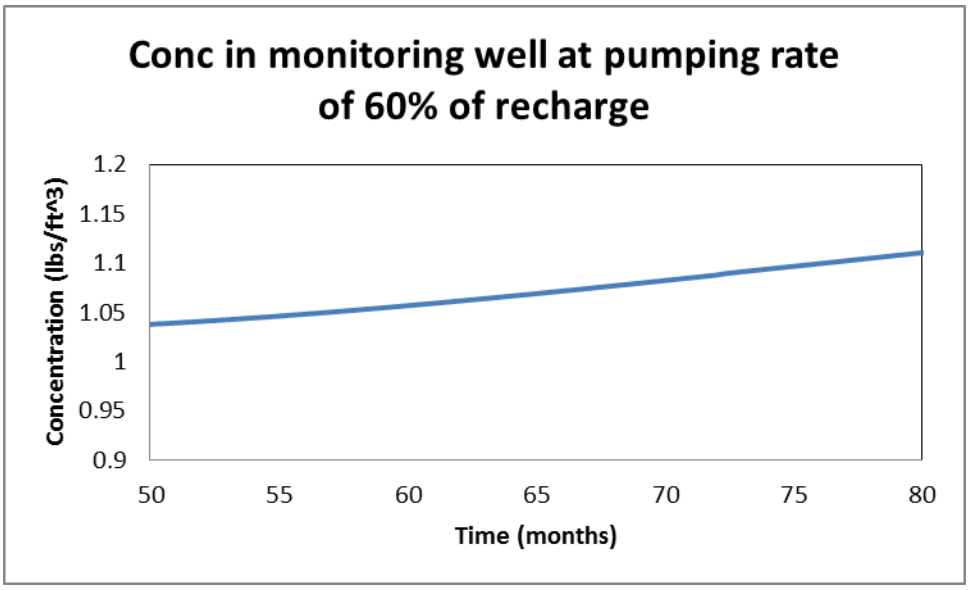

Figure 6-3. Concentration at Monitoring well, detected conc. of 1.09 lbs/ft^3 at 73 months

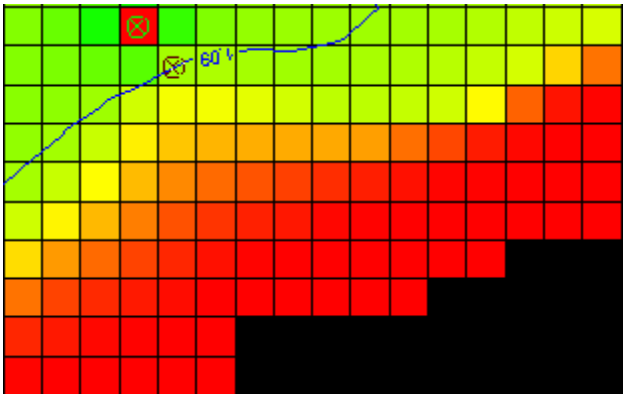

Figure 6-4. Isochlor 73 months, showing conc. of 1.09 lbs/ft^3 reaching the monitoring well.

6.4 Discussions

It is important to note that the ranges presented in the results for the two pumping scenarios are not claimed to be the sustainable yield pumping percentages for the entire aquifer. They are simply the ranges where saltwater contaminant might not occur in any of the wells in the pumping system.

While a formal optimization was not performed, it can still be conjectured that if Well 80 were to pump smaller amounts than the other wells and the difference was distributed between the seven remaining wells, the sustainable yield for the aquifer would go up substantially. The 50% isochlor did not approach any of the other wells closely, even when the pumping was increased to levels of approximately 70% of the annual recharge values.

Another important aspect observed in this study is that while the average recharge and pumping scenario and the varied recharge and pumping scenario gave different results, the results were still relatively similar. This would suggest that in some cases where screening calculations are needed for a very complex model, it would most likely be sufficient to use average annual recharge values for the entire simulation period.

7. Conclusions and Recommendations

A review of literature indicated that obtaining a relationship between land cover and groundwater recharge amounts was achieved in several locations in the United States. In this study, several methods were explored to estimate recharge at seven sites in the Southeast, and these recharge estimates were related to land cover by calculating the curve number for these sites and applying appropriate relationships. However, a consistent relationship was not found between the land cover of each site and the amount of groundwater recharge.

A calibrated, steady-state and transient model for Dauphin Island was successfully developed using SEAWAT. The groundwater model was calibrated against previously published results. By simulating a variety of scenarios we were able to test the sensitivity of the island's unconfined aquifer to parameters such as land-cover change, climate change, and increased pumping due to expected population growth. The Dauphin Island models that were developed could also be applied in the future to simulate other groundwater situations on the island.

The model predicted that a decrease in groundwater recharge due to climate change would have the greatest effect on the island's freshwater resources. This was determined by calculating the volume of freshwater contained in the aquifer at the end of each simulation. Additionally, it was observed that changing land cover, sea level rise, and the expected increased pumping level have a very little effect on the freshwater resources of the island. Saltwater intrusion was detected in several of the scenarios. While the total volume of freshwater did not decrease significantly with any of the scenarios simulated, lateral intrusion did suggest that the changing factors could eventually lead to saltwater contamination in the outer wells.

The existing Dauphin Island groundwater model used in the sensitivity analysis was subsequently utilized to determine a sustainable pumping amount for the Dauphin Island aquifer.

A monitoring well was positioned next to the pumping well most prone to saltwater contamination. Pumping amounts were expressed as a function of recharge amounts. It was found that approximately 50%-55% of recharge could be withdrawn from the aquifer under the uniform pumping scenario. The average of the actual percentage of recharge that was pumped in 2009-2010 was 39%. This indicates that the current pumping levels are relatively sustainable. However, further site specific field assessments need to be made to validate these predictions. The study also illustrated that using uniform average recharge values would likely be sufficient for large, complex groundwater models.

In conclusion, additional research is needed to establish a relationship between land cover and groundwater recharge amounts in the Southeast. Perhaps the study should first be done on a smaller scale until the method is refined, and then extended to a more regional scale. Further research is also needed to develop an optimization tool for locating pumping wells in Dauphin Island. By performing an optimization study, a more sustainable pumping pattern that could allow exploitation of the groundwater resource without the problem of saltwater intrusion would be developed.

8. References

Andersen, P. F., J. W. Mercer and H. O. White (1988). "Numerical Modeling of Salt Water Intrusion at Hallandale, Florida." *Groundwater* (26), 619-630.

Arnold, J. G. and N. Fohrer (2005). "SWAT2000: current capabilities and research opportunities in applied watershed modelling." *Hydrological Processes* (19), 563-572.

Arnold, J. G., R. S. Muttiah, R. Srinivasan and P. M. Allen (2000). "Regional estimation of base flow and groundwater recharge in the Upper Mississippi river basin." *Journal of Hydrology* (227), 21-40.

Arnold, J. G., J. R. Williams, R. Srinivasan and K. W. King (1996). "The Soil and Water Assessment Tool (SWAT) User's Manual." Temple, TX.

Balci, "Verification, Validation, and Testing", in J. Banks (Ed.), *Handbook of Simulation: Principles, Methodology, Advances, Applications, and Practice*, John Wiley & Sons, New York NY, 1998, pp. 335-393.

Barlow, P. M. and E. G. Reichard (2010). "Saltwater intrusion in coastal regions of North America." *Hydrogeology Journal* (18), 247-260.

Bedient, P. B. and W. C. Huber (1992). *Hydrology and floodplain analysis*, Addison Wesley Publishing Company.

Bras, R. L. (1990). *Hydrology: an introduction to hydrologic science*, Addison-Wesley Reading, Massachusetts, USA.

Caldwell, J (1996). "Dauphin Island Water and Sewer Report."

Cecan, L., G. Nelson, C. McLane, and M. Metheny (2008). Evaluating safe yield for supply wells in an aquifer with fresh water/salt water interface. In *Proceedings of the 20th Salt*

Water Intrusion Meeting, Naples, Florida, USA, ed. C.Langevin, L.Lebbe, M.Bakker, and C.Voss, 163–166. Reston, Virginia: USGS.

Chandler, R. V., B. Gillett and S. S. DeJarnette (1983). Hydrogeologic and water-use data for southern Baldwin County, Alabama, Geological Survey of Alabama, Hydrogeology Division.

Chang, S. W., T. Prabhakar Clement, M. J. Simpson and K. K. Lee (2011). "Does Sea-level Rise Have an Impact on Saltwater Intrusion?" *Advances in Water Resources*. (In Press)

Cherkauer, D. S. and S. A. Ansari (2005). "Estimating ground water recharge from topography, hydrogeology, and land cover." *Ground water* (43), 102-112.

Chesnaux, R. and D. M. Allen (2008). "Groundwater travel times for unconfined island aquifers bounded by freshwater or seawater." *Hydrogeology Journal* (16), 437-445.

Chow, V. T., D. R. Maidment and L. W. Mays (2005). *Applied hydrology*, McGraw-Hill New York,, USA.

Crosbie, R. S., P. Binning and J. D. Kalma (2005). "A time series approach to inferring groundwater recharge using the water table fluctuation method." *Water Resources Research* (41)

Crosbie, R. S., I. D. Jolly, F. W. Leaney and C. Petheram (2005). "Can the dataset of field based recharge estimates in Australia be used to predict recharge in data-poor areas?" *Hydrology and Earth System Sciences Discussions* 7.

Delin, G. N., R. W. Healy, D. L. Lorenz and J. R. Nimmo (2007). "Comparison of local- to regional-scale estimates of ground-water recharge in Minnesota, USA." *Journal of Hydrology* (334), 231-249.

Diersch, H.-J. G. (2005), FEFLOW: Finite Element Subsurface Flow and Transport Simulation System, Inst. for Water Resources Planning and System Res., Berlin.

Fetter, C.W., *Applied Hydrogeology*, 4th ed., Prentice Hall, Inc., New Jersey, 2001.

Fritz, H. M., C. Blount, R. Sokoloski, J. Singleton, A. Fuggle, B. G. McAdoo, A. Moore, C. Grass and B. Tate (2007). "Hurricane Katrina storm surge distribution and field observations on the Mississippi Barrier Islands." Estuarine, *Coastal and Shelf Science* (74), 12-20.

Goswami, R. R. and T. P. Clement (2007). "Laboratory-scale investigation of saltwater intrusion dynamics." *Water Resources Research* (43).

Guo, W. and C. D. Langevin (2002). User's Guide to SEWAT: A Computer Program for Simulation of Three-Dimensional Variable-Density Ground-Water Flow, United States Geological Survey.

Harbaugh, A.W., Banta, E.R., Hill, M.C., and McDonald, M.G., (2000), MODFLOW-2000, The U.S. Geological Survey Modular Ground-Water Model—User guide to modularization concepts and the ground-water flow process: U.S. Geological Survey Open-File Report 00-92, 121 p.

Henry, H. R. Effects of dispersion on salt encroachment in coastal aquifers. US Geological Survey Water-Supply Paper; 1964. p. C71–84.

Heppner, C. S., J. R. Nimmo and M. P. C. A. Geological Survey (2005). Computer Program for Predicting Recharge with a Master Recession Curve, United States Geological Survey.

Homer, C. C. Huang, L. Yang, B. Wylie and M. Coan. (2004). Development of a 2001 National Landcover Database for the United States. *Photogrammetric Engineering and Remote Sensing*, (70), 829-840.

Jocson, J. M. U., J. W. Jenson and D. N. Contractor (2002). "Recharge and aquifer response: northern Guam lens aquifer, Guam, Mariana Islands." *Journal of Hydrology* 260(1-4): 231-254.

Kalin, Latif. Class Lecture. Auburn University, Auburn, AL. 26 Jan 2010.

Kidd, R.E., (1988). Hydrogeology and Water-Supply Potential of the Water-Table Aquifer on Dauphin Island, Alabama. U.S. Geological Survey Scientific Investigations Report 87-4283, 49p.

Larabi, A., M. Faouzi and A. H. D. Cheng (2008). Assessment of Groundwater Resources in Rmel Coastal Aquifer (Morocco) by SEAWAT.

Lin, J., J. B. Snodsmith, C. Zheng and J. Wu (2009). "A modeling study of seawater intrusion in Alabama Gulf Coast, USA." *Environmental Geology* (57),119-130.

Liu, J., Rich, K., Zheng, C., 2007, Sustainability analysis of groundwater resources in a coastal aquifer, Alabama, *Environmental Geology* DOI 10.1007/s00254-007-0791-x.

Loáiciga, H. A., T. J. Pingel and E. S. Garcia (2011). "Sea Water Intrusion by Sea Level Rise: Scenarios for the 21st Century." *Ground water*.

Lyon, S. W., M.T. Walter, P. Gérard-Marchant, and T.S. Steenhuis (2004). "Using a topographic index to distribute variable source area runoff predicted with the SCS curve-number equation." *Hydrological Processes* (18), 2757–2771.

Mahesha, A. and S. H. Nagaraja (1996). "Effect of natural recharge on sea water intrusion in coastal aquifers." *Journal of Hydrology* (174), 211-220.

Martínez-Santos, P. and J. M. Andreu (2010). "Lumped and distributed approaches to model natural recharge in semiarid karst aquifers." *Journal of Hydrology* (388), 389-398.

Masterson, J.P. (2004). Simulated interaction between freshwater and saltwater and effects of ground-water pumping and sea-level change, Lower Cape Cod aquifer system, Massachusetts. USGS Scientific Investigations Report 2004–5014. USGS.

McElroy, Gary. "New Dauphin Island well will provide better water, say officials." Al.com. 8 January 2010. 26 April 2011. <http://blog.al.com/live/2010/01/new_dauphin_island_well_will_p.html>

Michel, C., A. Andreassian, and C. Perrin (2005). "Soil Conservation Service Curve Number method: how to mend a wrong soil moisture accounting procedure." *Water Resources Research* (41).

Mishra, S. K. and V. P. Singh (1999). "Another look at SCS-CN method." *Journal of Hydrologic Engineering* (257).

Mollema PN, Marco Antonellini, Tomaz Dentinho and Vasco R. M. Silva (2010). The Effects of Climate Change on the Hydrology and Groundwater of Terceira Island (Azores). In: Proceedings of the Salt Water Intrusion Meeting June 21-25 Sao Miguel Azores, Portugal.

Morton, R.A. (2008). "Historical changes in the Mississippi-Alabama barrier-island chain and the roles of extreme storms, sea level, and human activities." *Journal of Coastal Research,* (24), 1587–1600.

Murgulet, D. and G. Tick (2008). "The extent of saltwater intrusion in southern Baldwin County, Alabama." *Environmental Geology* (55), 1235-1245.

Nachabe, M., N. Shah, M. Ross, and J. Vomacka (2005). "Evapotranspiration of two vegetation covers in a shallow water table environment." *Soil Science Society of America Journal* (69), 492–499.

O'Donnell, Daniel. (2005) "Baseline Assessment Report 2005 for Dauphin Island Water and Sewer Authority's Public Water Supply Wells."

Praveena, S. M. and A. Z. Aris (2009). "Groundwater resources assessment using numerical model: A case study in low-lying coastal area." *International Journal of Environmental Science and Technology* (7), 135-146.

Rahmstorf, S. (2007). "A semi-empirical approach to projecting future sea-level rise." *Science* (5810), 368.

Ranjan, P., S. Kazama and M. Sawamoto (2006). "Effects of climate change on coastal fresh groundwater resources." *Global Environmental Change* (16), 388-399.

Rao, S. V. N., V. Sreenivasulu, S. M. Bhallamudi, B. S. Thandaveswara and K. P. Sudheer (2004). "Planning groundwater development in coastal aquifers." *Hydrological Sciences Journal* (49), 155-170.

Rutledge, A. T. (2007). "Update on the use of the RORA program for recharge estimation." *Ground water* (45), 374-382.

Samper, J. and B. Pisani (2009). "Aquifer recharge evaluation by a combination of soil water balance and groundwater flow models." *Estudios en la Zona no Saturada del Suelo* 19.

Scanlon, B. R., R. C. Reedy, D. A. Stonestrom, D. E. Prudic and K. F. Dennehy (2005). "Impact of land use and land cover change on groundwater recharge and quality in the southwestern US." *Global Change Biology* (11), 1577-1593.

Sherif, M. M. and V. P. Singh (1999). "Effect of climate change on sea water intrusion in coastal aquifers." *Hydrological Processes* (13), 1277-1287.

Singh, H. V. (2010) Modeling impact of Land Use/Cover changes on Water Quality and Quantity of Fish River Watershed (M.S. Thesis) Auburn University.

Soil Survey Staff, Natural Resources Conservation Service, United States Department of Agriculture. Soil Survey of Baldwin County, AL. (Online WWW) Available URL: "http://soildatamart.nrcs.usda.gov/Survey.aspx?County=AL003" (Accessed 5 March 2011).

Soil Survey Staff, Natural Resources Conservation Service, United States Department of Agriculture. Soil Survey of Covington County, AL. (Online WWW) Available URL: "http://soildatamart.nrcs.usda.gov/Survey.aspx?County=AL039" (Accessed 5 March 2011).

Soil Survey Staff, Natural Resources Conservation Service, United States Department of Agriculture. Soil Survey of Montgomery County, AL. (Online WWW) Available URL: "http://soildatamart.nrcs.usda.gov/Survey.aspx?County=AL101" (Accessed 5 March 2011).

Soil Survey Staff, Natural Resources Conservation Service, United States Department of Agriculture. Soil Survey of Escambia County, FL. (Online WWW) Available URL: "http://soildatamart.nrcs.usda.gov/Survey.aspx?County=FL033" (Accessed 5 March 2011).

Sophocleous, M. A. (1991). "Combining the soilwater balance and water-level fluctuation methods to estimate natural groundwater recharge: practical aspects." *Journal of Hydrology* (124), 229-241.

Sun, H. and P. S. Cornish (2005). "Estimating shallow groundwater recharge in the headwaters of the Liverpool Plains using SWAT." *Hydrological Processes* (19), 795-807.

Wang, H. F. and M. P. Anderson (1982). *Introduction to groundwater modeling*, Freeman.

Wang, R. (2011) Modeling Hydrologic and Water Quality Responses to Changing Climate and Land Use/Cover in the Wolf Bay Watershed, South Alabama (M.S. Thesis) Auburn University.

Webb, M. D. and K. W. F. Howard (2010). "Modeling the Transient Response of Saline Intrusion to Rising Sea Levels." *Ground water* (49), 560-569.

Zhang, Y. K. and K. E. Schilling (2006). "Effects of land cover on water table, soil moisture, evapotranspiration, and groundwater recharge: a field observation and analysis." *Journal of Hydrology* (319), 328-338.

Zheng, C., 1990. MT3D — A modular three-dimensional transport model for simulation of advection, dispersion and chemical reactions of contaminants in groundwater systems, U.S.E.P.A Report.

9. Appendix

9.1 Additional Data

Table 9-1. Recharge values in ft/month used in Scen 1.1 obtained using Soil Moisture method in SWAT

Stress Period	Recharge	Stress Period	Recharge
1	0.122	32	0.387
2	0.122	33	0.341
3	0.109	34	0.322
4	0.177	35	0.145
5	0.165	36	0.198
6	0.044	37	0.104
7	0.048	38	0.150
8	0.004	39	0.060
9	0.048	40	0.093
10	0.139	41	0.053
11	0.099	42	0.122
12	0.041	43	0.122
13	0.125	44	0.122
14	0.135	45	0.122
15	0.027	46	0.122
16	0.201	47	0.122
17	0.201	48	0.122
18	0.136	49	0.122
19	0.208	50	0.122
20	0.041	51	0.122
21	0.065	52	0.122
22	0.128	53	0.122
23	0.090	54	0.122
24	0.126	55	0.122
25	0.118	56	0.122
26	0.239	57	0.122
27	0.134	58	0.122
28	0.056	59	0.122
29	0.090	60	0.122
30	0.095	61	0.122
31	0.361		

Table 9-2. Recharge values in ft/month used in Scen 1.2 obtained using Plant ET method in SWAT

Stress Period	Recharge	Stress Period	Recharge
1	0.103	32	0.238
2	0.103	33	0.120
3	0.099	34	0.100
4	0.137	35	0.072
5	0.081	36	0.178
6	0.051	37	0.088
7	0.056	38	0.139
8	0.007	39	0.057
9	0.053	40	0.099
10	0.154	41	0.057
11	0.110	42	0.103
12	0.050	43	0.103
13	0.140	44	0.103
14	0.145	45	0.103
15	0.030	46	0.103
16	0.219	47	0.103
17	0.148	48	0.103
18	0.121	49	0.103
19	0.129	50	0.103
20	0.049	51	0.103
21	0.074	52	0.103
22	0.125	53	0.103
23	0.111	54	0.103
24	0.142	55	0.103
25	0.139	56	0.103
26	0.246	57	0.103
27	0.131	58	0.103
28	0.060	59	0.103
29	0.099	60	0.103
30	0.111	61	0.103
31	0.333		

Table 9-3. Recharge values in ft/month used for Scenario 2 with Land Cover Change taken into account

Stress Period	Recharge	Stress Period	Recharge
1	0.077	32	0.238
2	0.071	33	0.120
3	0.007	34	0.100
4	0.030	35	0.072
5	0.110	36	0.178
6	0.072	37	0.088
7	0.029	38	0.139
8	0.099	39	0.057
9	0.111	40	0.100
10	0.024	41	0.057
11	0.084	42	0.076
12	0.070	43	0.076
13	0.097	44	0.076
14	0.100	45	0.076
15	0.192	46	0.076
16	0.098	47	0.069
17	0.039	48	0.107
18	0.062	49	0.117
19	0.070	50	0.026
20	0.258	51	0.025
21	0.195	52	0.047
22	0.105	53	0.078
23	0.087	54	0.130
24	0.053	55	0.089
25	0.125	56	0.130
26	0.062	57	0.024
27	0.108	58	0.036
28	0.044	59	0.074
29	0.085	60	0.079
30	0.049	61	0.116
31	0.333		

Table 9-4. Recharge Values in ft/month for Scenario 3 (Dry Climate Change)

Stress Period	Recharge	Stress Period	Recharge
1	0.103	32	0.238
2	0.103	33	0.120
3	0.099	34	0.100
4	0.137	35	0.072
5	0.081	36	0.178
6	0.051	37	0.088
7	0.056	38	0.139
8	0.007	39	0.057
9	0.053	40	0.100
10	0.154	41	0.057
11	0.110	42	0.062
12	0.050	43	0.062
13	0.140	44	0.062
14	0.145	45	0.062
15	0.030	46	0.062
16	0.219	47	0.053
17	0.148	48	0.090
18	0.121	49	0.105
19	0.129	50	0.015
20	0.049	51	0.018
21	0.074	52	0.033
22	0.125	53	0.061
23	0.111	54	0.110
24	0.142	55	0.075
25	0.139	56	0.114
26	0.246	57	0.017
27	0.131	58	0.023
28	0.060	59	0.059
29	0.099	60	0.062
30	0.111	61	0.098
31	0.333		

Table 9-5. Recharge Values in ft/month for Scenario 4 (Wet Climate Change)

Stress Period	Recharge	Stress Period	Recharge
1	0.103	32	0.238
2	0.103	33	0.120
3	0.099	34	0.100
4	0.137	35	0.072
5	0.081	36	0.178
6	0.051	37	0.088
7	0.056	38	0.139
8	0.007	39	0.057
9	0.053	40	0.099
10	0.154	41	0.057
11	0.110	42	0.091
12	0.050	43	0.091
13	0.140	44	0.091
14	0.145	45	0.091
15	0.030	46	0.091
16	0.219	47	0.084
17	0.148	48	0.125
18	0.121	49	0.129
19	0.129	50	0.037
20	0.049	51	0.031
21	0.074	52	0.062
22	0.125	53	0.095
23	0.111	54	0.150
24	0.142	55	0.103
25	0.139	56	0.146
26	0.246	57	0.031
27	0.131	58	0.050
28	0.060	59	0.088
29	0.099	60	0.096
30	0.111	61	0.133
31	0.333		

Table 9-6. Pumping rates (in ft^3/month) for Dauphin Island wells.

Month-Year	Well ID #							
	10	20	30	40	50	60	70	80
Sep 2000	36997	35137	39763	38550	40100	38587	33430	32130
Oct 2000	35387	34048	41861	0	33706	33903	31659	29930
Nov 2000	28366	27307	34825	0	28328	26666	26159	26645
Dec 2000	30194	29490	36303	0	30877	28452	27910	26226
Jan 2001	24641	23680	30352	0	25397	23352	23510	22314
Feb 2001	25560	24119	32652	0	26075	24986	23381	21886
Mar 2001	47549	33676	45521	0	38633	37290	34677	32424
Apr 2001	39457	43353	48413	0	39657	37440	36173	33963
May 2001	49703	52426	58810	0	48377	45539	44481	41777
Jun 2001	55813	55168	66303	0	55237	50997	50983	47853
Jul 2001	61829	61280	71113	0	60884	56203	56665	53006
Aug 2001	42516	44061	50281	0	42127	41516	39535	37129
Sep 2001	40320	43387	50013	0	37756	41300	37480	34700
Oct 2001	37767	38820	47310	0	37514	36300	35100	32537
Nov 2001	39313	40693	44147	0	39050	37780	36220	33700
Dec 2001	33804	35497	33758	0	33583	32243	31229	29093
Jan 2002	45029	46624	45009	0	44519	43177	41329	38262
Feb 2002	30760	32072	30948	0	32676	32224	28296	26172
Mar 2002	39611	43154	41704	0	43290	40422	38250	35765
Apr 2002	49679	46173	44331	0	46321	42849	40666	37725
May 2002	58281	58813	58335	0	60313	57003	51106	49203
Jun 2002	60103	58239	60433	0	62073	59793	53820	48567
Jul 2002	66687	65676	66338	0	69190	66655	58345	52790
Aug 2002	58486	57897	58983	0	53584	60004	50622	49625
…	…	…	…	…	…	…	…	…
Jan 2009	29000	12000	23000	0	13000	19000	23000	21000
Feb 2009	28000	15000	25000	0	29000	0	23000	20000
Mar 2009	35000	2000	5000	0	41000	26000	34000	29000
Apr 2009	42000	15000	5000	0	45000	16000	35000	31000
May 2009	54000	56000	0	0	61000	0	40000	34000
Jun 2009	74000	78000	10000	0	80000	20000	37000	31000
Jul 2009	75000	74000	53000	0	80000	24000	34000	26000
Aug 2009	64000	69000	50000	0	68000	25000	40000	31000
Sep 2009	52000	61000	28000	0	56000	21000	37000	32000
Oct 2009	36000	27000	33000	0	38000	2000	28000	23000
Nov 2009	31000	19000	18000	0	31000	9000	18000	19000
Dec 2009	24000	16000	0	0	21000	19000	18000	18000

Jan 2010	32000	23000	0	0	32000	0	19000	28000
Feb 2010	23000	17000	0	0	23000	0	0	20000
Mar 2010	30000	22000	0	0	31000	0	0	25000
Apr 2010	56000	36000	0	0	57000	0	5000	34000
May 2010	64000	42000	0	0	60000	0	5000	28000
Jun 2010	61000	39000	0	0	59000	0	0	26000
Jul 2010	68000	45000	0	0	67000	0	0	36000
Aug 2010	73000	48000	0	0	74000	0	0	30000
Sep 2010	65000	43000	0	0	71000	0	0	19000
Oct 2010	38000	35000	0	0	58000	0	0	14000
Nov 2010	35000	28000	0	0	46000	0	10000	0
Dec 2010	21000	19000	0	0	33000	0	14000	0

Table 9-7. Pumping Values (in ft^3/month) used for Scenario 6 showing increased pumping

SP	10	20	30	40	50	60	70	80
1	181945	158560	117536	156748	0	0	0	0
2	181945	158560	117536	156748	186640	99592	114446	122696
3	181945	158560	117536	156748	186640	99592	114446	122696
4	181945	158560	117536	156748	186640	99592	114446	122696
5	181945	158560	117536	156748	186640	99592	114446	122696
6	181945	158560	117536	156748	186640	99592	114446	122696
7	181945	158560	117536	156748	186640	99592	114446	122696
8	147259	140750	166056	78426	150151	147474	132418	126255
9	110632	106395	136440	0	112581	105236	102697	98741
10	193468	137021	185217	0	157191	151726	141094	131927
11	160543	176395	196984	0	161357	152336	147181	138189
12	226965	229039	266136	0	223104	207156	206328	193453
13	157219	164944	174537	0	157929	155104	146192	135979
14	202135	187869	180375	0	188472	174345	165462	153496
15	247747	244765	248288	0	249378	247643	217573	203629
16	181945	158560	117536	0	186640	99592	114446	122696
17	181945	158560	117536	0	186640	99592	114446	122696
18	181945	158560	117536	0	186640	99592	114446	122696
19	181945	158560	117536	0	186640	99592	114446	122696
20	181945	158560	117536	0	186640	99592	114446	122696
21	181945	158560	117536	0	186640	99592	114446	122696
22	181945	158560	117536	0	186640	99592	114446	122696
23	132179	118625	146583	0	145819	101876	104387	102744
24	117996	48826	93583	0	52895	77307	93583	85445
25	113927	61032	101720	0	117996	0	93583	81376
26	156649	34585	20344	0	174959	85445	140374	122064

27	219716	227854	0	0	248198	0	162753	138340
28	269559	286851	143426	0	288886	91548	150546	122064
29	146477	109858	134271	0	154615	8138	113927	93583
30	126133	77307	73239	0	126133	36619	73239	77307
31	97652	65101	0	0	85445	77307	73239	73239
32	130202	93583	0	0	130202	0	77307	113927
33	93583	69170	0	0	93583	0	0	81376
34	122064	89514	0	0	126133	0	0	101720
35	244129	158684	0	0	238026	0	20344	126133
36	262439	170890	0	0	256335	0	0	126133
37	297023	195303	0	0	301092	0	0	122064
38	264473	174959	0	0	288886	0	0	77307
39	154615	142409	0	0	235991	0	0	56963
40	142409	113927	0	0	187165	0	40688	0
41	85445	77307	0	0	134271	0	56963	0
42	181945	158560	117536	0	186640	99592	114446	122696
43	186490	162521	120472	0	191302	102080	117305	125761
44	191149	166581	123482	0	196081	104630	120235	128903
45	195924	170742	126566	0	200979	107244	123239	132123
46	200818	175007	129728	0	205999	109923	126317	135423
47	205834	179379	132968	0	211145	112669	129472	138806
48	210976	183860	136290	0	216419	115483	132707	142274
49	216246	188452	139695	0	221826	118368	136022	145828
50	221648	193160	143184	0	227367	121325	139420	149470
51	227185	197985	146761	0	233046	124355	142902	153204
52	232860	202931	150427	0	238868	127462	146472	157031
53	238677	208000	154185	0	244835	130646	150131	160954
54	244639	213196	158036	0	250951	133909	153881	164974
55	250750	218521	161984	0	257220	137254	157725	169095
56	257014	223980	166030	0	263645	140683	161665	173319
57	263434	229575	170178	0	270231	144197	165703	177649
58	270015	235310	174429	0	276981	147799	169843	182087
59	276760	241188	178786	0	283900	151491	174085	186635
60	283673	247213	183252	0	290992	155276	178434	191297
61	290759	253388	187830	0	298261	159154	182891	196076

Sample Calculations

First cut calculations can be done in order to estimate the amount of water contained in the Dauphin Island Water-Table aquifer. By doing these rough calculations, we can check the volumes that are calculated in Section 5.4 and confirm that they are the same order of magnitude.

As shown in the Figure 8-1, by multiplying the area of the island by the depth of the aquifer we will get a volume of the study area. To obtain the volume of water contained in the groundwater, we multiply the volume by the porosity, 0.3. Next, we will assume that the saltwater takes up about 30% of this volume and subtract that out to obtain a rough estimate for freshwater volume.
Area of study area = 58982294 ft^2
Depth of Aquifer= 42 ft
Volume of study area= 58982294 ft^2 * 42 ft = 2477256361 ft^3
[3067739136*0.7]*0.3= <u>520223836 ft^3</u> of freshwater
This is the same order of magnitude as the values calculated in Section 5.4. For example, the volume of freshwater for the aquifer after the simulation of Scenario 1.1 was <u>526248576 ft^3</u>.